1-27-2022

Motor Network Reorganization During Chronic Stroke Recovery Using a Contralesional Brain-Computer Interface

Joseph Humphries
Washington University in St. Louis

WASHINGTON UNIVERSITY IN ST. LOUIS

McKelvey School of Engineering and Applied Science
Department of Biomedical Engineering

Dissertation Examination Committee:
Eric Leuthardt, Chair
Dennis Barbour
Alexandre Carter
ShiNung Ching
Nico Dosenbach

Motor Network Reorganization During Chronic Stroke Recovery Using a Contralesional Brain-Computer Interface
by
Joseph Benjamin Humphries

A dissertation presented to
The Graduate School
of Washington University in
partial fulfillment of the
requirements for the degree
of Doctor of Philosophy

December 2021
St. Louis, Missouri

Table of Contents

List of Figures

List of Tables

<u>Acknowledgments</u>

<div align="right">Joseph Benjamin Humphries</div>

Washington University in St. Louis

December 2021

Dedicated to my wife and family.

ABSTRACT OF THE DISSERTATION

Motor Network Reorganization During Chronic Stroke Recovery Using a Contralesional Brain-

Computer Interface

by

Joseph Benjamin Humphries

Doctor of Philosophy in Biomedical Engineering

Washington University in St. Louis, 2021

Professor Eric Leuthardt, Chair

Professor Alexandre Carter, Co-Chair

Stroke is a leading source of adult disability. Many chronic stroke patients never fully regain the

use of their affected limb. Providing effective rehabilitation to chronically hemiparetic stroke

patients is crucial for improving the lives of these patients. Brain-computer interfaces (BCIs)

have emerged as a promising approach for developing new, effective therapies for both acute and

chronic stroke patients. Specifically, an EEG-based BCI using signals from motor regions of the

non-lesioned hemisphere was shown to promote clinically significant upper motor rehabilitation

in a chronic stroke population. This is a major advance for expanding therapy access to patients

who previously did not substantially benefit from existing therapies. However, we do not yet

fully understand how BCIs effect change in the functional organization of the brain to drive

motor recovery. Determining how contralesional BCI therapy affects the brain will enable

further improvements to BCI therapy systems, as well as targeted approaches for individual

patients. Comparing therapy approaches may also inform how the brain generally reacts to stroke

rehabilitation. This project examines changes in the resting-state functional organization of the brain by comparing shifts in fMRI and EEG connectivity to contemporaneous motor function improvement in a cohort of chronic stroke patients using a contralesional BCI for 12 weeks. We were particularly interested in the reorganization of the motor network as it related to motor recovery. We measured changes in functional connectivity between several cortical and cerebellar motor regions using fMRI data. Overall, motor network connectivity decreased in these patients, and this decrease correlated with motor recovery. The specific ROI pairs driving this decrease varied among patients. A comparison group of chronic stroke patients using intensive physical therapy to achieve motor recovery did not show these same effects. Contralesional BCI therapy may therefore promote recovery differently from standard approaches. The EEG data offers a complementary perspective to the fMRI data, as it provides a detailed measurement of activity in a few cortical areas as opposed to coarse signal measurements in many specific regions. Alpha-band (8-12 Hz) coherence between two motor electrodes increased following 12 weeks of contralesional BCI therapy, and this increase correlated with motor recovery. Delta (1-4 Hz), alpha, and beta (13-30 Hz) band activity have all been previously implicated in stroke recovery, but we observed effects only in alpha. Although at first glance, an increase in motor coherence and a decrease in BOLD connectivity may seem to disagree with each other, but these signals have different physiological sources. An increase in motor alpha coherence may be driven by a decrease in activity in inhibitory thalamocortical circuits which are thought to drive the alpha rhythm. Future BCI systems may specifically modulate alpha coherence or thalamocortical activity to further boost recovery. Additional research is necessary to improve BCI design, and to potentially enable them to change their behavior to provide the best therapy possible for each individual patient.

Chapter 1: Introduction

1.1 Clinical Significance

Chronic upper motor weakness, or hemiparesis, following stroke remains a significant problem. Upper motor weakness is the most common outcome in stroke survivors.[1] Motor rehabilitation becomes more difficult after three months post-stroke, and a majority of hemiparetic stroke patients report continued motor weakness six months post-stroke.[2–6] Some specific therapies, such as constraint-induced movement therapy, can be effective in the chronic state. However, patients with severe motor impairment are not able to use this technique.[7–13] The development of a contralesional brain-computer interface (BCI) system for upper motor rehabilitation in chronic stroke patients was driven by the lack of options available to these patients. A series of previous studies showed the feasibility of contralesional control and the efficacy of a contralesional BCI system in promoting stroke recovery.[14,15] This new system offers a path to motor rehabilitation for a population of patients with few options previously available.

1.2 Project Overview

The core implementation of the contralesional BCI system is effective at promoting upper motor rehabilitation in a chronic stroke population. However, it is not year clear how contralesional BCI works to effect recovery. To optimize therapy efficacy and target patients that would most benefit from BCI therapy, it is necessary to determine what changes in the brain during contralesional BCI therapy. These changes may then be targeted for further enhancement in the future.

We approached this goal by measuring changes in brain function with two noninvasive modalities. A cohort of chronically hemiparetic stroke patients used the contralesional BCI for therapy over a three-month period. Before and after this therapy period, resting-state EEG and functional MRI data was acquired from each patient. We also evaluated motor function at these times. Resting-state BOLD data from fMRI scans were used to determine changes in functional connectivity in cortical and cerebellar motor regions that corresponded with motor recovery. The EEG data was similarly used to find changes in the resting-state organization of oscillatory brain activity at central motor, frontal, and parietal electrode sites. These approaches complement one another by providing spatially-specific (fMRI) and frequency-specific (EEG) perspectives into the function of the brain during recovery. This work establishes a strong foundation for determining the mechanism driving chronic stroke rehabilitation with a contralesional BCI.

1.3   Dissertation Organization

This dissertation is organized into five chapters. Chapter 2 describes the existing body of relevant literature to best understand the presented work. First, an overview of rehabilitation strategies and methods of recovery prediction are presented. Brain-computer interfaces are then introduced as a comparison to existing therapies. Discussions of structural and functional plasticity measured primarily via EEG and MRI during acute and chronic stroke rehabilitation follow.

Chapter 3 describes resting-state changes in the fMRI-BOLD motor network accompanying chronic stroke recovery with a contralesional BCI system. Functional connectivity in select motor regions pre- and post-therapy are compared with motor recovery over the same time period. This chapter focuses on changes to functional organization within motor areas of the brain.

Chapter 4 complements Chapter 3 by examining resting-state changes in oscillatory brain activity. EEG signals provide much better temporal resolution than fMRI data at the cost of coarse spatial resolution. Alpha-band coherence change between several electrode pairs was compared to contemporaneous motor rehabilitation. These findings provide an additional perspective of how the functional organization of the resting brain changes.

Finally, Chapter 5 summarizes the previous chapters into a brief, coherent narrative. Key points of the results, implications for stroke rehabilitation, and potential future research directions are discussed.

Chapter 2: Background

2.1 Stroke Rehabilitation Overview

Stroke is a leading cause of adult disability in the United States and affects approximately

800,000 people annually.[16] The individual impact of stroke on patients varies dramatically. Some

stroke survivors experience minimal long-term issues related to their stroke, while others may

suffer from severe cognitive, language, or motor deficits. Unilateral upper motor weakness or

paralysis, also known as hemiparesis, is observed in 77% of new stroke cases and is the most

commonly observed post-stroke deficit.[1] The ability to recovery from hemiparesis varies from

patient to patient. Predicting and promoting individual ability to recovery has been a major focus

of stroke rehabilitation research. Several biomarkers have been observed for predicting the

ability of each patient to achieve upper motor recovery.[17]

2.1.1 Recovery Strategy and Prediction

The PREP-2 algorithm contains one such set of biomarkers and can predict recovery in 75% of

patients. The strongest predictors of recovery are the ability to achieve a motor evoked potential

(MEP).[18] MEPs are observed by stimulating motor cortex with transcranial magnetic stimulation

and measuring the resulting electrical response in arm muscles.[19] The presence of an MEP

indicates that the neural circuitry responsible for transmitting motor signals from motor cortex to

the muscles is intact. Age and baseline motor function supplemented prediction in MEP positive

patients, while lesion load was the strongest secondary predictor of recovery in MEP negative

patients.[9,18] Sensorimotor tract lesion load and MEP potential both serve as measures of how a

given stroke has impacted the patient's ability to successfully transmit a motor control signal

from motor cortical regions to the affected limb. Initial motor deficit has also been identified as

a predictor of recovery. Patients are often observed to regain about 70% of lost function, in a pattern known as the Proportional Recovery Rule (PRP).[20,21] However, about 30% of hemiparetic stroke patients are "non-fitters" who do not follow this rule.[17,22] Some of these non-fitters lack the necessary corticospinal tract integrity to achieve meaningful or proportional recovery of upper motor function.[23,24] The PRP has recently come under criticism as being potentially attributable to a statistical error arising from correlating the change of a measure with the baseline value of that same measure.[25] The utility of the PRP is under active debate among neurorehabilitation researchers.[25,26]

Post-stroke hemiparesis frequently persists into the chronic stage of stroke; about 65% of chronic stroke patients continue to experience hemiparesis 6 months after stroke.[2,3] Upper motor recovery is generally thought to plateau approximately 3 months after stroke, and very few patients achieve meaningful recovery after this time.[4–6,27–30] Furthermore, any motor function improvement that does happen after 3 months post-stroke is usually attributed to intentional behavioral adaptations as opposed to the spontaneous recovery of function.[29] Many therapy strategies have been developed for post-stroke hemiparesis, but most are not effective in the chronic stage of stroke. Constraint-induced movement therapy (CIMT) is a rare example of a motor rehabilitation strategy that is effective in both the sub-acute and chronic stages of stroke.[7,8,10] CIMT consists of limiting the movement of the unaffected limb to encourage the use of the affected limb and combat learned non-use (i.e. behavioral maladaptation).[7,10,11] While effective at all stages of stroke, CIMT unfortunately requires a relatively high level of retained function in the affected limb, which excludes severely impaired patients from benefitting.[10–13,18] Thus, chronic stroke patients with substantial hemiparesis are have few options for achieving further rehabilitation. Recently, brain-computer interfaces (BCIs) have emerged as a promising

approach for upper motor recovery in stroke patients in all stages of stroke and with a wide range of deficits.

2.1.2 Brain-Computer Interfaces for Stroke Rehabilitation

Early evidence suggests that BCI-based approaches are a versatile and effective method for upper limb rehabilitation post-stroke.[31] The breadth of design decisions around type and method of feedback, control, and stimulation in the BCI system allows for personalization to individual patients, but also makes comparison among different approaches difficult. The mechanisms driving BCI-assisted recovery are also not well-understood.[31] Generally, BCIs are thought to promote activity-dependent plasticity to aid in recovery.[32,33] The specific changes to the brain likely vary based on BCI design. Mrahacz-Kersting and colleagues have shown that BCIs are able to pair brain activity with an associated external stimulus.[34] This pseudo-Hebbian framework of pairing a stimulus with a desired pattern of neural activity is an appealing strategy for achieving motor recovery.

BCI Design Considerations

BCI-based therapy approaches vary drastically in terms of design and efficacy, and possibly in mechanism of action for promoting recovery. Understanding these mechanisms is vital for improving therapeutic strategies and personalizing rehabilitation to individual patient needs. Feedback to the user is one aspect of BCI design, and is vital for learning to perform a BCI task.[35] Vibration, visual images or animations, assisted limb movement (proprioception), and combinations thereof have all been used in therapeutic BCIs to provide feedback.[36] Neither specific feedback timing nor differentiating between realistic and abstract imagery appear to strongly influence BCI performance.[37,38] Direct stimulation to the subject, separate from control feedback, is frequently used for therapeutic BCIs as well. This typically takes the form of

assisted movement via robotic orthosis or electrical stimulation to the muscles of the impaired limb.[31] Both methods promote movement of the impaired limb when a desired brain signal is observed and may therefore have similar effects on neural reorganization. Finally, the method of BCI control is yet another design choice which may affect system efficacy. For upper motor rehabilitation in stroke patients, motor imagery and attempted motor execution are the most common control methods.[31] Motor imagery calls for a vivid imagining of a movement, while attempted execution asks subjects to try to perform a physical task. Both methods elicit similar neural activity as detected through EEG.[39] Attempted execution may be frustrating for subjects with severe deficits who are unable to perform the movement. Additionally, execution may be more susceptible to movement-driven (i.e. EMG) artifacts in EEG recordings. Within this large space of design decisions to choose from, there is likely no single best approach. However, it is important to determine what types of BCIs will work best for an individual patient based on their specific needs and abilities.

Stroke patients with severe upper motor deficits or large cortical lesions may find controlling a BCI through traditional contralateral motor signals difficult. Motor function in subjects with cortical strokes tends to remap to the perilesional cortex during recovery.[40–42] However, a large disruption to the location and organization of primary motor areas would disrupt the measurement of motor activity with non-invasive methods. In EEG for example, motor activity on the left side of the brain is typically recorded primarily via the C3 electrode, approximately over the left primary motor cortex. Remapping of motor function may result in measurements from ipsilesional motor electrodes becoming less reliable for BCI control. This issue is potentially addressable by performing source localization with motor task data to estimate motor activity at the remapped brain location.[43] However, this is computationally intensive and requires

a dense electrode placement. A series of reports from the Leuthardt Lab and others has highlighted the function of the ipsilateral (contralesional) hemisphere in coordinating motor activity and its feasibility as a substrate for BCI control.[14,15,44] Contralesional motor areas may be more reliable for post-stroke BCI control in patients with cortical lesions.

2.2 Structural Influences on Rehabilitation

The effects of lesion size and location on motor deficits have been extensively studied and debated. Numerous studies have observed the presence [45–48] or absence [49,50] of associations between lesion size or location and the severity of sensorimotor deficits. Potential sources of disagreement among these studies are the variance between motor outcome measures, follow-up durations, and the consideration of only lesion size or location, as opposed to studying the two factors in combination [51]. Chen et al. combined lesion size and location into a "brain lesion profile" measure with strongly correlated with recovery [51]. Brain lesion profiles in this study were computed across brain regions consisting of either gray or white matter (e.g. thalamus, internal capsule, etc.). More recent efforts have focused on the descending cortico-spinal tract (CST) as a particularly important structure to examine following stroke. A previously discussed study by Stinear et al. found that CST integrity is a strong predictor of motor recovery in MEP-negative patients using a decision tree model [9]. Lesion load in the CST during the acute stage of stroke has also been used as an effective univariate predictor of motor recovery [52]. Subcortical strokes are likely to cause white matter (i.e., CST) damage and comprise a majority of stroke cases. Subcortical strokes also may result in more severe motor outcomes with less successful recovery and increased contralesional excitability.[53–55] Further complicating lesion effects is the lack of observed associations between white matter-based structural connectivity and resting-state functional connectivity in healthy subjects.[56] The specific impact of spatial lesion

8

characteristics is still actively studied, and is critical for assigning patients to optimal, individualized therapies.

Structural Plasticity During Recovery

Structural changes in the brain occur following stroke as a response to brain injury. White matter integrity is estimated using measures of "directionality" assessed from diffusion tensor imaging scans. Fractional anisotropy (FA), radial diffusivity (RD), axial diffusivity (AD), and mean diffusivity (MD) are used in conjunction to assess the impact of lesions on white matter tracts.[57] Immediately following stroke, white matter integrity in the lesioned hemisphere decreased sharply, and continued to decline over the following three months (due to Wallerian degeneration).[58] Patients with less severe behavioral deficits showed smaller decreases in white matter tract integrity.[58] White matter plasticity has also been observed in the non-lesioned hemisphere. Structural remodeling of white matter tracts opposite the lesion is associated with better clinical outcomes.[59,60] Although the corticospinal tract is the primary white matter pathway associated with motor function, secondary tracts have been identified as potentially useful for facilitating stroke recovery. Both the reticulospinal and rubrospinal tracts show structural change to compensate for lost upper motor function following stroke.[61–63] The rubrospinal tract may also provide a pathway for the contralesional motor cortex to control the paretic limb.[64] Structural plasticity may be both a complement and an enabling substrate to functional plasticity during rehabilitation.

2.3 The Complex Role of the Contralesional Motor Cortex

Ipsilateral motor signals have been continuously studied for decades.[65–68] As BCIs became more widely used in research environments, ipsilateral motor signals were identified as a possible platform for BCI control. Several studies used invasive electrophysiology (primarily

electrocorticography, ECoG) in humans and non-human primates to characterize these ipsilateral

signals as generally similar to contralateral signals in their cortical activation patterns and ability

to decode motor activity.[69,70] Wisneski and colleagues additionally noted some key differences,

such as the lower optimal control frequency of ipsilateral signals compared to contralateral

signals.[44] Importantly, each of these studies highlighted the potential for ipsilateral motor signals

as a platform for neuroprosthetics. This potential was further explored by Bundy and colleagues,

who confirmed that ipsilateral motor signals could indeed be used as a robust primary control

feature of a BCI [14]. These results were further expanded upon with a clinical trial testing the

efficacy of such a device in promoting upper motor recovery in a chronic stroke population [15].

Despite the variety of rehabilitative BCIs for stroke patients, this remains the only example of a

contralesionally-controlled BCI for stroke rehabilitation. Efforts to further understand the

contributions of ipsilateral motor cortical regions are ongoing; Bundy and colleagues recently

showed via ECoG that 3D arm movement kinematics are encoded by ipsilateral motor cortex .[71]

The study of how the ipsilateral motor cortex contributes to motor control is continually

developing. In addition, the role of this brain region specifically in the context of stroke recovery

is hotly debated.[72,73]

2.3.1 Contralesional Motor Activity Following Stroke

The role of the contralesional hemisphere in stroke recovery is not well-understood currently.

Conflicting evidence suggests that it may actively hinder recovery by inhibiting the lesioned

hemisphere, or support recovery by compensating for lost motor function. Following stroke,

functional activations shift contralesionally and later remap to the ipsilesional hemisphere in

patients who achieve motor recovery.[41,74,75] The degree of the initial shift in functional mapping

as well as the remapping back to the ipsilesional hemisphere depend on the severity of initial injury and the degree of recovery.[41,76–78] Patients with greater contralesional functional activity tend to have more severe deficits, and decreases in activity in the unaffected hemisphere are correlated with motor recovery.[41,74,75,79–83] This trend supports the notion that increased contralesional activity following stroke is a biomarker for poor recovery and may be partially responsible for the prevention of recovery. Additionally, inhibitory repetitive transcranial magnetic stimulation (rTMS) of the contralesional motor cortex improved motor function in the affected limb of stroke subjects in several studies.[84–86] Generally, these experiments support the hypothesis that the contralesional hemisphere impede recovery via abnormal transcallosal inhibition (TCI). However, there is also a large body of evidence that suggests contralesional motor activity may be primarily compensatory in nature as opposed to inhibitory.

2.3.2 Interhemispheric Inhibition Framework

Although TCI is a common framework for explaining the impact of the contralesional hemisphere on stroke recovery, there is some evidence that increased contralesional activity and bihemispheric communication between motor regions promotes motor function. Greater integrity of transcallosal M1-M1 white matter tracts was shown to facilitate interhemispheric interaction and improve motor function in stroke patients.[61,87–94] The benefit of inhibitory rTMS to contralesional primary motor cortex has also been shown to be time-dependent; although effective in a subacute stroke population, it is not beneficial for chronic stroke patients.[86] Other studies examining interhemispheric inhibition (IHI) demonstrated differences between subjects with cortical and subcortical strokes.[95] Furthermore, increased contralesional M1 excitability elicited via paired-pulse TMS did not causally result in altered IHI for a subacute population.[95] However, in the specific context of a pre-movement interval in a chronic stroke population,

11

increased IHI from contralesional to ipsilesional M1 was observed.[96] Studies of stroke rehabilitation methods on the contralesional hemisphere are also useful in determining how this brain region may influence recovery. For example, CIMT increases contralesional activity and is an effective method for improving motor function in stroke patients with some remaining ability in the affected limb.[80,97] This tangle of seemingly conflicting and nuanced evidence has more recently been examined through the lens of precision medicine, suggesting a spectrum of interactions among lesion size, location, and deficit severity.

Many of the commonly observed findings described above appear at first to directly conflict with each other. However, patterns of effects begin to emerge when considering the specific differences between the studies describing these findings. Di Pino and colleagues proposed a bimodal model that in part explains these disparate findings. The model suggests that the probability of recovery is a function of both IHI post-stroke as well as the reserve of intact structural pathways to support function.[92] Further work by Plow and colleagues identified response curves for ipsilesional and contralesional substrates of motor function based on the degree of motor system damage or functional deficit.[98,99] This allows for the empirical derivation of a functional threshold, above which ipsilesional motor regions are more likely to recover, and below which contralesional motor systems may be a more appropriate target for rehabilitation.[98] As this work continues, a more complete understanding of the function and role of the contralesional hemisphere in stroke will be developed.

Rehabilitation Summary

The contralesional primary motor cortex is a promising target for noninvasive stroke rehabilitation, especially in chronic stroke patients exhibiting severe motor deficits. Early results using contralesionally-controlled BCI suggest that this specific method of rehabilitation may be

effective.[15] The effects of this therapeutic BCI system on the organization of the brain, especially on the function of the contralesional motor cortex, are critical to understand in order to improve the system and target the patient population most likely to benefit from its use.

2.4 Functional Plasticity During Stroke Rehabilitation

Strokes elicit changes in the molecular ecosystem of the brain which result in increased plasticity and functional reorganization to drive recovery.[29,100–107] This is an area of active research, but there is ample evidence of altered levels of neurotransmitters and proteins in the extracellular environment following stroke. Several days after a stroke primarily affecting the M1 hand area, neurons in the nearby ventral premotor hand area express vascular endothelial growth factor (VEGF).[104,108] This protein is associated with angiogenesis and neuroprotection, and likely aids in post-stroke functional remapping.[104,105] Additional studies in ischemic rats have observed increased expression of GAP-43, a protein associated with axonal sprouting.[102] Most genes associated with axonal sprouting show higher levels post-stroke.[107] Extracellular matrix structures known as perineuronal nets (PNNs) interface with GABAergic neurons to stabilize existing neural circuitry and downregulate plasticity.[105] Decreased PNN counts were observed in perilesional cortex after stroke, indicating increased perilesional plasticity.[105,109] These changes are thought to be an innate mechanism of recovery and are primarily observed in the acute and sub-acute phases of stroke.[105] Despite the extracellular environment returning to normal over time, functional reorganization may still occur in the chronic stage.

The reorganization of brain function has been linked to recovery in all stages of stroke, across multiple deficits, and with a variety of modalities, including EEG, MEG, task fMRI, and resting state fMRI.[41,75,110–113] The wealth of studies investigating each of these facets of recovery provides a rich context for exploring how stroke changes the brain, how the brain heals itself,

and how various interventions may work to promote further recovery. Each of these recording modalities examines signals generated by different physiological processes. EEG and MEG measure the electrical and magnetic signals generated by neuronal activity with high temporal resolution. However, they offer poor spatial resolution relative to fMRI data. This is especially true of EEG, which at best can localize signals to an area of a few centimeters on the cortical surface.[114] This results in a tradeoff compared to fMRI data, which measures hemodynamic signals slower than 1 Hz in approximately 1 cubic millimeter voxels.[115] Thus, separately using each of these modalities to observe functional reorganization is necessary for a holistic view of how the brain changes during recovery.

2.4.1 EEG Measures of Oscillatory Activity

Stroke-induced functional changes in the brain have been explored with a wide variety of electrophysiology techniques. Disruptions to event-related synchronization and desynchronization (ERS/ERD) patterns associated with movement have been observed in both acute and chronic stroke patients. In healthy subjects, alpha (8-12 Hz) and beta (13-30 Hz) band oscillations show a well-documented pattern of activity around movement. Power in both frequency bands decreases during movement preparation and execution (ERD). This is followed by a post-movement ERS where power increases above baseline before returning to normal levels.[116–121] The alpha band exhibits a stronger movement-related ERD than the beta band, while the post-movement beta ERS is stronger than the alpha ERS.[116] The temporal structure of these ERDs does not appear to be strongly affected by stroke; however, changes in ERD strength and location have been observed in several studies. Stępień and colleagues investigated changes in alpha ERD in an acute stroke population using a sensorimotor task. They found that contralateral alpha ERD decreased during movement of the paretic limb, while ipsilateral alpha

ERD amplitude increased.[122] Alpha ERDs during non-paretic limb movement were not strongly

affected in this population. Another study showed a decrease in movement-related beta ERD

amplitude in the lesioned hemisphere during paretic limb movement.[123] Similar effects have been

reported elsewhere, with an additional finding that ERD amplitude modulation and peak ERD

location shifts based on the specific stroke-related deficits exhibited by each group of subjects.[124]

In addition to changing event-related EEG signals, stroke also impacts the functional

organization of EEG signals at rest. Resting delta-band power in the subacute phase of ischemic

stroke increases and becomes more symmetrical across the brain.[125–128] Delta coherence,

especially between ipsilesional M1 and contralesional M1, similarly increased following

stroke.[126] Resting power of alpha- and beta-band frequencies tends to decrease in stroke patients

when delta power increases.[125,127,129,130] These effects have been associated with more severe

ischemic injury, greater infarct volume, and greater motor deficits.[126,131,132] Alpha power

fluctuations in stroke have also been observed across brain networks. MEG-based alpha power

connectivity in the sub-acute phase of stroke showed increases in perilesional cortical regions

and bilateral cerebellum, as well as decreases in contralesional cortical motor areas. Importantly,

these changes correlated with motor recovery.[113] Another study using high-density resting EEG

found correlations between motor alpha coherence and motor function 3 months post-stroke

[129,130]. Alpha coherence in other regions of the brain similar correlated with language function

and spatial working memory; the regions with correlations were previously known to be

involved in those functions (e.g. the inferior frontal gyrus for language function) [129,130]These

spatially distributed changes associated with motor recovery indicate that a network-level

examination of plasticity is necessary to characterize the impact of stroke as well as the effects of

rehabilitation. Combinations of these band-limited electrophysiology effects have been used as

clinical biomarkers to detect and assess acute strokes. Specifically, the ratio of delta power to alpha power (delta-alpha ratio or DAR) was able to differentiate between acute ischemic stroke patients and age-matched healthy controls.[133] DAR may also be linked to cognitive deficit severity following stroke.[134–136] Varied electrophysiological approaches to measuring neural function post-stroke and throughout rehabilitation are vital for understating how to best promote recovery.

2.4.2 Shifts in Functional MRI Activity

Brain function following stroke has been widely studied with noninvasive functional imaging as well. Functional MRI is a particularly common imaging modality for stroke populations, although several prominent studies have used PET imaging. The high spatial resolution and access to subcortical grey matter structures make fMRI and PET strong complements to EEG. Decades of research have shown task-related BOLD activations that deviate from healthy activity post-stroke. The redistribution of functional activation patterns in the cortex following stroke and throughout motor recovery tends to follow a stereotyped pattern.[75,80,137,138] In healthy patients, fMRI BOLD activations during a motor task are almost entirely contralateral to the side of the body engaged in motion. These activation patterns become weighted towards the contralesional hemisphere in stroke patients, and the degree of functional redistribution is proportional to the motor deficit. In patients who achieve motor function recovery, these activation patterns shift back to the ipsilesional hemisphere (i.e., they become similar to healthy subject activations.[41,74,75,80] In a population of well-recovered chronic stroke patients, fMRI-BOLD activation maps during a finger-movement task were not significantly different from healthy controls performing the same task.[139]

Correlated networks of spontaneous brain activity during rest have also been extensively

described using BOLD signals acquired with fMRI [140–142]. These resting-state networks are

defined by patterns of functional connectivity (FC) – a term used to describe BOLD signal

similarities between brain regions at rest. Disruptions of healthy FC are observed throughout the

acute and chronic stages of stroke.[110,112,143,144] The extent of this network disruption was

correlated with the severity of post-stroke impairment in multiple behavioral domains (e.g.

motor, language, etc.).[110,143–145] For example, after stroke, network modularity typically

decreased and then partially recovered in association with behavioral improvements [110,146,147].

Additionally, performance in motor and attention tasks post-stroke correlated with

interhemispheric connectivity in the somatomotor (SMN) and dorsal attention (DAN) networks,

respectively.[112,148] Connectivity changes between specific regions have also been implicated in

stroke recovery.[149–151] However, stroke- or recovery-related connectivity changes between

specific brain regions frequently differ among studies due to variance in treatment, population, or

analysis technique.

Measuring the impact of stroke on the functional organization of the brain is a vital step in

understanding the mechanisms driving rehabilitation with a variety of interventions. Future

research may eventually be able to identify optimal therapies for individual patients based on

these noninvasive evaluations of brain function.

2.5 Summary and Conclusion

Chronic stroke rehabilitation is difficult and complex. Rehabilitation is influenced by many

factors, both within and out of the control of physicians and patients. Even for rehabilitation aids

proven to be effective, not all patients will have access due to varying personal circumstances

such as disability or lack of financial resources. Furthermore, rehabilitation techniques and tools

that are effective on average may not be appropriate for each patient. Therefore, identifying optimal individual rehabilitation strategies is vital for improving both the quality of and access to therapy for stroke patients.

Brain-computer interfaces are a flexible platform for providing therapy to stroke patients. However, these various therapy strategies must be better understood to effectively match individual rehabilitation techniques with patients. Noninvasive acquisition of neural data such as fMRI and scalp EEG allow for the study of brain function and organization at any point during the recovery process. Contralesional BCIs specifically provide a novel view into the mechanisms of rehabilitation. These tools are necessary for understanding how the brain reacts to BCI therapy, and how changing the application of BCI therapy may change functional reorganization in the brain. Additionally, further study of stroke rehabilitation with BCI, EEG, and fMRI will facilitate the development and implementation of individualized, targeted therapy techniques to enhance recovery for stroke patients.

Chapter 3: Motor Network Reorganization Induced in Chronic Stroke Patients with the Use of a Contralesionally-Controlled Brain Computer Interface

3.1 Introduction

Stroke causes adult disability in approximately 800,000 adults annually in the United States.[16]

Unilateral upper motor weakness, known as hemiparesis, occurs in 77% of new stroke cases.[1]

Hemiparesis frequently persists into the chronic stage of stroke; 65% of chronic stroke patients

report reduced motor function 6 months after stroke.[2,3] Patients rarely obtain substantial motor

improvement 3 months after a stroke, with residual motor deficits effectively becoming

permanent.[4–6,27–30] Behavioral adaptations instead of spontaneous recovery generally underlie

subsequent improvements.[29] Recent innovations in rehabilitation techniques, however, offer new

opportunities for motor recovery, even in the chronic stage.

The efficacy of brain-computer interfaces (BCIs) for post-stroke motor rehabilitation has been

demonstrated with a variety of designs.[31] However, there is a lack of consensus regarding the

neurophysiological mechanisms driving recovery through BCI [75,87,152,153], which necessitated

further study. We previously showed functional rehabilitation in a severely impaired chronic

stroke population treated with a BCI system using signals from the contralesional motor cortex.[15]

The former study used cortical EEG signals to control a robotic hand orthosis. Additionally, the

efficacy of BCI on motor recovery was linked to changes in EEG activity in motor regions

within frequencies used for BCI.[15] We hypothesized BCI may have affected neural circuitry to

facilitate motor recovery on the basis of the similarity of EEG frequencies used for BCI control and those recorded from motor cortex. However, previously recorded EEG signals were only from cortical regions directly contacted by recording electrodes. Here we used functional MR imaging to study whether BCI therapy affected functional connectivity organization in the motor cortex and cerebellum.

Networks of correlated spontaneous brain activity during rest have been extensively described using functional MRI (fMRI).[140–142] Strokes disrupt "functional connectivity" networks.[110,112,143,144] Furthermore, the extent of network disruption correlated with stroke induced impairments in multiple behavioral domains.[110,143–145] Strokes altered network modularity, typically by a decrease and then a partial recovery in association with behavioral improvements.[110,146,147] Connectivity changes between specific regions have also been implicated in stroke recovery.[149–151] Further, task performance after a stroke covaried with interhemispheric motor network connectivity.[112,148] Thus, recovery from stroke induced by BCI might involve changes in resting-state functional connectivity (rsFC).

The objective of the current study was to determine whether an EEG-driven BCI controlled by motor signals from the unaffected hemisphere reorganized brain networks for motor control. We hypothesized the BCI system would change motor network connectivity during rehabilitation, and that BCI induced rsFC changes in motor systems would correlate with the strength of recovery. Increases in interhemispheric connectivity, and decreases in intrahemispheric connectivity have previously been reported during stroke recovery s.[110,112,148,149,154,155] Consequently, we hypothesized motor recovery via BCI would lead to similar patterns of change in inter- and intrahemispheric rsFC. The unexpected findings in this study provide intriguing

evidence for a novel recovery mechanism associated with BCI induced recovery in chronic stroke.

3.2 Materials and Methods

3.2.1 Patient Demographics

Eight enrolled patients had an upper limb hemiparesis (Median upper extremity portion of the Fugl-Meyer Assessment (UEFM) = 21.75) at least 6 months post-stroke. Exclusion criteria included evidence of memory loss, severe aphasia, joint contractures in the upper limb, unilateral neglect, or an inability to generate a consistent BCI control signal. **Table 3.1** lists patient demographics. **Table 3.S1** lists patient-specific information**. Figure 3.1** documents patient recruitment and attrition Every patient provided written informed consent before data collection. A total of fifty-six patients provided written consent. The Washington University Institutional Review Board approved this study. Patients were recruited via referrals from neurologists and physiotherapists, as well as via emails to the Washington University Research Participant Database. Informed consent and data collection took place at Washington University. Recruitment began 04/26/2018 and ended 03/01/2020. Data collection ended 03/18/2020. The authors confirm that all ongoing and related trials for this drug/intervention are registered. A cohort of twenty-six chronic stroke patients with upper limb hemiparesis who participated in a study of task-specific physical therapy (PT) training served as a comparison group. Data description is available in Lang et al. and Waddell et al.; **Table 3.1** presents summary demographics.[156,157]

Consented (n= 56)

Did not meet inclusion/
exclusion criteria (n= 20)

BCI Task screening
(n = 36)

Inconsistent EEG signal
generation (n = 6)

Withdrew prior to therapy
start (n= 2)

Initiated therapy
(n = 28)

Interrupted by COVID-19
pandemic (n= 11)

Discontinued intervention for
personal reasons (n = 4)

Discontinued by research
staff due to noncompliance
(n= 1)

Post-Therapy motor
evaluation and fMRI
scan (n= 10)

MRI Contraindication (n= 2)

Poor fMRI data quality (n= 2)

Analysis (n= 8)

Figure 3.1. CONSORT Recruitment and Attrition Flowchart. Fifty-six patients consented to participate. Thirty-six patients met criteria to perform BCI task screening. Twenty-eight patients initiated therapy. Ten patients completed therapy and performed final motor evaluations and MRI scans. Eight subjects passed quality assurance checks.

For analyses, comparison patients were split into therapy responders (PT-R, n = 12) and

nonresponders, (PT-NR, n = 14) based on whether they surpassed the minimal clinically

important difference (MCID) threshold of 5.7 points on the Action Research Arm Test

(ARAT).[158] The UEFM and ARAT measures are highly correlated.[159] Although each measure

scales similarly with improving motor function, direct statistical tests between motor outcomes

in the two groups are not appropriate due to the different designs of the tests. Specifically, The

UEFM is a measure of impairment while the ARAT is a measure of function.[158,160–164] Therefore,

the PT group is an appropriate comparison group for determining if functional imaging findings

in the BCI group reflect either non-specific changes due to a general increase in activity, or

changes that are specific to BCI training.

Table 3.1. Demographic Information.

Group	Age (y)	Time post-stroke (months)	Gender	Affected Limb	Motor Baseline (BCI: UEFM, PT: ARAT)	Motor Final (BCI: UEFM, PT: ARAT)	Motor Change (BCI: UEFM, PT: ARAT)
BCI (n=8)	58	62	4 F/8 M	5 R/3 L	21.75	30.5	7.25
PT Responders (n=12)	59	N/A	4 F/7M	10 R/2 L	37.5	43	8.5
PT Nonresponders (n=14)		N/A		9 R/5 L	32.5	30.5	1

Age and Gender for 3 nonresponders, Affected Limb for 2 nonresponders, and Time post-stroke
for all PT patients were unavailable.

3.2.2 EEG Screening

Patients performed an EEG screening task to identify a brain signal associated with motor

imagery of the affected hand from the contralesional hemisphere (i.e., the BCI control feature).

Patients had to generate the motor imagery EEG signal consistently for the BCI therapy task.

Initially, patients rested quietly for approximately 7 minutes during recordings of baseline EEG

activity. Patients then performed a series of paired trials of quiet rest and imagined movement of

their left, right, or both hands at the same time. Trial duration was 8 seconds with an inter-trial

interval of 3 seconds. A single EEG screening session included acquisition of approximately 45

trials of rest and each type of imagined hand motion. Patients had to avoid moving or talking

during EEG recordings. Screenings paused automatically for patients to rest in absence of a

specific task at 25% completion intervals for the full duration of the screening. Each patient

performed at least 2 screening sessions. A third session was necessary when detected feature

frequencies were erratic or EEG signal quality was low in a prior session. Excluded patients had

low quality EEG data in all screening sessions, showed no reliable feature frequency, or could

not regularly perform the BCI task.

3.2.3 BCI Feature Frequency

Control of the BCI device was through a 1 Hz wide feature frequency distinctly identified from

EEG screening data in each patient. The band-limited power of the feature frequency determined

whether the orthosis opened (decreased power) or closed (increased power) during BCI therapy.

A measure of the variance in each feature frequency from each patient was its coefficient of

determination (R^2), calculated from the difference in quiet rest and impaired hand imagery task

states in each screening session. Negative R^2 values indicated a power decrease during motor

imagery relative to rest. Selected from each patient were feature frequencies with the largest

negative R^2 value within mu or beta frequency bands (8-25 Hz) dependably produced across

screening sessions.

3.2.4 Intervention Protocol

The study timeline started with screening sessions over 1-2 weeks, followed by pre-therapy

motor assessments and resting-state fMRI (**Fig. 3.2A**). Next, patients trained to use the BCI

device. They subsequently received a complete set of equipment to use at home. Patients then

performed 12 weeks of home BCI therapy sessions, when they used the equipment for 1 hour per

day, 5 days per week. The assigned therapy sessions totaled 60 hours. Although all patients were assigned the same amount of BCI therapy, usage varied among patients. Therapy dosage for BCI patients was estimated by summing the number of runs with at least 10% accuracy on both movement imagery and rest trials. Five BCI runs were approximately one hour of therapy. Patients either performed the therapy and device setup alone or with a caretaker based on their specific needs and living situation. Members of the research team were available via phone and email to assist with technical issues. Excluded from the study were patients unable to use the BCI device. Patients had to enter their usage on a provided tracking sheet, which assisted them in documenting therapy times and any problems experienced with the equipment. Clinicians assessed motor function once per month (**Fig. 3.2A**). After 12 weeks of BCI therapy, patients received a post-therapy motor assessment and second resting-state fMRI scan. Patients in the comparison group received intensive physical therapy in an 8-week task-specific training program.

The comparison group intervention is described in detail in a previous study.[156] Briefly, chronic hemiparetic stroke patients were assigned to groups with varying therapy intensities quantified by repetitions per 1-hour session. These PT patients attended 4 sessions per week for 8 weeks. Specific actions during therapy were selected by therapists based on the ability level of each patient. Therapy activities engaged patients in reaching, grasping, manipulating, and releasing components.
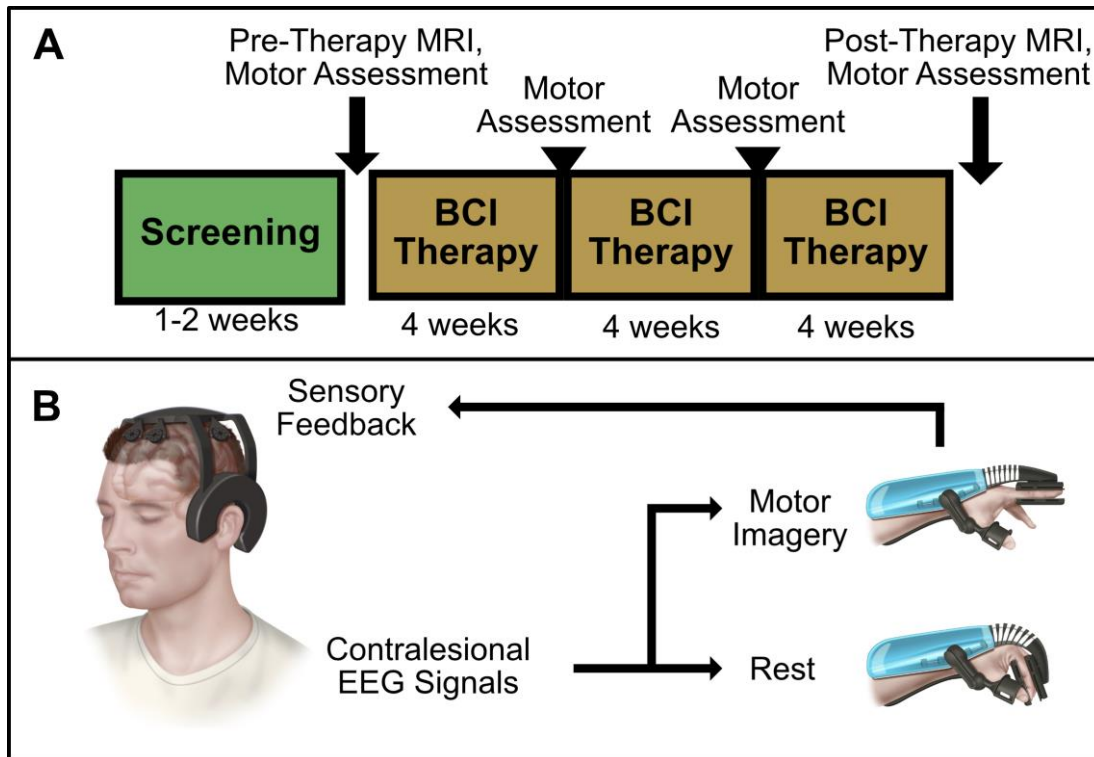
Figure 3.2. BCI Intervention Protocol and System Design Overview. A) Protocol Timeline. Screening for EEG feature frequency and inclusion and exclusion criteria occur over several sessions in a 1-2 week period. Following screening, patients undergo an MRI scan and motor assessments before receiving their BCI device. Patients perform BCI therapy for 12 weeks at home, returning every 4 weeks for motor assessments. A final MRI scan and motor assessment is performed after 12 weeks of therapy. **B)** BCI System Design.

3.2.5 BCI System Design

Components of the BCI system included a motorized hand orthosis and wireless EEG headset

with dry, active electrodes (**Fig. 3.2B**). A Windows tablet connected via bluetooth to the EEG

headset to record signals from the electrodes. A local Wi-Fi network generated within the

orthosis supported communications between the tablet and a computer within the orthosis. The

computer controlling orthosis received commands to open or close the hand via the tablet

through these communications.

BCI therapy sessions involved multiple steps: (1) Patients put on the BCI headset and hand

orthosis, turned on system components, and confirmed correct communications through a series

26

of automated test outputs. (2) Next, signal quality assessments involved comparing low amplitude rest signals to noisy signals activated by jaw clenches. The tablet informed patients of obtained signal quality. When signals were too noisy, patients could improve electrode connections by manually adjusting the headset and electrodes to facilitate contact with the scalp, rotating electrodes to push through hair, and waiting for a gradual decline in dry electrode impedance. Therapy did not proceed until signal quality improved with a subsequent assessment. (3) Patients began the BCI therapy task following a one-minute recording of an at-rest signal and 8 repetitions each of quiet rest and motor imagery trials. These recordings enabled threshold adjustments for orthosis control for each session. During therapy, patients received a cue to remain quietly at rest or perform vivid motor imagery of their affected hand. Analysis of EEG signals acquired during BCI therapy extracted the band-limited power of the patient-specific contralesional BCI feature frequency. The hand orthosis opened in a 3-point grip (**Fig. 3.2B**, upper right) after power of the feature frequency dropped below the threshold. The orthosis remained closed at higher feature frequency power levels (**Fig. 3.2B**, lower right). Patients received an instruction to attempt opening the orthosis by thinking about moving during motor imagery trials, and kept the hand closed by clearing their thoughts during rest trials. Patients thereby received proprioceptive and visual sensory feedback from the orthosis based on the EEG signals they generated. Individual trials lasted 8 seconds followed by a 3-second inter-trial interval.

3.2.6 Motor Function Assessment

The upper extremity portion of the Fugl-Meyer Assessment functioned as the primary motor outcome due to its wide use and high inter- and intra-rater reliability.[165–167] UEFM is a 66-point measurement of reaching and grasping ability with several hand orientations and ranges of

motion. Secondary outcomes included grip strength, Motricity Index, Modified Ashworth Scale (MAS), and Arm Motor Ability Test (AMAT). Motor function assessment to establish a stable baseline occurred twice before commencing therapy. Baseline motor function was the average of two assessments (pre_1 and pre_2). Further assessments occurred at 4-week intervals during therapy, and at 6-months post-therapy completion. Calculation of motor improvement followed the formula:

$$UEFM_{post} - \frac{UEFM_{pre_1} + UEFM_{pre_2}}{2} , \qquad (3.1)$$

 i.e., the post-therapy motor function score minus the average of the baseline motor function scores. Occupational and physical therapists assessed motor function. Motor function assessments for the comparison group data ensued before and after an 8-week course of task-specific training using the ARAT, a validated and widely used 57-point measure of upper motor function.[160,168] The UEFM and ARAT measures are highly correlated in their estimates of initial impairment and motor function change during therapy.[159,164]

3.2.7 MRI Acquisition Protocol

MRI scans with a Siemens Prisma 3T scanner included structural images from T1-weighted MP-RAGE, T2-weighted fast spin echo, and fluid attenuation inversion recovery (FLAIR) sequences. Scanning sessions occurred within 2 weeks of initiating and completing the 12-week therapy protocol. Capture of BOLD signals for resting-state data utilized a 64-channel head coil and a gradient echo EPI sequence (voxel size = 2.4 x 2.4 x 2.4 mm; TR=1070 ms; TE=30 ms; flip angle = 70°; multi-band factor 4). Each of three, approximately 7-minute scans collected 400 frames of resting-state functional MRI data, for a total of 1200 frames over 21 minutes. We acquired distortion maps immediately prior to each resting-state BOLD scan.

Comparison group MRI scans included similar T1- and T2-weighted structural images with a

Siemens TRIO 3T scanner. Resting state BOLD data acquisition included the following

parameters: 4 mm isotropic voxels; TR = 2000 ms; TE = 27 ms; 12 channel head coil; 4 scans

with 128 frames each.

3.2.8 MRI Preprocessing

A previously described pipeline preprocessed all functional MRI data.[169] The 4dfp suite

(4dfp.readthedocs.io) of preprocessing steps comprised slice-time correction, removal of odd-

even slice intensity differences, rigid body motion correction, affine transformation to a $(3 \text{ mm})^3$

atlas space, spatial smoothing with a 6 mm FWHM Gaussian kernel, voxelwise linear

detrending, and a temporal low pass filter (0.1 Hz cutoff). Freesurfer software performed cortical

surface segmentation. Regression of nuisance waveforms, derived from motion correction

timeseries, CSF signal, white matter signal, and the whole brain ("global") signal, reduced

spurious variance.[170,171] High-motion frames were removed from the analysis.[169] Fisher z-

transforms were applied to Pearson correlation coefficients prior to statistical analysis.

3.2.9 Seed-Based Functional Connectivity Calculations

Analysis of preprocessed MRI data utilized MATLAB (MathWorks, Natick, MA) unless

otherwise noted. Cortical regions, previously implicated in motor control served as *a priori*

regions of interest (ROIs), included the hand region of bilateral primary dorsal motor cortex

(M1), dorsal premotor area (PMA), and supplementary motor area (SMA). We used

Neurosynth.[172] for all ROI coordinates. Peak Z-scores for each ROI served as centers for 8mm

diameter spheres. Extracted mean BOLD timeseries were from each ROI. Generation of two

aggregate cerebellum (CBL) ROIs were from somatomotor regions in anterior CBL lobules.

Separately averaged left and right CBL somatomotor regions formed the basis of left and right

CBL mean timeseries.[173] Then, labelling these left and right side timeseries as contralesional and ipsilesional was relative to the left/right stroke brain location. Cerebellar laterality was in correspondence to motor network membership (i.e., left cerebellum and right primary motor cortex were in the same functional hemisphere). Excluded ROIs overlaid the stroke lesion. Analyses were of functional connectivity, defined as the Pearson correlation of paired mean ROI timeseries and between select ROIs and all other voxels in the brain. Pre- and post-therapy connectivity differences indicated changes in functional connectivity.

3.2.10 Functional Connectivity Analyses

A twofold focus of the functional connectivity analysis was: 1) define changes in cortical and subcortical connectivity topography and 2) define alterations in magnitude of connectivity in known motor network ROIs. For network topography, primary analyses performed on fMRI data included voxel-based functional connectivity between ROI in contralesional M1, ipsilesional M1, contralesional CBL, and ipsilesional CBL and the rest of the brain. Findings assessed connectivity changes at specific ROIs following BCI therapy. We examined only statistically significant functional connectivity maps by applying a threshold of $z = 0.3$. Obtained maps were from pre- and post-therapy timepoints in BCI patients and PT responders. Counts of suprathreshold voxels in each connectivity map tracked spatial distributions for pre- and post-therapy MRI scans. Voxel counts were from the whole brain and each hemisphere. Wilcoxon signed-rank tests compared pre- and post-therapy timepoints for whole-brain voxel counts. Timepoints here refers to MRI scans at baseline before any therapy (pre-therapy) and after 12 weeks of therapy for BCI patients or 8 weeks for PT patients (post-therapy). Suprathreshold voxel counts for each patient and ROI evaluated relationships between functional topography plasticity and motor recovery. The subtraction of pre- from post-therapy voxel counts quantified

changes. Spearman rank correlations estimated the relationship between motor recovery and change in number of suprathreshold voxels.

Evaluations of motor network connectivity changes following therapy relied on assessments of network strength through pairwise functional connectivity (FC) measurements between ROIs. Median adjacency matrices generated from Pearson correlation coefficients between each ROI pair visualized FC strength in the pre-therapy state as well as changes in FC following therapy. Adjacency matrices were converted into circular graphs for visualization using the Python NetworkX package.[174] Circular graph nodes were per ROI. Color of edges (lines) connecting nodes mark the z-score value of Pearson correlations (i.e., connectivity strength).

Pairwise connectivity measurements were grouped into the following subsets: all motor ROI pairs, interhemispheric ROI pairs contralesional intrahemispheric pairs, and ipsilesional intrahemispheric pairs. Interhemispheric ROI pairs indicated FC strengths between contra- and ipsilesional ROIs. For each ROI pair within these groupings, FC strengths across all cases were combined into distributions showing the proportion of each FC strength value at pre- and post-therapy timepoints. Similarly, distributions of all FC z-values for each ROI pair and per patient showed individual differences in changed FC strengths between pre- and post BCI therapy. Wilcoxon signed-rank tests assessed differences between pre- and post-therapy FC strength distributions relative to the number of correlation z-scores of a given magnitude. The formula listed below estimated the Wilcoxon signed-rank effect sizes:

$$r = Z/\sqrt{N}, \tag{3.2}$$

with r the effect size, Z the signed-rank test Z-statistic, and N the sample size. The Spearman rank correlation between Wilcoxon effect sizes and increases in UEFM scores examined the relationships between FC change and motor recovery.

31

3.3 Results

3.3.1 Motor Rehabilitation

All BCI patients showed an increase in UEFM score after 12 weeks of contralesional BCI

therapy. Clinically meaningful recovery occurred in seven of the eight patients who reached a

minimal clinically important difference (MCID) threshold of at least a 5.2 point score

increase.[175] Median increase in UEFM score was 7.25. **Figure 3.3** illustrates progressive

longitudinal motor recovery from baseline in each case. Most patients passed the clinically

significant threshold by 8 weeks. Wilcoxon signed-rank test also found significant improvement

($p < 0.05$) in grip strength, Motricity Index score, and AMAT scores (see Supplemental Material

for more detail). Median changes included increased grip strength (3.75 pounds, $p = 0.0234$),

Motricity Index (2 points, $p = 0.0156$), and AMAT (5 points, $p = 0.0156$). The Modified

Ashworth Scale, a measure of spasticity, showed median changes of 0 at the elbow and 0.125 at

the wrist. No MCID comparisons were available for these measures. **Figure 3.4** compares

baseline and final motor recovery scores in patients receiving BCI and PT therapies, with lines

indicating each patient. Patients who reached the MCID for the UEFM or ARAT are marked

with red, while those who did not reach clinically significant recovery are marked with gray.

Initial impairment relative to the range of each measure scale is similar between groups. Median

baseline UEFM scores of patients who completed the study (Baseline = 21.75) and those who

were not included in the final analysis (Baseline = 22) were similar.
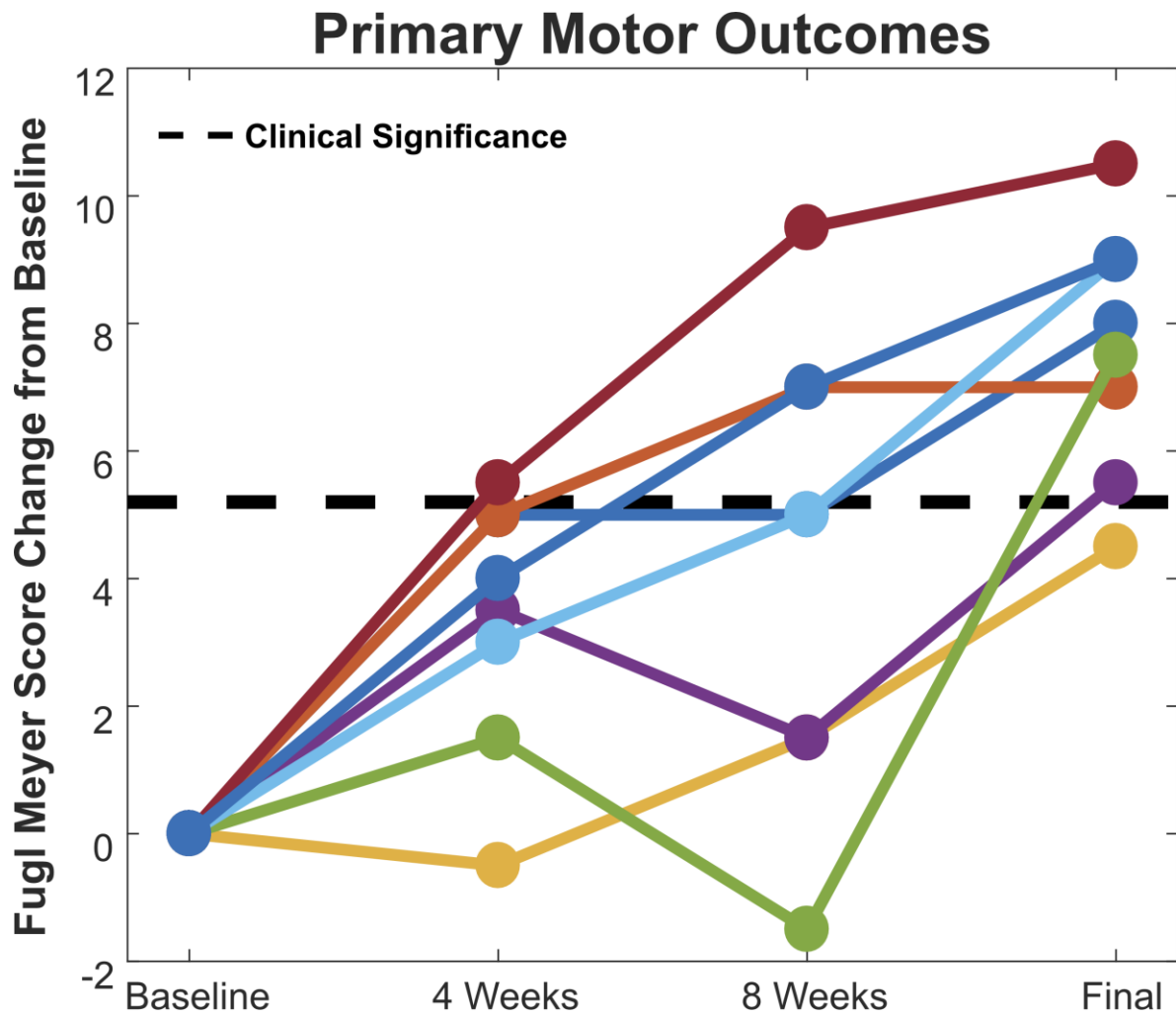
Figure 3.3. Longitudinal BCI Primary Motor Outcomes. Longitudinal change in UEFM score from baseline. Each patient represented as a different line color. Dotted black line indicates minimal clinically important difference of 5.2 points on the UEFM.

Dosages of therapy between the BCI and PT groups were similar despite the different intervention periods. BCI patients received a mean therapy dosage of 29.2 hours compared to a flat 32 hours for PT patients (**Figure 3.S3**).
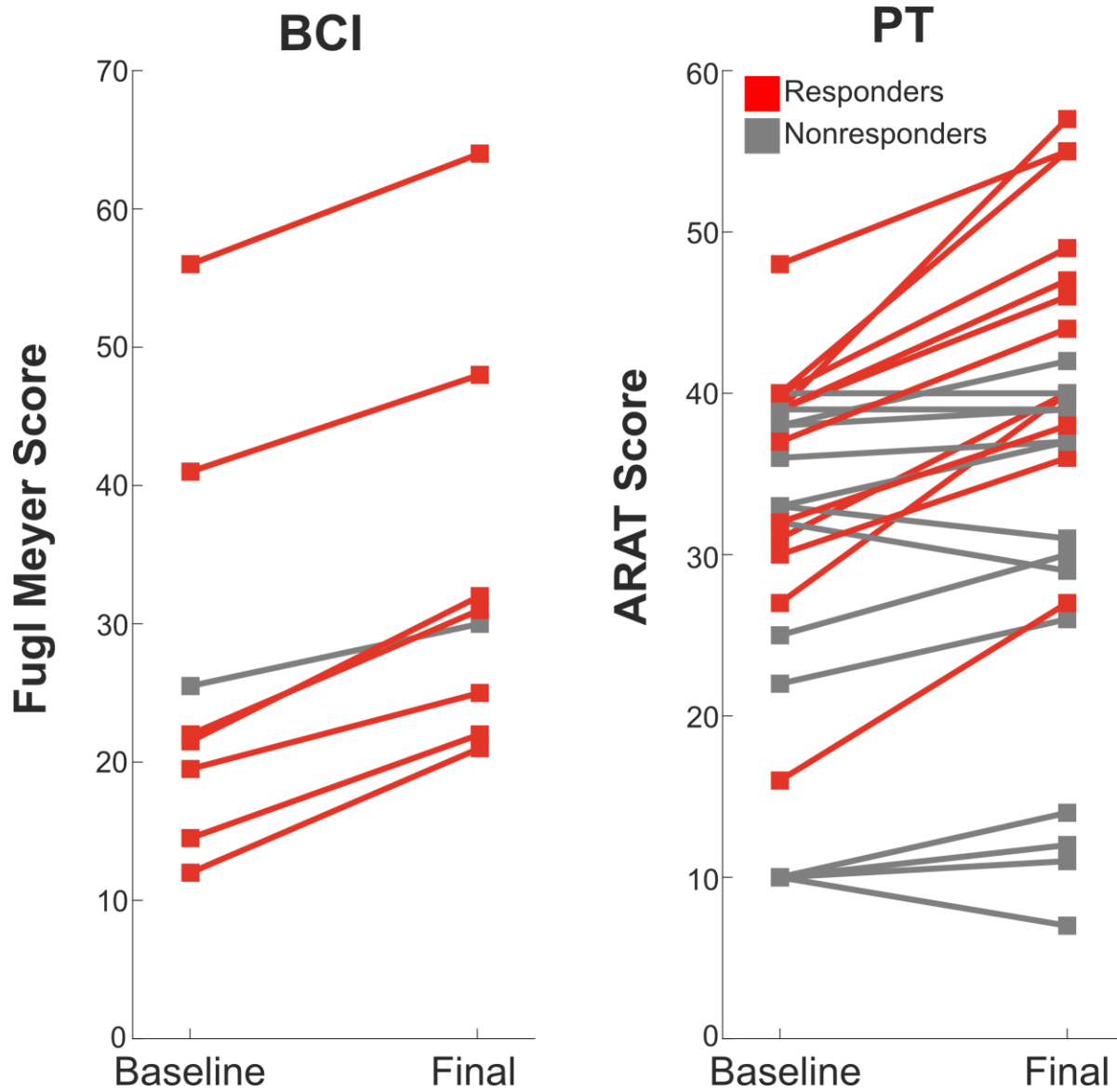
Figure 3.4. Comparison of Motor Recovery Between Cohorts. Upper motor function change from pre- to post-therapy in BCI patients (**A**) and PT patients (**B**). BCI recovery was measured with UEFM score, and PT recovery was measured with ARAT score. Red markers indicate therapy responders, and gray markers indicate nonresponders.

3.3.2 BCI Performance

Patients generally used their BCI systems effectively, achieving median move and rest success rates of 78.5% and 35%, respectively. A definition of a successful trial was reaching the BCI activation threshold for at least 1 second for move trials or staying under the activation threshold for the entire trial duration for rest trials. Most patients showed greater success rates with movement imagery trials due to restrictive criteria for success on rest trials. Although we accepted feature frequencies in both alpha (8-12 Hz) and beta (13-25 Hz) bands, six out of eight patients had beta feature frequencies. **Table 3.2** contains BCI performance data including feature frequencies, trial success rates, signal error (Sum of Squares), and coefficients of determination (R^2).

Table 3.2. BCI Performance Data.

Subject	Move Success Rate (%)	Rest Success Rate (%)	Move Error (SS)	Rest Error (SS)	R^2	Total Sessions	Total Trials	Feature Frequency (Hz)
1	84	15	3.7	2.7	0.089	47	6120	21
2	49	48	3.9	4.1	0.102	62	9660	15
3	34	60	2.8	2.8	0.089	19	2790	19
4	92	23	3.6	3.8	0.256	50	8250	15
5	73	37	3.1	3.2	0.239	61	9750	16
6	31	62	4.7	4.9	0.128	29	3690	11
7	**96**	**33**	**18.5**	**4.1**	**4.145**	**86**	**9420**	**10**
8	**91**	**22**	**18.5**	**3.3**	**3.341**	**26**	**3090**	**18**

SS: Sum of Squares, R^2: Coefficient of Determination, Bold denotes updated hardware algorithm which changes estimation of error and R^2.

3.3.3 Spatial Distributions of Voxel-Based Functional Connectivity in Select ROIs

BCI therapy induced changes in spatial connectivity patterns in contralesional and ipsilesional primary motor cortex and cerebellum from pre- and post-therapy in group average functional connectivity maps (z > 0.3), as shown in **Figure 3.5**. Qualitatively, contralesional and ipsilesional M1 (**Fig. 3.5A,B**) and cerebellar (**Fig. 3.5C,D**) ROIs showed decreased spatial distributions functional connectivity voxels post therapy (**Fig. 3.5A-D**). Smaller extents of functional connectivity appeared especially in ipsilesional M1 (**Fig. 3.5B**) and contralesional cerebellum (**Fig. 3.5C**).
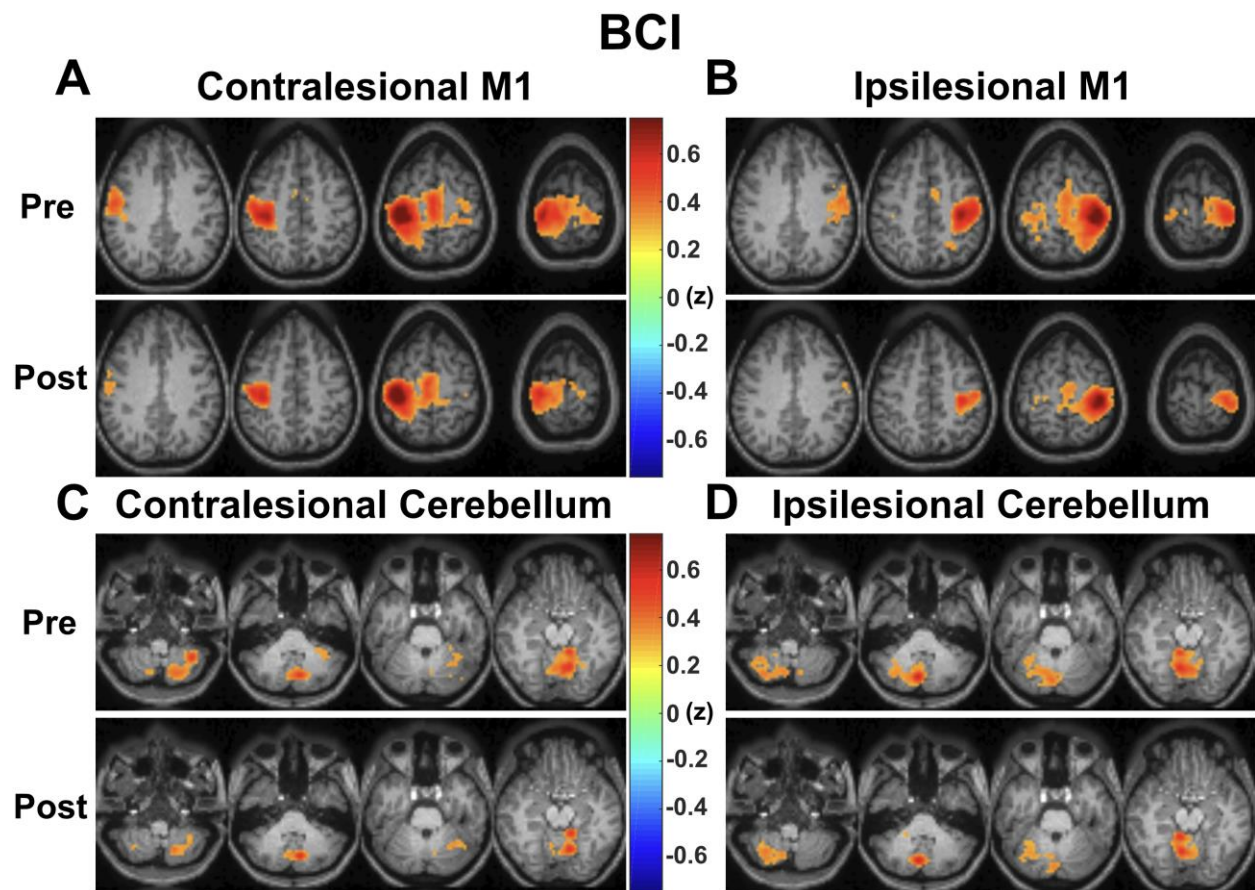
Figure 3.5. Spatial Connectivity Distributions Change Following BCI Therapy. Pre- and post-therapy maps of group average voxelwise functional connectivity (z > 0.3) are shown for contralesional M1 (**A**), ipsilesional M1 (**B**), contralesional cerebellum (**C**), and ipsilesional cerebellum (**D**). Pre-therapy maps are shown above their post-therapy equivalents.

Figure 3.6 shows changes in topographic connectivity extent for PT responders using the same set of four ROIs. Little to no change occurred in the topographic extent of connectivity to any PT group ROIs.
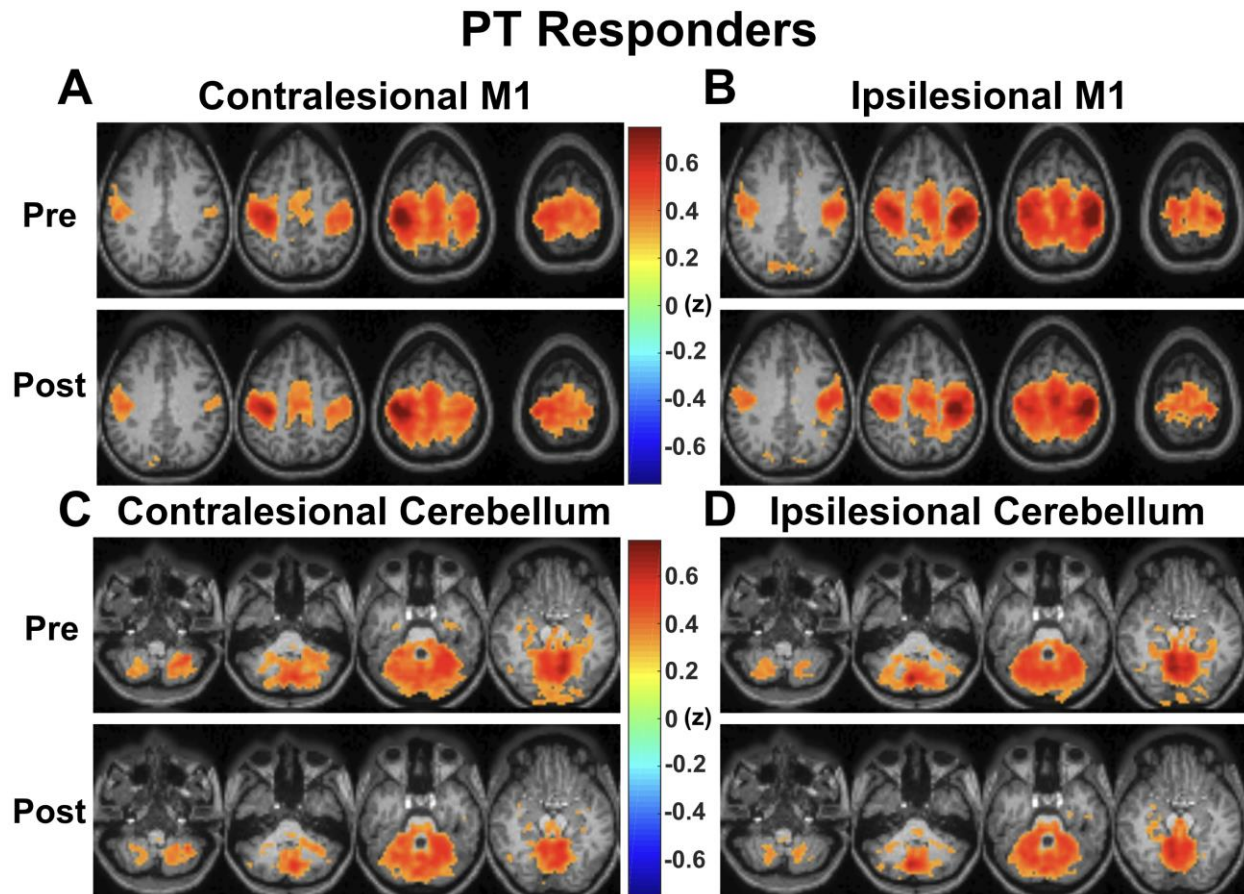
Figure 3.6. Spatial Connectivity Distributions in Physical Therapy Responders. Pre- and post-therapy maps of group average voxelwise functional connectivity (z > 0.3) are shown for contralesional M1 (**A**), ipsilesional M1 (**B**), contralesional cerebellum (**C**), and ipsilesional cerebellum (**D**). Pre-therapy maps are shown above their post-therapy equivalents.

Quantitatively, suprathreshold voxel counts significantly decreased for ipsilesional M1 following BCI therapy (**Fig. 3.7B**, Wilcoxon signed-rank test, $p = 0.0156$). Differing MRI acquisition

parameters between BCI and PT patients prevented direct statistical comparisons. To compare

relative changes between the two cohorts, we normalized suprathreshold voxel count changes as

a difference relative to baseline for each patient and measurement. Normalized changes for each

ROI and each patient group are shown in **Figure 3.7**. Suprathreshold voxel counts to ROIs in PT

responders and non-responders showed no statistically significant differences. Box and-whisker

plots of pre- and post-therapy counts of voxels surpassing the functional connectivity statistical

significance threshold ($z > 0.3$) show decreased variance following BCI therapy, but not

following PT (**Fig. 3.S4**). No statistically significant correlations were observed between voxel

count changes and motor recovery in BCI or PT patients (**Fig. 3.S5-S7**).
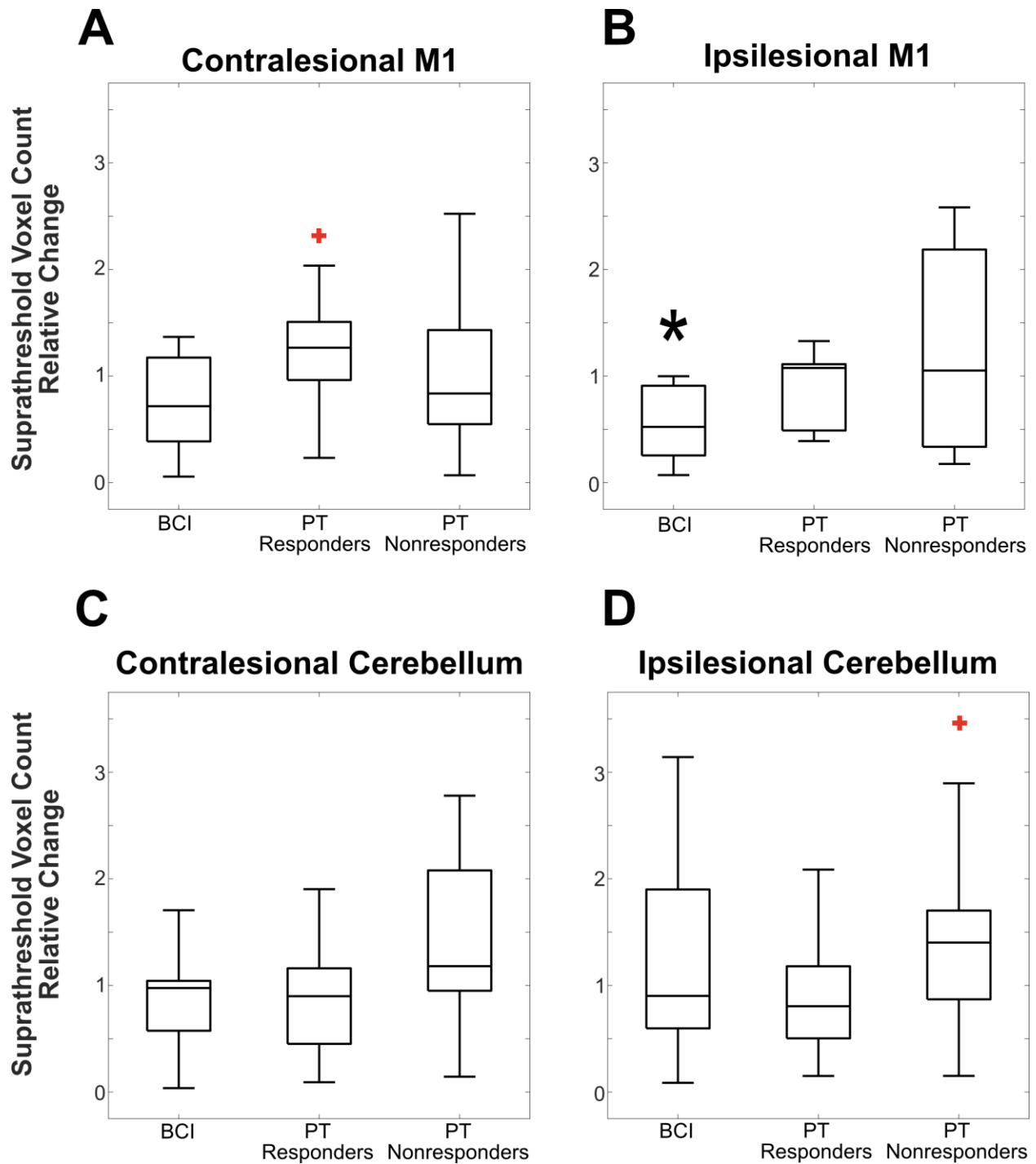
Figure 3.7. Normalized Voxel Count Changes in Select ROIs. Difference relative to baseline for the number of voxels with statistically significant functional connectivity (z > 0.3) to contralesional M1 (**A**), ipsilesional M1 (**B**), contralesional cerebellum (**C**), and ipsilesional cerebellum (**D**) in chronic stroke patients pre- and post-therapy for BCI therapy groups and PT responders and non-responders. Box-and-whisker plots indicate median values. Red markers indicate outliers. Value of 1 indicates no change. **A, C, D)** No statistically significant differences

observed. **B)** The post-BCI therapy timepoint showed a statistically significant reduction in number of suprathreshold voxels compared to the pre-therapy timepoint with a Wilcoxon signed-rank test (p = 0.0156).

3.3.4 ROI-ROI and Interhemispheric Connectivity

Circular graph representations show median functional connectivity strengths pre-therapy for

contra- and ipsilesional ROIs, based on z-scores of Pearson correlations between paired ROI

nodes (**Fig. 3.8A,B**). Strong connectivity strengths (z > 0.6) characterized links between cortical

motor ROI with connections located entirely contralesional or ipsilesional and most

interhemispheric links (**Fig. 3.8A**). Relatively weaker connectivity strengths (z < 0.5) occurred

between interhemispheric CBL and motor ROIs (e.g., cSMA to iPMA or iM1; cM1 to iM1 or

iPMA). Generally, many nodes showed connectivity above the threshold to other motor ROIs, an

expected feature of the motor network. Median connectivity strength pre-therapy PT responders

was similar in structure and magnitude of connectivity (**Fig. 3.8B**). All suprathreshold

connectivity changes in BCI patients were negative from pre- to post-therapy timepoints,

regardless of whether paired ROI were contralesional, ipsilesional or interhemispheric and

irrespective of whether interhemispheric ROI matched. (**Fig. 3.8C**). Not shown are median

connectivity changes of |z| < 0.1. PT responders showed changes over time surpassing the |z| <

0.1 threshold in only three ROI pairs. Two of these correlations were negative (both to

ipsilesional PMA), while one was positive (contralesional M1 to contralesional CBL) (**Fig.

3.8D**).
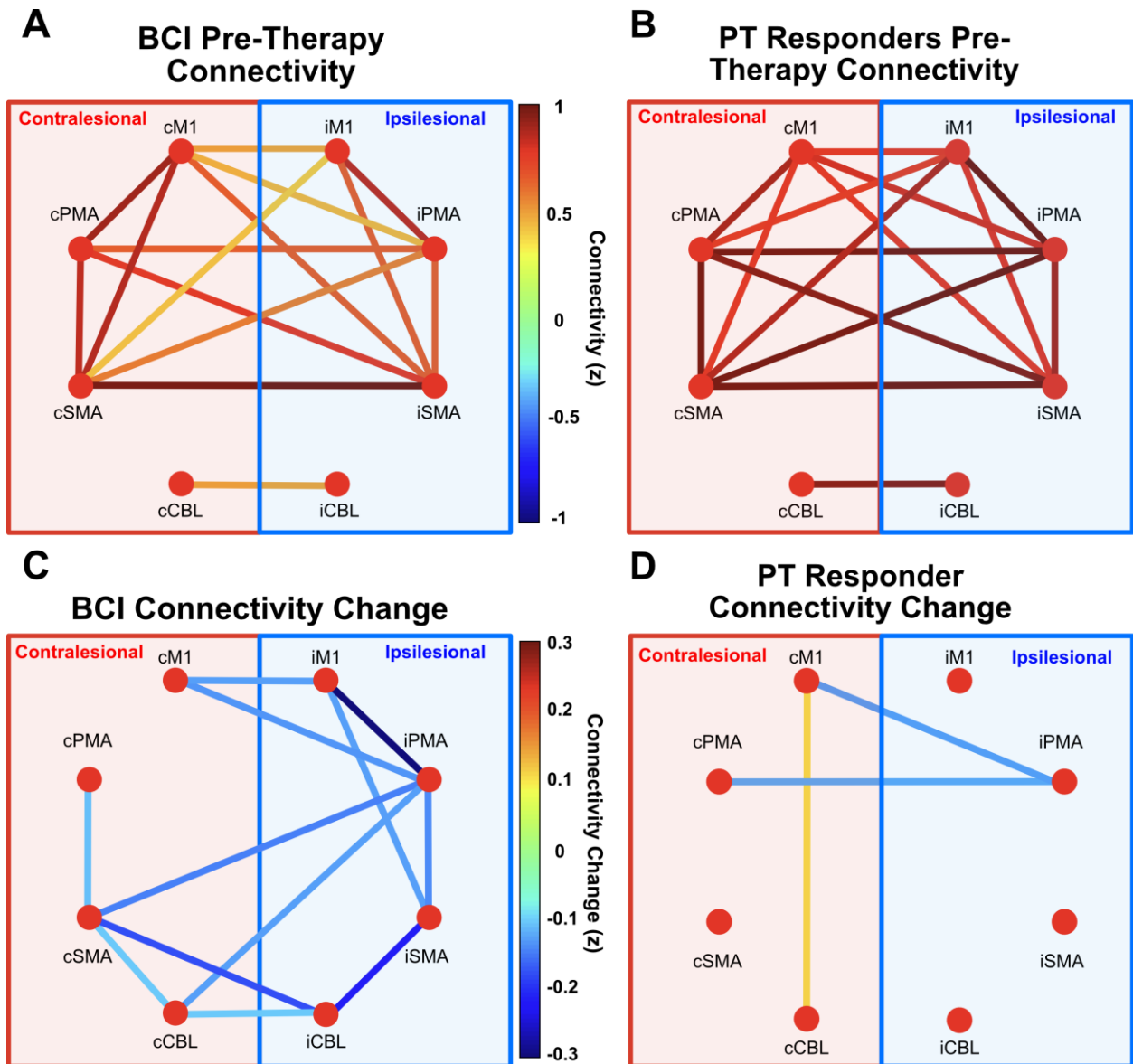
Figure 3.8. Functional Connectivity Changes in Motor Regions. A, B) Median pre-therapy functional connectivity between motor ROI pairs in BCI patients (**A**) and PT responders (**B**). Primary motor, premotor, supplementary motor, and cerebellar ROIs used. Each node marks an ROI with a prefix specifying laterality (e.g. cSMA is contralesional supplementary motor area). Nodes in red and blue background areas are contralesional and ipsilesional ROIs, respectively. Line color indicates connectivity strength. Threshold of $z = 0.3$ applied to connectivity graph. **C, D)** Median change in connectivity from pre-therapy to post-therapy timepoints (post − pre) in BCI patients (**C**) and PT responders (**D**). Threshold of $z = 0.1$ applied to connectivity graph.

Functional connectivity strength in BCI patients was significantly lower post-therapy compared to pre-therapy. Normalized distributions of functional connectivity strengths are shown in **Figure 3.9**. The analysis included all ROI pairs regardless of a threshold of $z > 0.3$ for results shown in Fig. 5. A Wilcoxon signed-rank test found statistically significant decreases from pre- to post-therapy timepoints across all motor ROIs and patients ($p = 1 \times 10^{-6}$), all interhemispheric motor ROI ($p = 0.006$), all ipsilesional intrahemispheric ROI pairs (**Fig. 3.9D**, $p = 0.003$), but not any contralesional intrahemispheric ROI pairs (**Fig. 3.9C**, $p = 0.071$). These results showed contralesional BCI therapy significantly decreased motor network connectivity strength, regardless of hemisphere in relation to stroke location. Results from PT responders analyzed similarly found no evidence of motor connectivity change (**Fig. 3.10**). Pre-therapy distributions in PT responders were qualitatively similar to those in pre-therapy BCI patients. Pre- and post-therapy distributions in PT responders also revealed no statistically significant changes in Wilcoxon signed-rank tests (and non-responders, **Fig. 3.S10**).
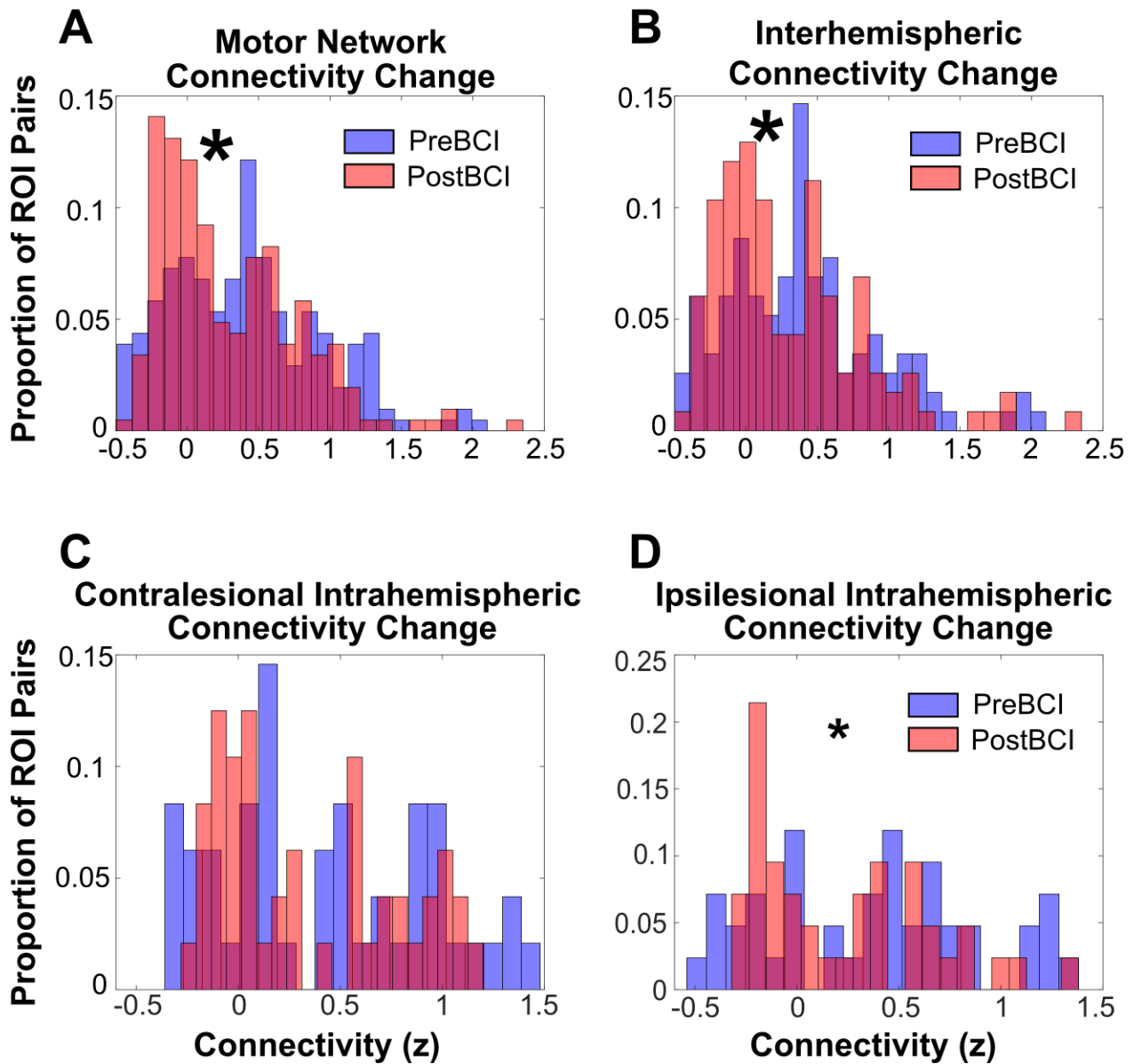
Figure 3.9. Motor Connectivity Decreases Following BCI Rehabilitation. Histograms constructed from motor ROI sets across all BCI patients at pre-therapy (blue) and post-therapy (red) timepoints. Overlapping histograms shown in purple. Histograms displays the normalized distribution of Z-transformed functional connectivity. ROI sets include all motor ROI pairs (**A**), interhemispheric ROI pairs (**B**), contralesional intrahemispheric ROI pairs (**C**), and ipsilesional intrahemispheric ROI pairs (**D**). Decreased post-therapy motor FC is statistically significant via Wilcoxon signed-rank test for full motor ROI set ($p = 1 \times 10^{-6}$), interhemispheric ROI set ($p = 0.006$), and ipsilesional intrahemispheric ROI set ($p = 0.003$). Contralesional intrahemispheric connectivity decreased, but this change was not statistically significant ($p = 0.071$).
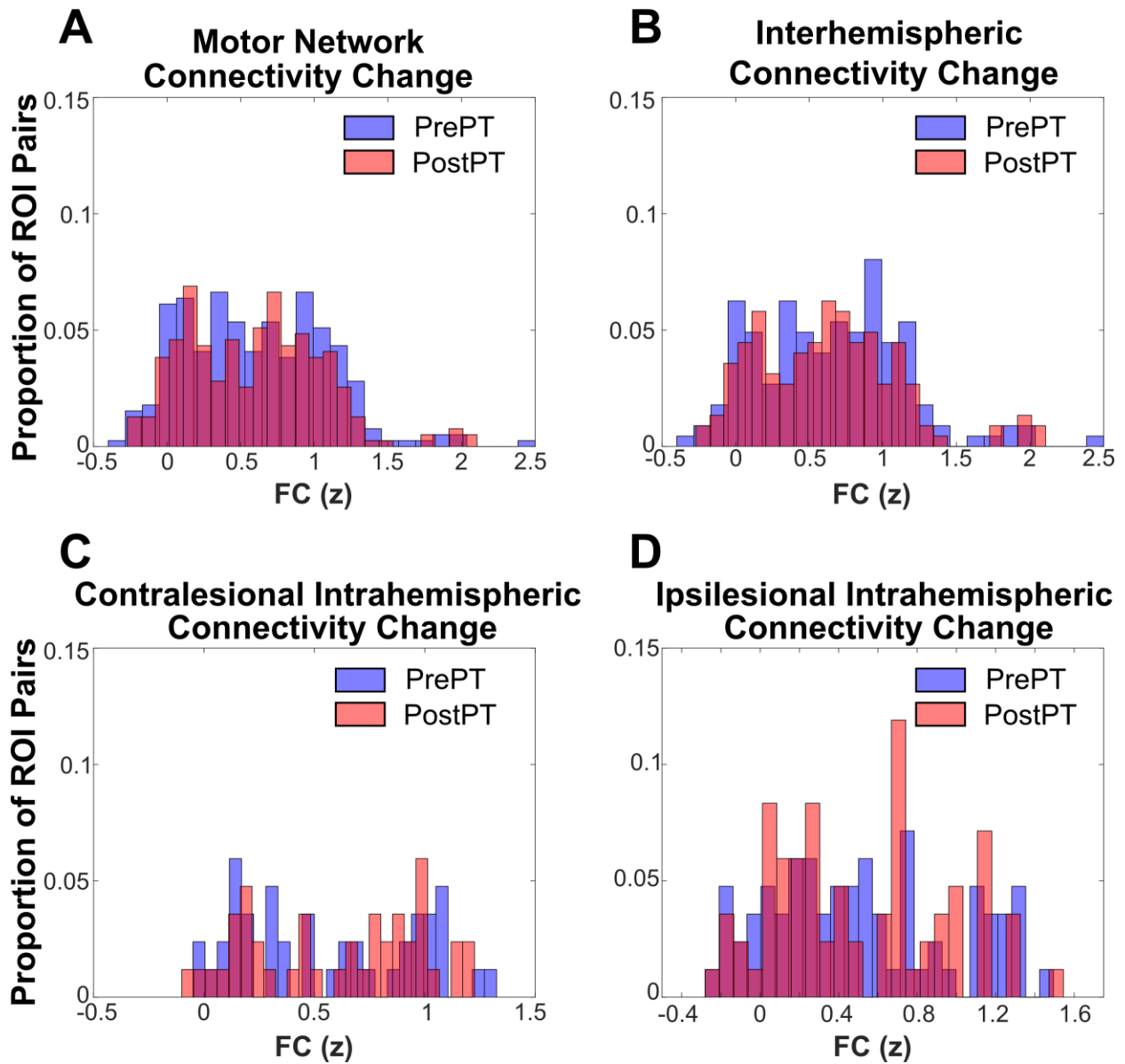
Figure 3.10. Motor Connectivity Distributions in PT Responders. Histograms constructed from motor ROI sets across PT responders at pre-therapy (blue) and post-therapy (red) timepoints. Overlapping histograms shown in purple. Histograms displays the normalized distribution of Z-transformed functional connectivity. ROI sets include all motor ROI pairs (**A**), interhemispheric ROI pairs (**B**), contralesional intrahemispheric ROI pairs (**C**), and ipsilesional intrahemispheric ROI pairs (**D**). No distributions showed statistically significant change over time.

A key issue was whether motor recovery corresponded with decreases in motor connectivity. A nonparametric rank correlation analysis sorted patients by change in FC strength and extent of motor recovery. The analysis found that larger decreases in motor FC strength correlated with greater motor recovery (**Fig. 3.11A** r = 0.77, p = 0.033). These significant findings indicated motor rehabilitation through contralesional BCI therapy resulted in decreased overall motor intra-network functional connectivity. No other ROI sets showed connectivity changes correlated with recovery (**Fig. 3.11B-D**).
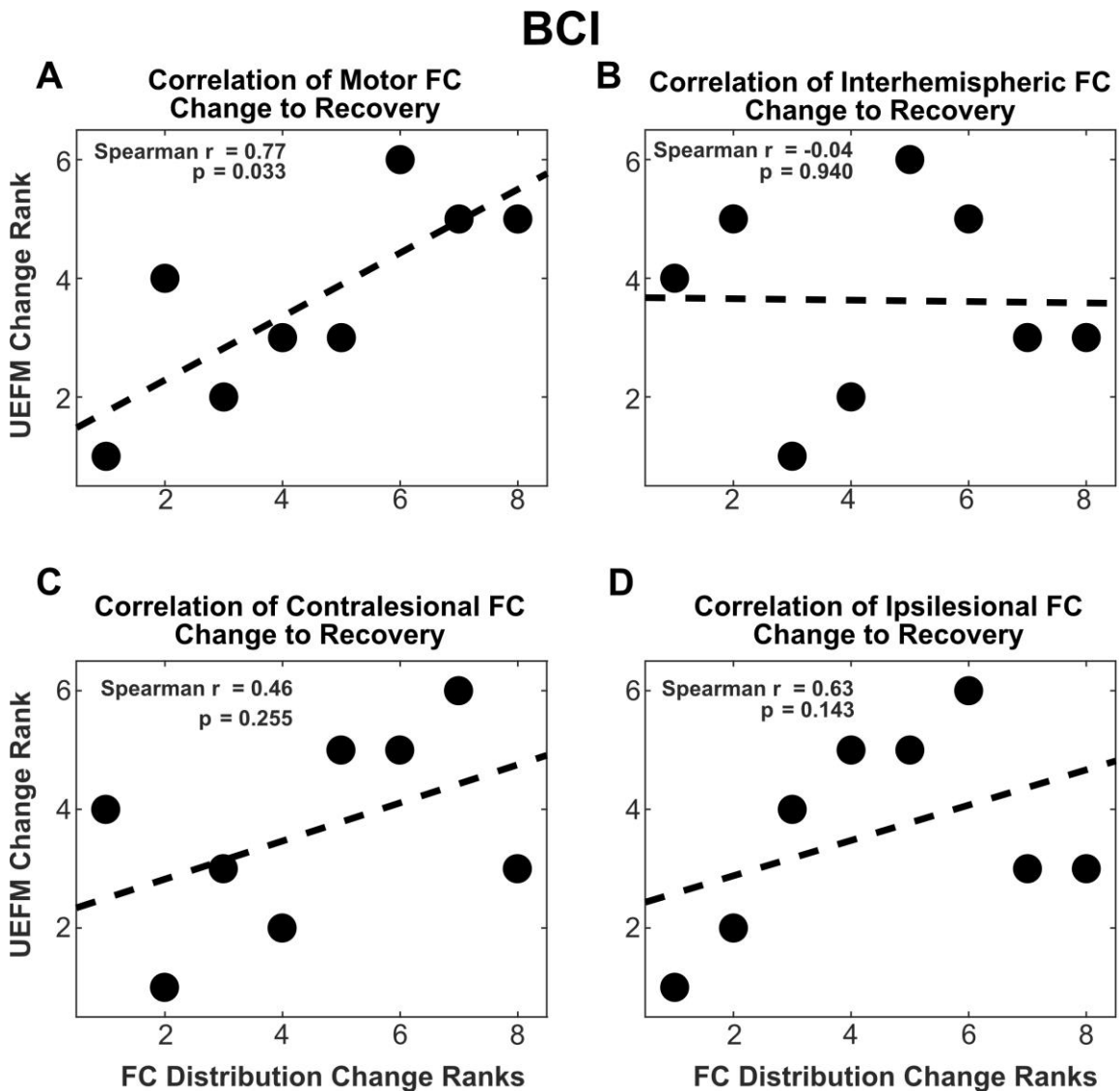
Figure 3.11. Correlation Between Connectivity Change and BCI Motor Recovery. Spearman correlations between motor ROI connectivity change and motor recovery. Data represented in ranked form. The dotted line represents a least-squares regression fit onto the ranked data. Connectivity change in four ROI sets measured as shown in **Figure 3.8**. The correlation between connectivity change in all motor ROIs and motor recovery was statistically significant.

There was no finding of functional connectivity changes in PT responders (or nonresponders,

Fig. 3.S11) showing statistically significant correlations with motor recovery in any motor

network ROI sets (**Fig. 3.12**).
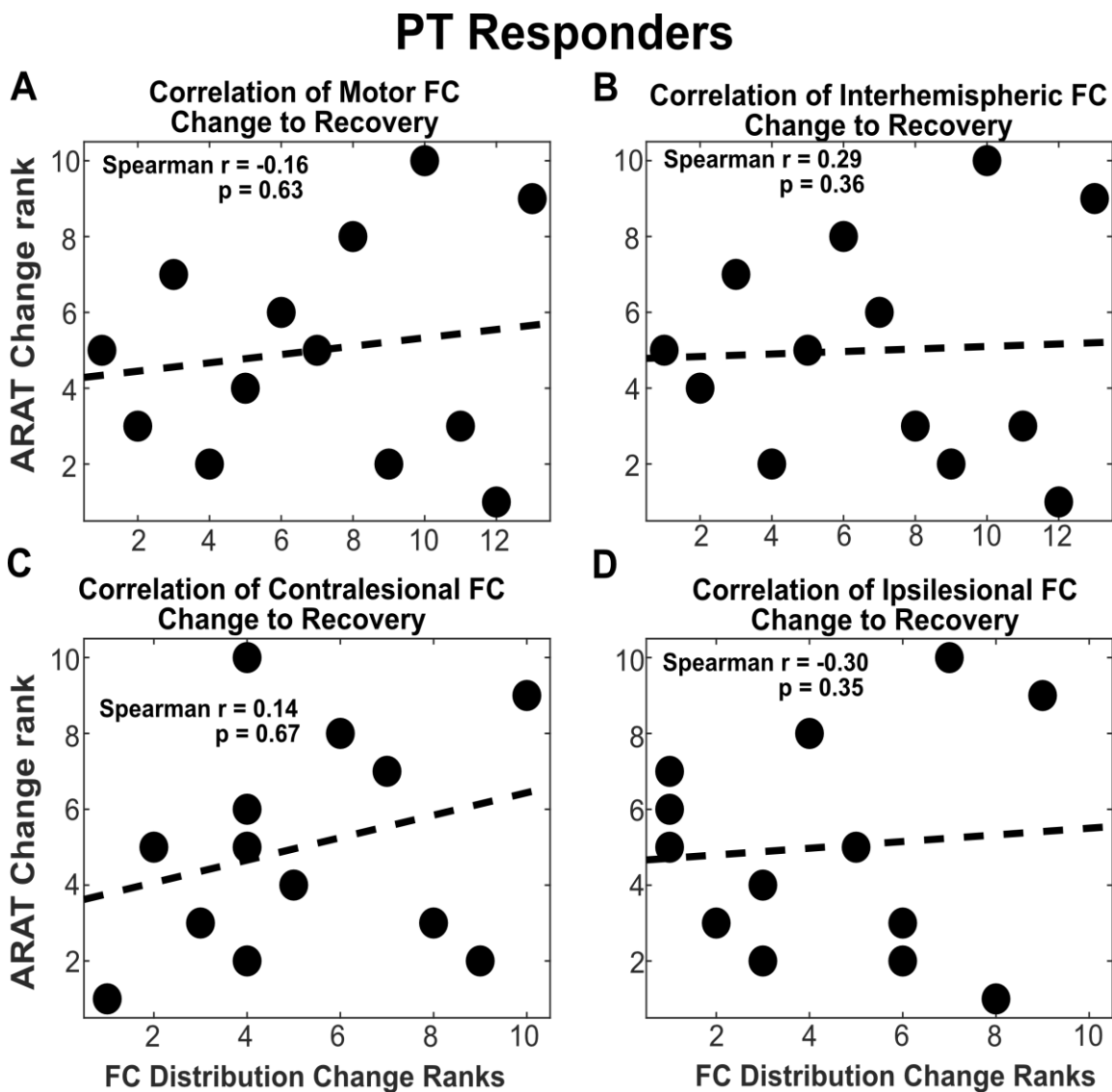
Figure 3.12. No Correlation Between Connectivity Change and PT Motor Recovery. Spearman correlations between motor ROI connectivity change and motor recovery. Data represented in ranked form. The dotted line represents a least-squares regression fit onto the ranked data. Connectivity change in four ROI sets measured as shown in **Figure 3.9**. No correlations were statistically significant.

3.4 Discussion

Upper extremity motor function improved in a chronic stroke population following 12 weeks of training with a noninvasive, contralesionally-controlled brain-computer interface. Decreases in functional connectivity strength and topography in motor cortex ROIs were concurrent with upper limb motor improvements. Reductions in topographic connectivity to ipsilesional MI also correlated with recovery. Motor recovery levels significantly correlated with a reduction in functional connectivity strengths. Functional topography of connectivity to the ipsilesional primary motor cortex also showed decreases following BCI therapy. These findings were from a small sample without a contemporaneous control group. However, chronic stroke patients receiving intensive physical therapy showed few functional connectivity changes, indirectly substantiating the notable effects specific to BCI therapy. Specifically, while there were significant differences in motor cortex ROI functional connectivity before and after BCI therapy, functional connectivity changes in patients receiving intensive PT were much less prevalent. These combined findings provide intriguing evidence for a potential mechanism suggesting that contralesional BCI-induced motor rehabilitation of chronic stroke patients by widespread decreases in motor network functional connectivity.

Of particular importance was finding contralesional BCI therapy effectively enabled rehabilitation for chronic hemiparesis. Chronic hemiparetic stroke patients usually experience poor motor recovery after 3 months post-stroke.[4–6,27,29] Studied patients were at a median of 62 months post-stroke. Nevertheless, 7 out of 8 patients made clinically significant improvements in

upper limb motor function following contralesional BCI therapy. Ipsilesional BCI therapy for both acute and chronic hemiparesis has been previously implemented in a variety of configurations.[31] Robotic orthoses, electrical stimulation, and visual imagery feedback have all been used in combination with ipsilesional BCI systems with variable success.[75,152,176,177] The current contralesionally-driven BCI therapy method and intervention protocol replicated BCI-mediated recovery reported previously, thus confirming motor recovery with contralesional BCI therapy.[15] Critically, patients achieved motor improvement using BCI in a home therapy setting, with patients or their caretakers operating the BCI system. The current BCI approach advantageously expanded a therapy method previously confined to in-person clinical settings. Acquisition of noninvasive functional neuroimaging concurrent with BCI therapy additionally revealed unexpected motor network changes during rehabilitation. Decreases in motor network functional connectivity strength suggest different network dynamics occur during recovery in chronic stroke compared to (sub)acute stroke. Typically, acutely injured networks characteristically showed increased intra- and decreased interhemispheric resting-state FC strength.[110,112,148,149,154,155] Task-based BOLD activations during motor tasks also became lateralized towards the contralesional hemisphere.[41] With functional recovery in the subacute stage, brain function gradually reverted towards the pre-stroke state with increased interhemispheric connectivity and a return of ipsilesional cortical activation during a motor task.[41,75,147,149,150,154,178] Functional organization with more successful behavioral recovery resembled that of a healthy brain.[147,149,150,178] In contrast, contralesionally-driven BCI therapy resulted in broadly decreased motor network intra- and interhemispheric connectivity strength. The findings also were not an epiphenomenon given a significant correlation between connectivity change and motor recovery. The relative lack of significant functional connectivity

changes even in PT responders emphasizes an important distinction from effects of BCI therapy in altering motor networks in the brain. PT and BCI therapy both induced clinically significant motor recovery, yet only BCI therapy resulted in significantly reduced motor network connectivity correlated with recovery.

Contralesionally-driven BCI rehabilitation in chronic stroke may operate by affecting inhibitory circuit activity through experience-dependent plasticity. Studies in whisker barrel cortex suggest a possible model in which loss of incoming sensory input (e.g., removal of a whisker) resulted in robust alteration in the activity, connectivity, and structure of neural circuits.[179] Loss of input to a deprived barrel column precipitated a loss of inhibitory firing in that column. Unmasked horizontal excitatory connections possibly provoked expanded adjacent receptive fields serviced from neighboring columns linked to intact whiskers. These changes might be a consequent pathologic expansion of local connectivity.[180] Similar changes in cortical topographical maps arose from peripheral loss in nonhuman primates and other animal models.[181,182] A possible mechanism affecting these network changes might be injury-induced downregulation of inhibitory circuits,[182–184] allowing increased neural activity via *pre-existing* thalamocortical and intracortical connectivity as opposed to *de novo* sprouting.[185–187] Similarly provoked increases in intracortical connectivity might occur following stroke-mediated white matter transections in human cortex.[188] Consequently, chronic loss of motor output from stroke might pathologically diminish inhibitory activity, resulting in a net increase in maladaptive connectivity of the remaining motor network. This connectivity increase probably does not represent a compensatory mechanism, but rather a long-term pathologic end point of an injury. Thus, a consistent engagement of thalamocortical inhibitory motor rhythms with BCI usage may reverse this chronic state of maladaptive, decreased inhibitory activity.[119] A consequence of the reversal

could be the observed reduced motor functional connectivity, which may result from restored inhibitory activity. Further, enhanced inhibition might lead to increased functional specialization within the motor network, consistent with current findings of reduced nodal connectivity and diminished topographic distributions of connectivity (most notably in ipsilesional M1). Ipsilesional primary motor cortex in BCI patients was the only ROI that showed a statistically significant change in suprathreshold voxels. Previous studies into motor network connectivity following acute stroke typically reported positive associations between ipsilesional M1 connectivity or activity and motor recovery – this does not match the presented findings.[41,75,112,150] While we observed no correlations between the degree of motor recovery and the change in ipsilesional M1 connectivity extent, there was an observed increase in a patient population achieving clinically significant recovery. The discrepancy may be due to the specific design of the BCI device used for therapy. By promoting contralesional activity during therapy, activity-dependent plasticity may have altered functionally relevant ipsilesional activity. Extensive contralesional BCI use potentially resulted in reduced ipsilesional M1 connectivity specifically, in addition to the general decrease in motor network connectivity.

The current findings of BCI effects on motor recovery and decreased motor network connectivity indicate the importance of further optimization of BCI-mediated therapies. Previously, Bundy et al. demonstrated functional recovery correlated with patient accuracies of BCI control.[15] In the current study, motor recovery was associated with reduced motor network functional connectivity. Methods to improve BCI control may further facilitate recovery. Specifically, current methods used for BCI control were relatively simple. The BCI system was controlled by the signal from a single electrode and a 1-Hz wide EEG frequency band associated with motor imagery. More elaborate control algorithms reliant on different EEG features may enhance

rehabilitative effects. Further, other methods of feedback could include functional electric stimulation or virtual representations of a paretic hand moving.[31,152,176,189–191] In particular, the current feedback was only through proprioceptive sensation from moving the hand. Abundant evidence showed robotic manipulation of an affected limb has provided substantive benefit.[31,152,176,189–191] Designing an optimal feedback regimen to best affect identified motor network changes will require further research, possibly piloted initially in an animal model.

We executed a small, non-randomized, prospective study, which constrained the impact of these findings. The small sample size also constrained statistical testing to less powerful non-parametric tests, which may unreliably detect results from small effect sizes. The study had a target sample size of 20 based on an *a priori* power analysis indicating a $d_z = 0.66$ for paired *t*-tests and $|\rho| = 0.66$ for linear correlations. Due to study interruption by the COVID-19 pandemic, data collection was ended prematurely. Alternative statistical tests were implemented to estimate network-wide effects of BCI rehabilitation, as the study was no longer powered to statistically investigate effects on individual ROI pairs. Two BCI patients had multiple stroke lesions, which may have further affected motor connectivity. However, we assumed these patients achieved full recovery from non-motor deficits due to our strict inclusion and exclusion criteria. Despite additional stroke effects in these cases, seven of eight patients showed clinically significant upper motor recovery after BCI therapy which coincided with decreased in motor network connectivity.

We compared results from BCI therapy to a cohort of chronic stroke patients treated with PT, especially PT responders, as a comparison to the BCI effects. Collected MRI data differed between the BCI and PT groups, weakening direct comparisons between functional connectivity in each group. Consequently, only paired tests assessed changes in each therapy group to avoid

invalid comparisons. An alternative BCI control group would have been patients using BCI with movements decoupled from neural activity. Despite these caveats, only cases receiving BCI therapy showed decreases in motor network connectivity that correlated with motor recovery. No comparable rsFC changes in PT responders correlated with motor recovery. These contrasting findings emphasize that contralesional BCI therapy resulted in motor network reorganization distinct from any changes caused by successful PT. The cause of these different results will be an important target for future studies.

In summary, we have shown that chronic stroke patients used a contralesionally-controlled BCI system to achieve clinically significant upper motor rehabilitation. Motor recovery coincided with decreases in resting-state functional connectivity among motor ROIs. These findings are notably different from those in the subacute stage of stroke, and in chronic stroke patients receiving physical therapy. Future studies need to explore the influence of BCI as a therapy for strokes affecting motor behavior.

3.5 Supplemental Material

Table 3.S1. Demographic Information.

Patient ID	Age (y)	Time Post-Stroke (mo.)	Gender	Lesion Location	Affected Limb	UEFM Baseline	UEFM Final	UEFM Change
1	55	183	F	L SMC	R	56	63	7
2	55	54	F	L BG, Thal	R	41	48	7
3	60	119	M	R BG, CST, L Thal	L	25.5	30	4.5
4	56	34	M	L BG, CST	R	19.5	25	5.5

5	68	46	M	L BG, Thal, CST	R	14.5	22	7.5
6	74	26	F	R BG, CST	L	12	21	9
7	63	71	M	L BG, CST, R BG	R	21.5	32	10.5
8	38	70	M	R BG, Thal, CST	L	22	31	9
Median	**58**	**62**				**21.75**	**30.5**	**7.25**

SMC: Somatomotor Cortex, BG: Basal Ganglia, Thal: Thalamus, CST: Corticocospinal Tract

Secondary motor outcomes included grip strength (in pounds) acquired via dynamometer, the Modified Ashworth Scale (MAS) at the elbow and wrist, the Arm Motor Ability Test (AMAT), and the Motricity Index (MI). These measures were acquired at the same timepoints as the UEFM – twice at baseline and once every 4 weeks of therapy. **Table 3.S2** lists the final values and mean values of the two baseline measurements for each patient and outcome. Wilcoxon signed-rank tests statistically examined changes over time. MAS was not evaluated with a Wilcoxon test due to the 5 ordinal values comprising the scale. Grip strength, AMAT score, and MI score all showed statistically significant improvements. Median MAS score did not change at the elbow or wrist.

Table 3.S2. Secondary Motor Outcomes.

Patient	Grip (Base)	Grip (Final)	MAS (Base, Elbow/Wrist)	MAS (Final)	AMAT (Base)	AMAT (Final)	MI (Base)	MI (Final)
1	37.5	36	1 / 0	1 / 0	104.5	128	12	13
2	18.5	47	1+ / 1	1+ / 1	86	91	10	10
3	25.5	40	3 / 1.25	3 / 1+	53	52	6	11
4	8	9	1 / 1+	1 / 1	24	31	4	6
5	11.5	14	1 / 0	1 / 1	32	38	5	7
6	7	12	1 / 1.25	1 / 2	32	36	5.5	8
7	22	24	1.75 / 3	1+ / 1+	41	46	7.5	10
8	16	22	2 / 2.5	2 / 3	38.5	41	7.5	9
Median	**17.25**	**23**	**1.25 / 1.25**	**1.25 / 1.25**	**39.75**	**43.5**	**6.75**	**9.5**

Leave-one-out variations of each of the BCI analyses were performed to more fully capture the variance of the data given the small sample size. Each analysis was performed on a subset of 7 subjects to generate a range of test statistics. Upper and lower bounds of each of these measures are described in **Table 3.S3**.

Table 3.S3. Leave-One-Out Results.

Test and Measure	ROI or Subset	Point Estimate	Lower Bound	Upper Bound
Suprathreshold Voxel Count (Signed-rank effect size)	Contralesional M1	0.25	0.14	0.41
	Ipsilesional M1	**0.59**	0.59	0.63
	Contralesional CBL	0.14	0	0.32
	Ipsilesional CBL	0.14	0	0.27
Connectivity Distribution Change (Signed-rank effect size)	**Motor Network**	**0.24**	0.11	0.35
	Interhemispheric	**0.22**	0.09	0.31
	Contralesional Intrahemispheric	0.18	0.06	0.31
	Ipsilesional Intrahemispheric	**0.30**	0.21	0.40
Correlation of Motor Improvement to Connectivity Change (Spearman coefficient)	**Motor Network**	**0.77**	0.65	0.87
	Interhemispheric	-0.04	-0.22	0.16
	Contralesional Intrahemispheric	0.46	0.33	0.74
	Ipsilesional Intrahemispheric	0.63	0.41	0.99

Figure 3.S1 shows montages of individual lesion locations. Red highlights lesioned voxels. Slices selected to show lesion spread for each patient. **Figure 3.S2** illustrates all lesion locations overlaid onto a summary map. Each lesion mask consists of an atlas-registered volume where each voxel contains a value of 1 where a lesion has been identified, and a value of 0 elsewhere. The summary map was built by adding these lesion mask volumes together. Thus, the value indicated on the summary map is the number of patients with a lesion in that voxel.
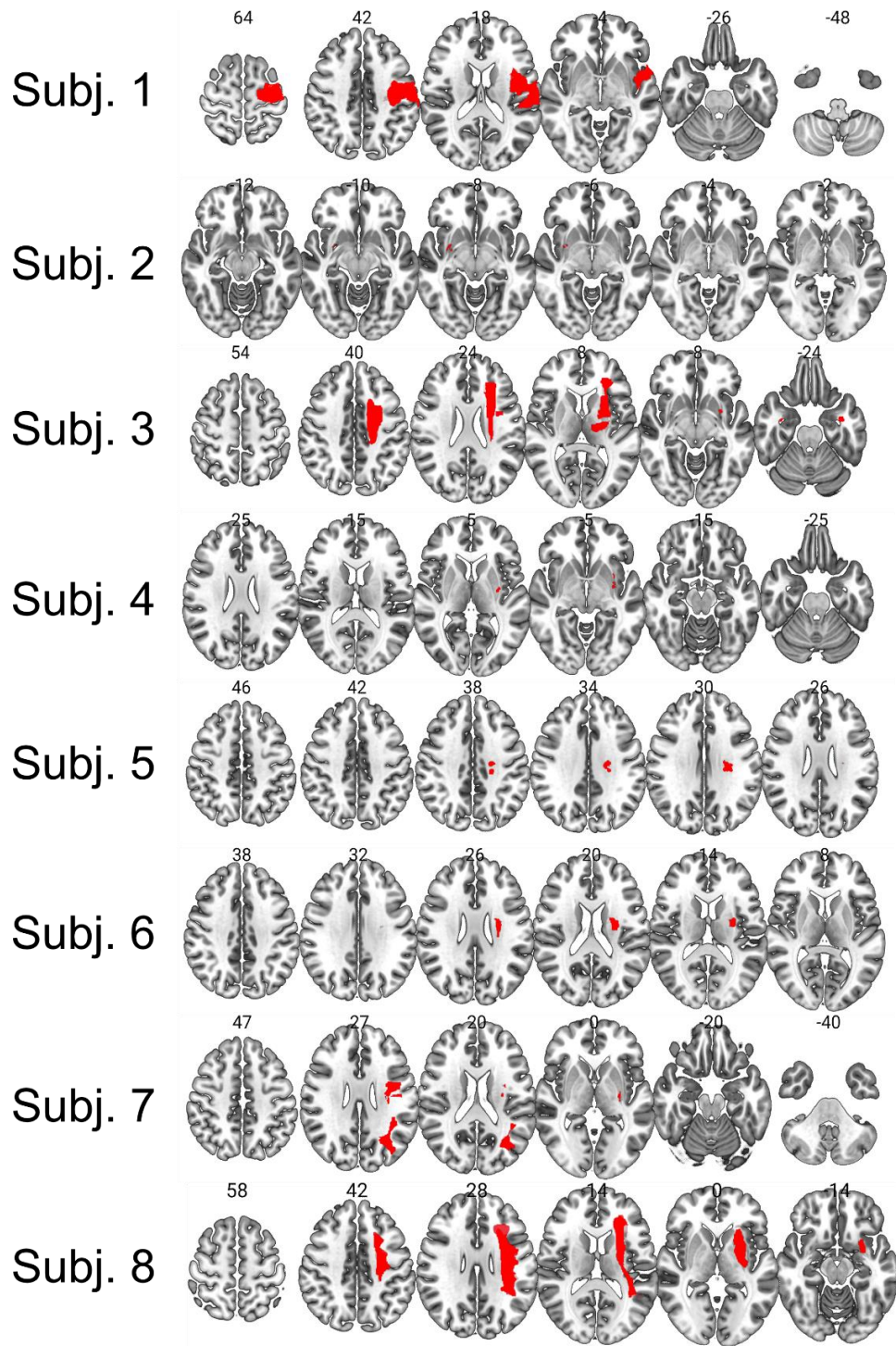
Figure 3.S1. Lesion Locations by Patient. Lesion locations for each patient indicated with red shading on an atlas T1 image. Six selected slices show the extent of the lesion in a row for each patient.
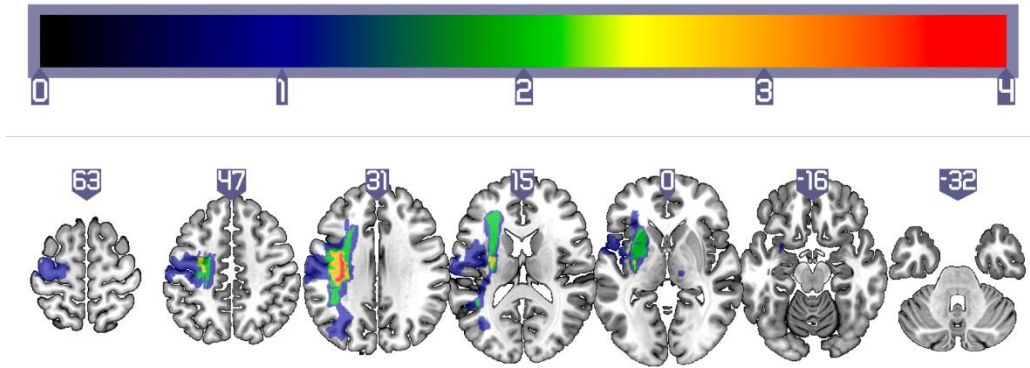
Figure 3.S2. Lesion Location Summary. Summary map of lesion locations generated by summing binary masks of individual lesions. Colormap indicates the number of patients with lesions in a given voxel. Lesions were flipped to correspond on the same brain hemisphere.

Figure 3.S3 compares therapy dosages of physical therapy and BCI patients. BCI therapy was variable due to patients controlling their own therapy in a home environment. Average dose was similar between the groups.
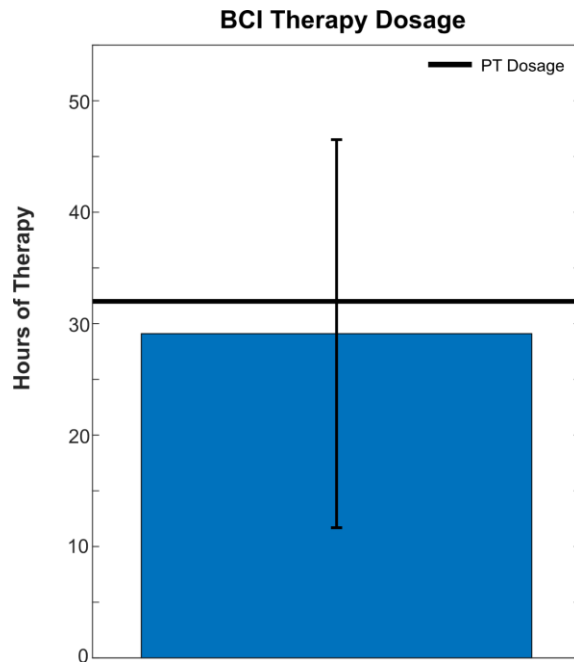
Figure 3.S3. BCI Therapy Dosage. Mean hours of BCI therapy (29.2) indicated by vertical bar. Error bars indicate standard deviations. The PT dosage of 32 hours is represented by a horizontal black line.
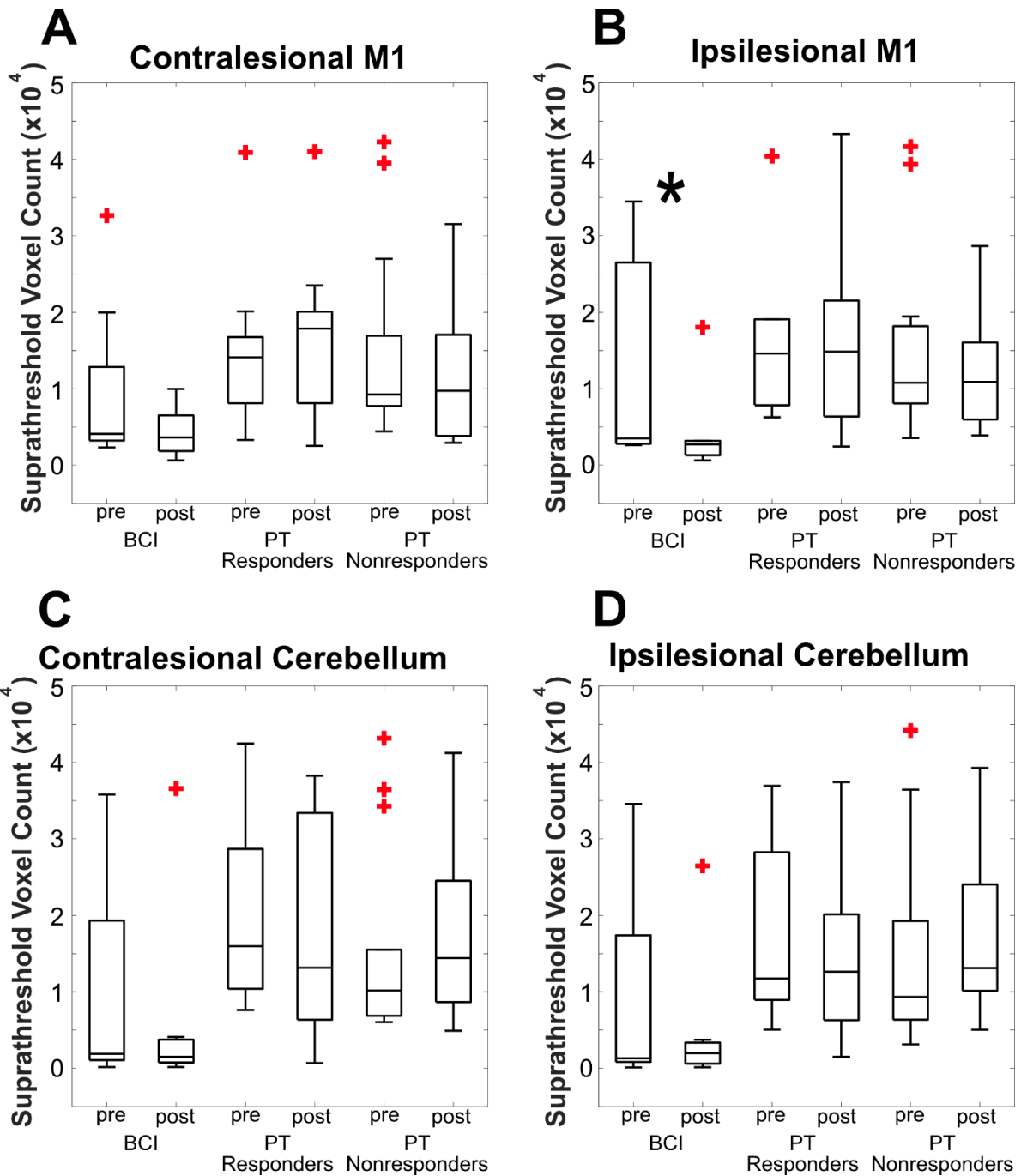
Figure 3.S4. Median Suprathreshold Voxel Counts Pre- and Post-Therapy. Pre- and post-therapy suprathreshold voxel counts in BCI patients and PT responders and non-responders in contralesional M1 (**A**), ipsilesional M1 (**B**), contralesional CBL (**C**), and ipsilesional CBL (**D**). Ipsilesional M1 showed a statistically significant decrease in voxel count after BCI therapy, as reported in main text. No other effects were statistically significant.
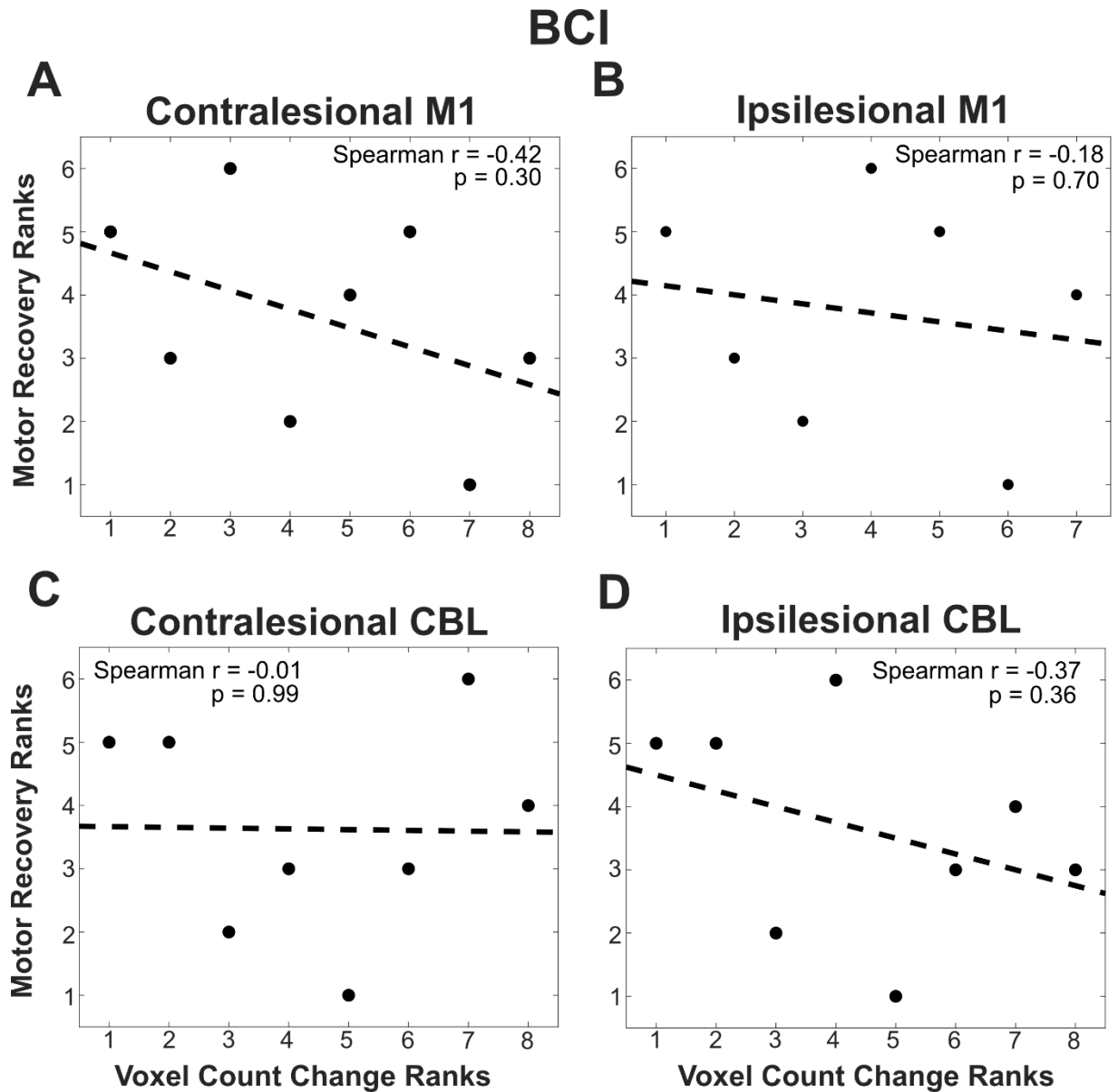
Figure 3.S5. Correlation Between Voxel Count Change and Motor Recovery in BCI Patients. Rank correlations of change in number of suprathreshold voxels and motor recovery for functional connectivity to contralesional M1 (**A**), ipsilesional M1 (**B**), contralesional cerebellum (**C**), and ipsilesional cerebellum (**D**). Least-squared regression lines show linear trends. No correlations reached statistical significance.
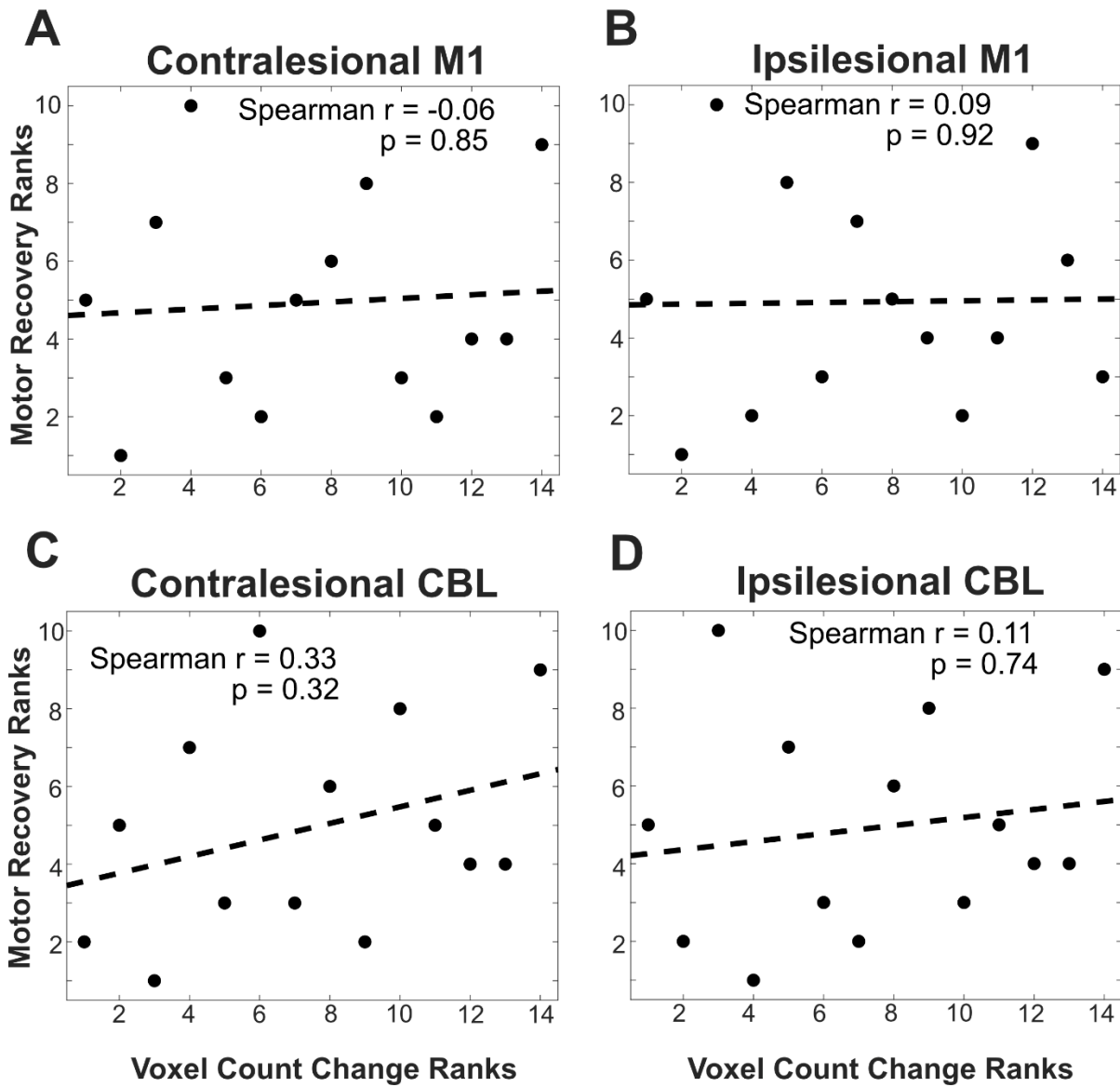
Figure 3.S6. No Correlation Between Voxel Count Change and Motor Recovery in PT Responders. Rank correlations of change in number of suprathreshold voxels and motor recovery for functional connectivity to contralesional M1 (**A**), ipsilesional M1 (**B**), contralesional cerebellum (**C**), and ipsilesional cerebellum (**D**). Least-squared regression lines show linear trends. No correlations reached statistical significance.

Figure 3.S7 No Correlation Between Voxel Count Change and Motor Recovery in PT Nonresponders. Rank correlations of change in number of suprathreshold voxels and motor recovery for functional connectivity to contralesional M1 (**A**), ipsilesional M1 (**B**), contralesional cerebellum (**C**), and ipsilesional cerebellum (**D**). Least-squared regression lines show linear trends. No correlations reached statistical significance.

PT Nonresponders

A Contralesional M1

B Ipsilesional M1

C Contralesional Cerebellum

D Ipsilesional Cerebellum
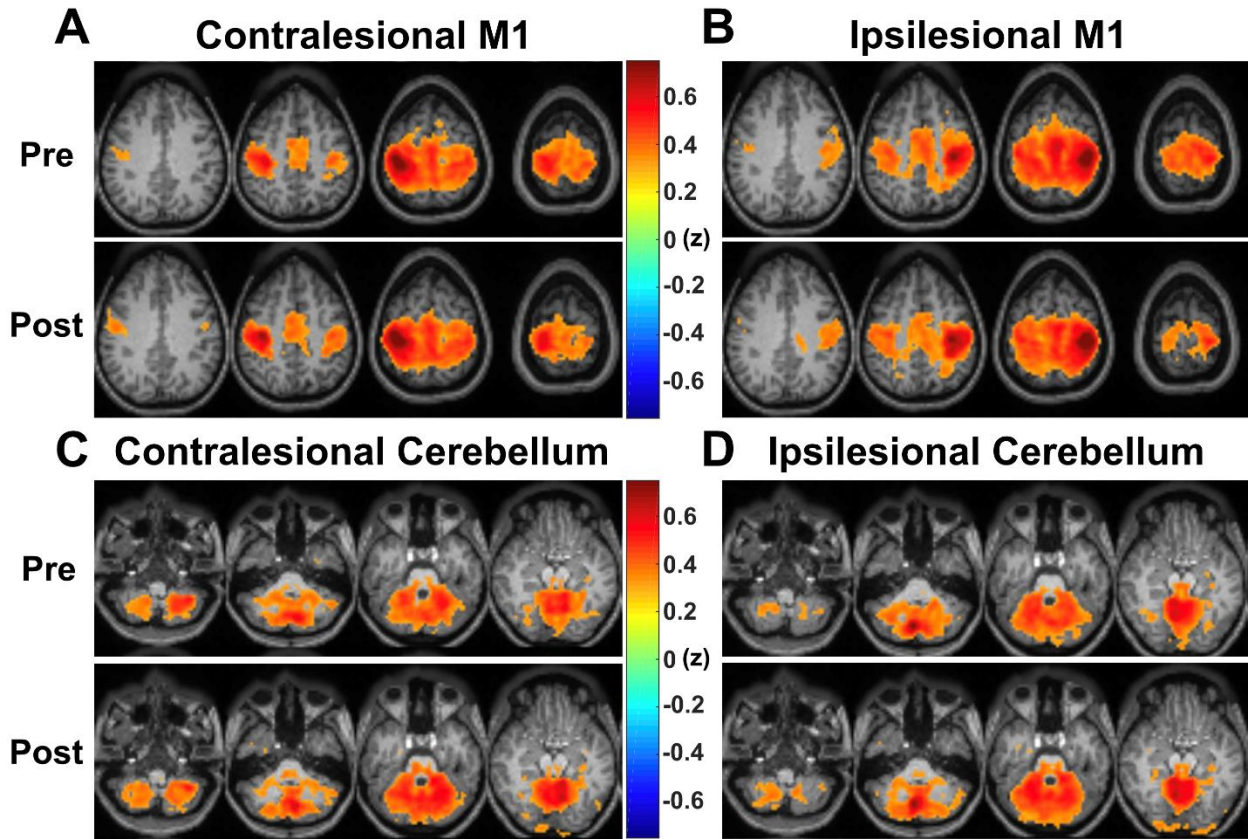
Figure 3.S8. Spatial Connectivity Distributions in PT Nonresponders. Pre- and post-therapy maps of group average voxelwise functional connectivity (z > 0.3) are shown for contralesional M1 (**A**), ipsilesional M1 (**B**), contralesional cerebellum (**C**), and ipsilesional cerebellum (**D**). Pre-therapy maps are shown above their post-therapy equivalents.

PT Nonresponders Pre-Therapy Connectivity

PT Nonresponder Connectivity Change
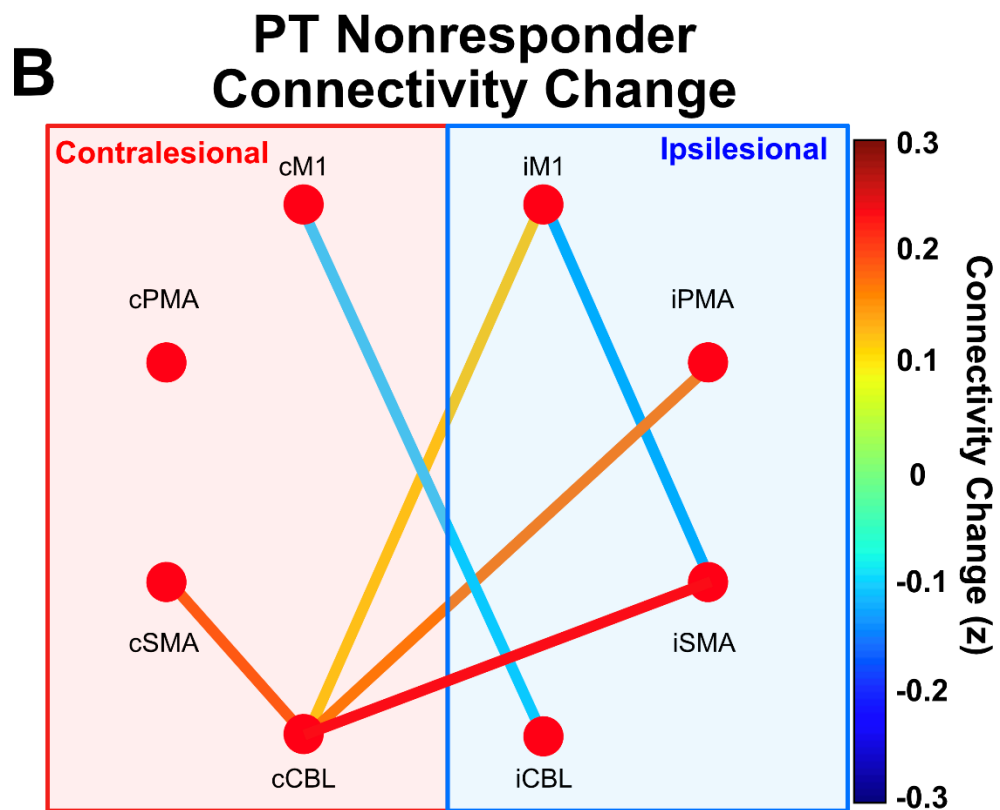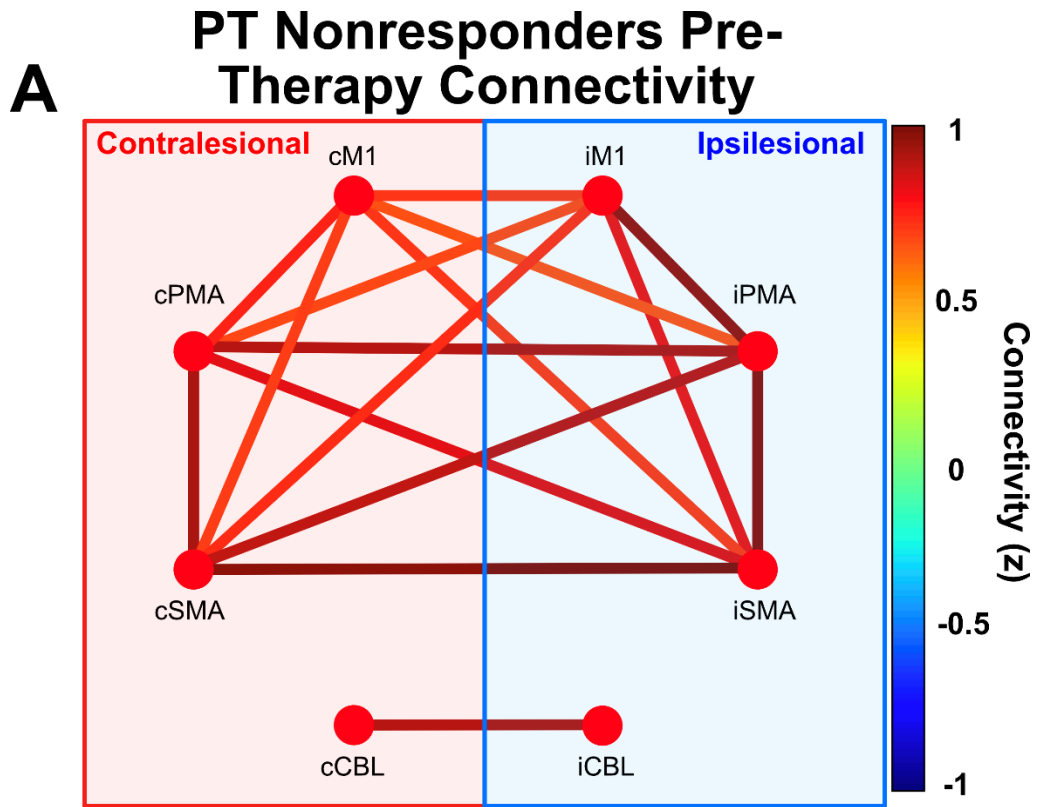
Figure 3.S9. Functional Connectivity in Motor Regions in PT Nonresponders. A) Median pre-therapy functional connectivity between motor ROI pairs. Primary motor, premotor, supplementary motor, and cerebellar ROIs used. Nodes in red and blue background areas are contralesional and ipsilesional ROIs, respectively. Threshold of z = 0.3 applied to connectivity graph. **B)** Median change in connectivity from pre-therapy to post-therapy timepoints (post – pre). Threshold of z = 0.1 applied to connectivity graph.
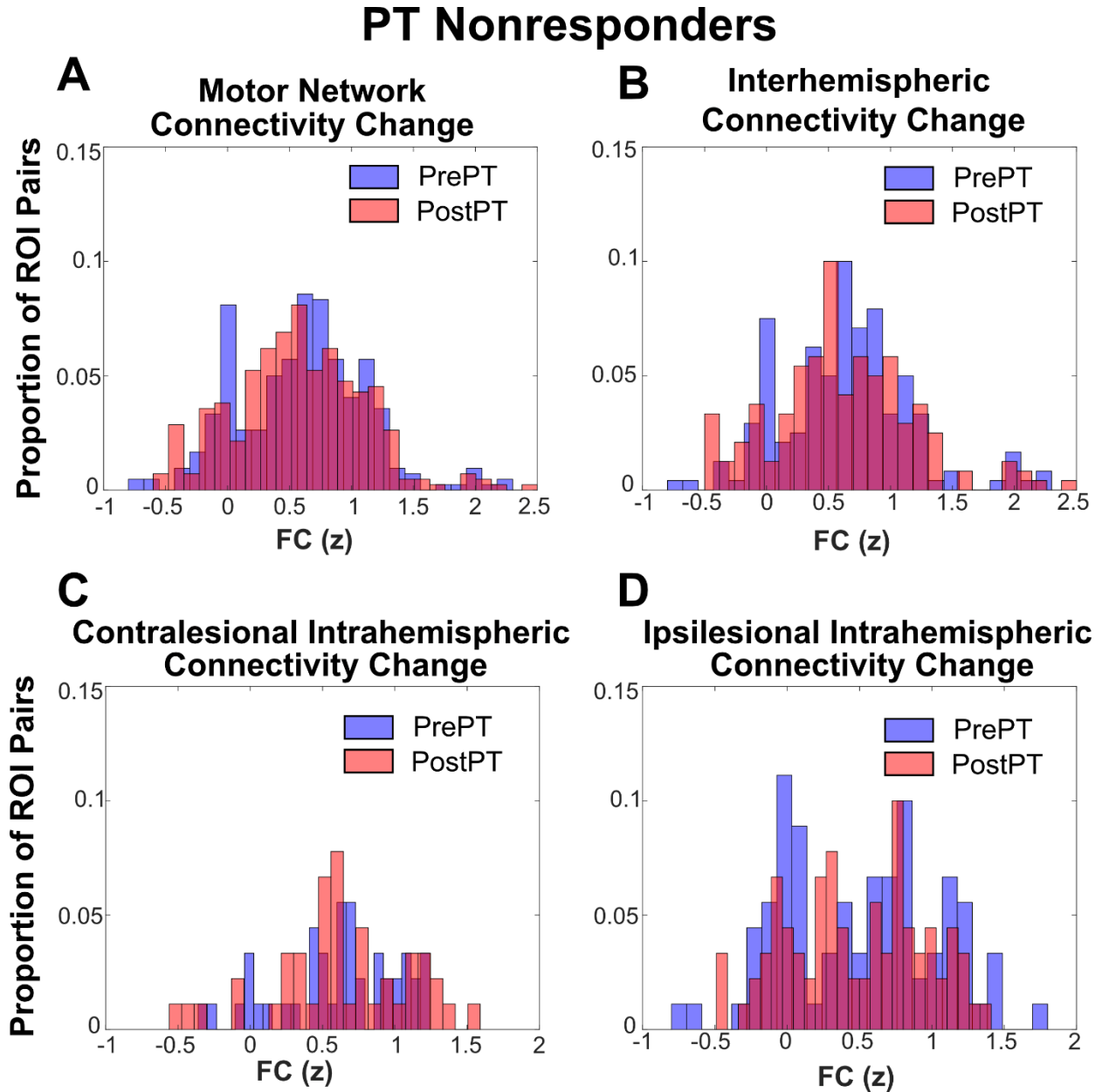
PT Nonresponders

Figure 3.S10. Motor Connectivity Distributions in PT Nonresponders. Histograms constructed from motor ROI sets across PT nonresponders at pre-therapy (blue) and post-therapy (red) timepoints. Overlapping histograms shown in purple. Histograms displays the normalized

distribution of Z-transformed functional connectivity. ROI sets include all motor ROI pairs (**A**), interhemispheric ROI pairs (**B**), contralesional intrahemispheric ROI pairs (**C**), and ipsilesional intrahemispheric ROI pairs (**D**). No distributions showed statistically significant change over time.

Nonresponders
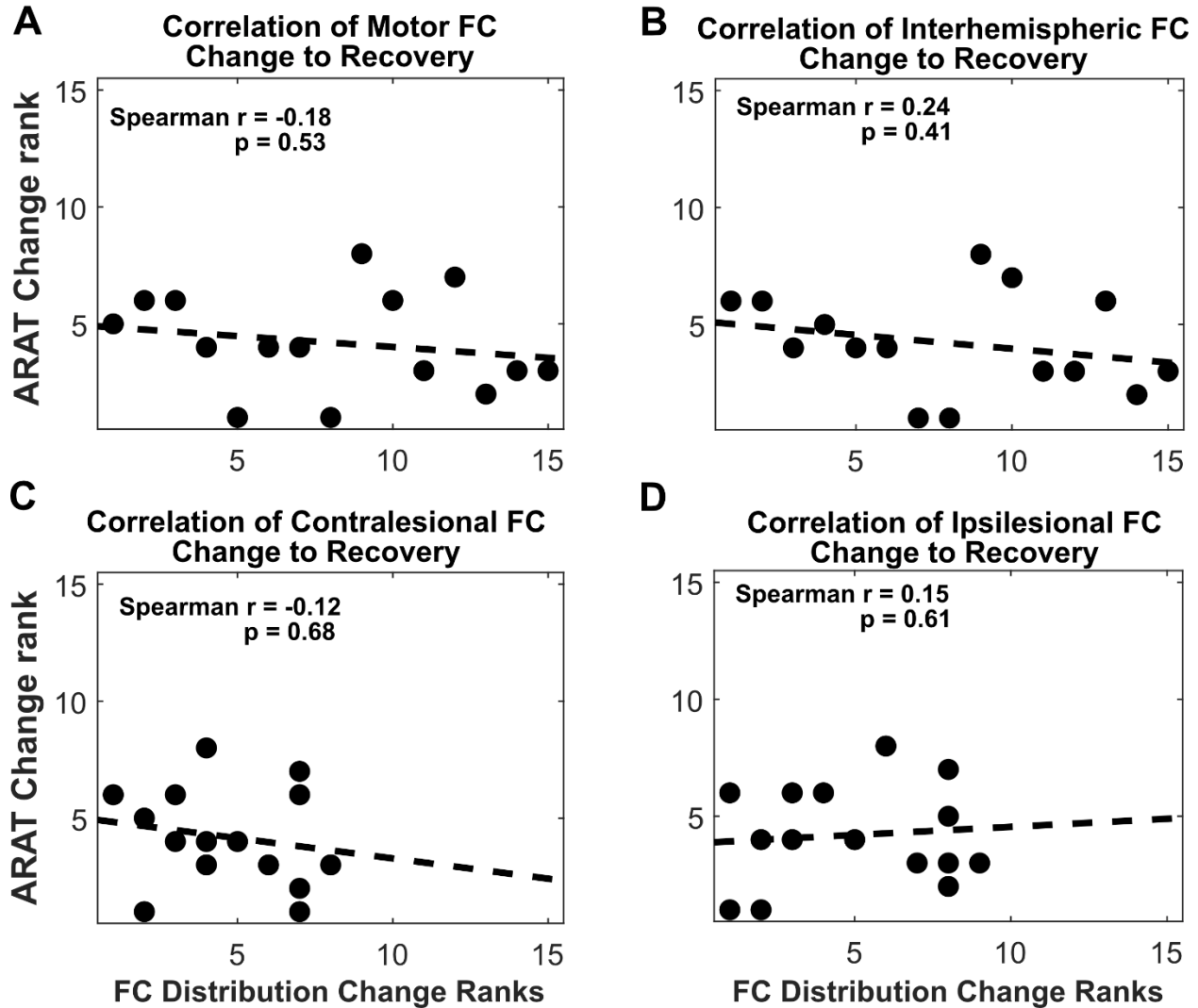
Figure 3.S11. No Correlation Between Connectivity Change and Motor Recovery in PT Nonresponders. Spearman correlations between motor ROI connectivity change and motor recovery. Data represented in ranked form. The dotted line represents a least-squares regression fit onto the ranked data. Connectivity change in four ROI sets measured as shown in **Figure 3.S10**. No correlations were statistically significant.

Chapter 4: Alpha Coherence Increases with Motor Recovery During Chronic Stroke Rehabilitation with Contralesional EEG-BCI

4.1 Introduction

Approximately 77% of stroke patients exhibit upper motor hemiparesis and about 65% of these

are unable to use their affected hand six months after stroke.[1–3] Upper motor rehabilitation in a

chronic stroke population remains a significant challenge. Prior studies reported a plateau in

motor recovery at 3 months post-stroke.[4–6] Brain-computer interface (BCI) mediated

rehabilitation, however, has shown that functional improvements can be accomplished in the

chronic phases of stroke.[15,31] Systems using control signals from the injured hemisphere vary in

their efficacy to accomplish a rehabilitative benefit.[75,87,176,189,192] Consistent motor recovery has

been demonstrated using a BCI-controlled robotic exoskeleton with electroencephalographic

(EEG) signals acquired from motor cortex contralesional to the stroke.[14,15] Regular home use of

the contralesional BCI system facilitated motor recovery that on average exceeded the minimal

clinically important difference (MCID).[15] Rehabilitation effects from contralesional BCI are

encouraging, but there is limited knowledge of the underlying mechanisms. Examining the

changes in cortical electrophysiology associated with a contralesionally-driven BCI

rehabilitation intervention will better inform the neurological underpinnings of recovery and

inform further refinement of BCI strategies in the future.

There is ample evidence that strokes disrupt cortical oscillations. Specifically, changes occur in

canonical delta (1-4 Hz), alpha/mu (8-12 Hz), and beta (13-30 Hz) frequency bands.

[113,123,124,126,193,194] Normally, alpha and beta rhythm power decreases in motor areas with

movement intention. [195] After stroke, there is an attenuation of this beta-band power decrease,

which has been associated with motor deficit severity. [123] In addition to alteration in task-

induced activation, resting state cortical dynamics are also perturbed. Resting delta power is

positively correlated with infarct volume in both subacute and chronic stroke patients, and with

motor ability in chronic patients.[126,194] Beta power and the ratio of alpha to delta power at rest

negatively correlate with infarct volume immediately post-stroke.[194] Changes in connectivity

between different brain regions have been demonstrated as well. Reduced pre-therapy alpha/mu

rhythm MEG coherence in subacute and chronic stroke patients was predictive of better motor

recovery.[113] Delta coherence in both motor and frontal regions correlated with motor status in the

subacute phase, but this effect was not observed in chronic stroke patients.[126] Between

rehabilitation facility admission and discharge, decreased interhemispheric motor coherence in

the delta band correlated with recovery.[126]

Given the broad disruption to oscillatory brain function caused by stroke, we expected that BCI-

induced recovery in motor function in the chronic stroke setting would also induce changes in

these rhythm dynamics. The current study examined resting state cortical activity via scalp EEG

in patients with chronic stroke throughout their use of a contralesionally controlled BCI to

recover hand. The EEG-BCI system used contralesional signals associated with affected hand

motor imagery to control the affected hand via a powered exoskeleton. Resting state coherence

between EEG electrodes over motor regions was measured throughout a 3-month period.

Because a BCI controlled via motor imagery has the potential to alter the functional organization

of motor systems, we hypothesized that the baseline dynamics of the rhythms involved in motor

control (i.e. alpha and beta) would be affected. Further, given the prior evidence showing the link

between delta oscillations and post-stroke motor function, we also hypothesized that these

rhythms would also be altered.[126,132,135] The findings in this study highlight the important role of interhemispheric motor networks in facilitating motor recovery.

4.2 Materials and Methods

4.2.1 Study Population

Seventeen chronic stroke patients with upper-limb hemiparesis completed the full course of BCI therapy. All patients suffered a first-time hemispheric stroke at least 6 months previously. Patients were recruited concurrently at sites in Saint Louis, MO and San Francisco, CA. **Table 4.1** lists patient demographics. The primary motor function outcome measure was the Upper Extremity of the Fugl-Meyer Assessment (UEFM). Secondary outcome measures included the Motricity Index (MI), the Arm Motor Ability Test (AMAT) the modified Ashworth Scale (MAS) at the wrist and elbow, and grip strength. Two separate baseline measurements were acquired to ensure motor function stability. Each patient gave written informed consent prior to any data collection. The study was approved by Institutional Review Boards at each study site.

Table 4.1. Demographics and Motor Recovery

	Age (y)	Time Since Stroke (mo.)	Lesion Side	Gender	Initial UEFM	Final UEFM	UEFM Change
Mean	54.9	64.4	9 L/8 R	7 F/10 M	33.3	41.4	7.9

4.2.2 BCI System Design

The BCI system consisted of a powered exoskeleton hand orthosis (Neurolutions Corp., Santa Cruz, CA), and an EEG amplifier and EEG cap with active electrodes (Wearable Sensing, LLC, San Diego, CA). The system is diagrammed in **Figure 4.1A**.
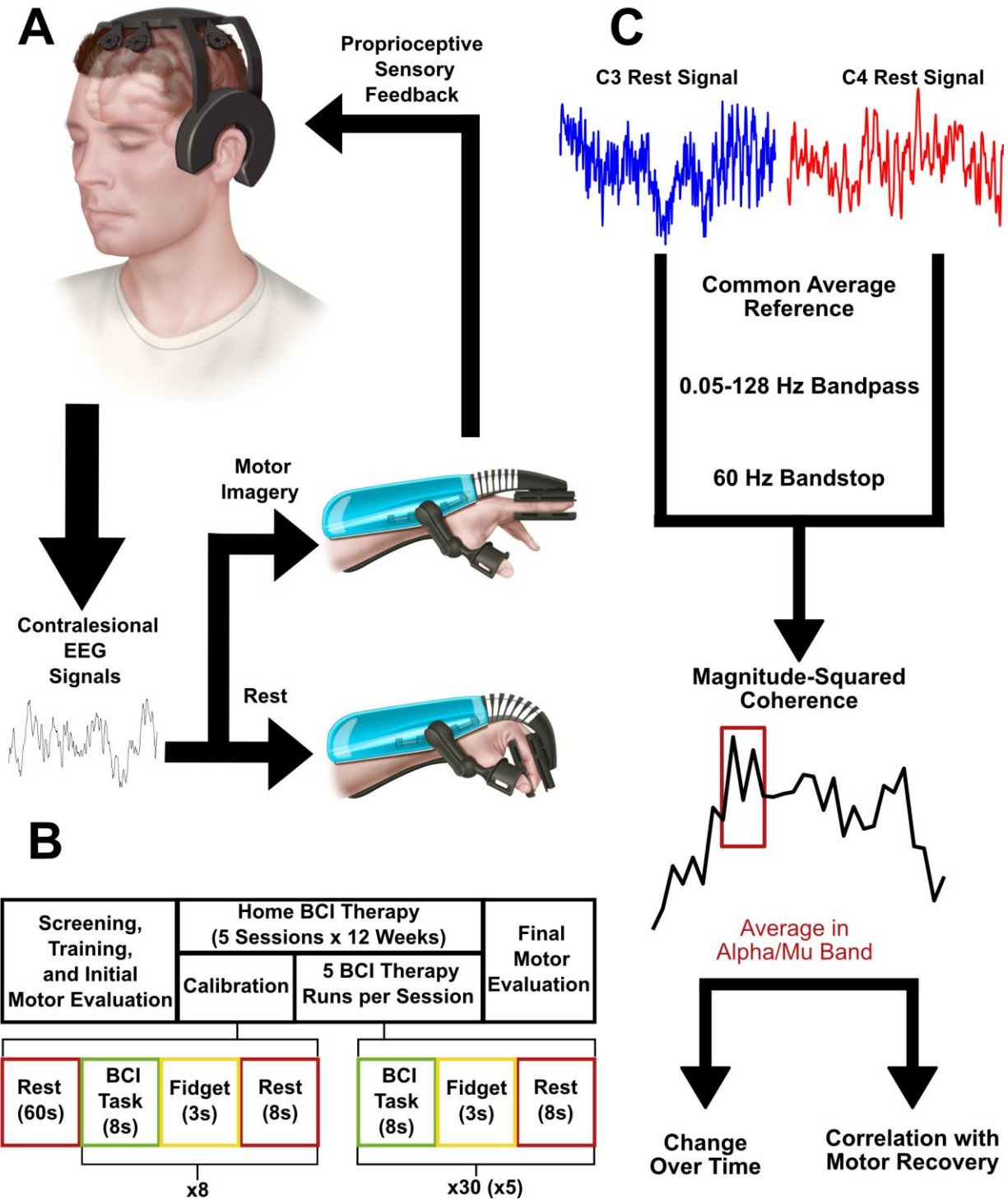
Figure 4.1. BCI Design, Intervention Timeline, and Analysis Outline. A) BCI system design. Patients perform motor imagery or quiet rest. Contralesional EEG signals are translated into commands to open the or close the orthosis based on the detected signal power. Orthosis movements then provide sensory feedback to the patient as they perform these mental tasks. **B)** Intervention timeline. Patients are screened for ability to perform the BCI task and receive

equipment to perform therapy at home for 12 weeks. Daily sessions consist of calibration (Extended rest period, alternating motor imagery and rest trials with inactive orthosis) and 5 BCI runs (150 total trials each of motor imagery and rest with active orthosis). **C)** Coherence analysis pipeline. EEG time series are passed through filters to clean the data, then coherence calculations are performed. Coherence within canonical frequency bands are averaged. Statistical tests are performed on the change in coherence over time and correlation with motor recovery.

The orthosis opened and closed in a 3-finger pinch grip, which occurred in response to changes in the power of a patient-specific control feature during the BCI therapy task. A Windows tablet guided patients through BCI tasks and translated spectral power changes into orthosis control. Patients performed the BCI task by imagining movement with their affected hand to open the exoskeleton or resting quietly to keep the exoskeleton closed. EEG data from a pre-task calibration session and from the BCI task were transmitted to a remote server for storage. During EEG screening sessions prior to therapy implementation, patients performed a series of rest and motor imagery trials. Screening data was analyzed to identify a 1 Hz wide frequency band to use as a BCI control feature. The chosen feature showed spectral power modulation best corresponding to the difference between rest and motor trials. Choosing a narrow frequency band allowed for specific targeting of the peak frequency for optimal BCI control, as opposed to a wider canonical band which may have blurred the optimal feature with other activity. The feature was always within the mu (8-12 Hz) or beta (13-30 Hz) canonical frequency bands and stayed consistent for each patient throughout the study.

4.2.3 Intervention Protocol

The intervention timeline is visualized in **Figure 4.1B**. Patients were first screened for inclusion and exclusion criteria and the ability to perform the BCI task. Patients with an identifiable feature frequency consistent over two EEG screens proceeded in the study. Motor function evaluation was performed twice before therapy initiation by physical and occupational therapists. Research team members then trained patients in the use of the BCI system. After training,

70

patients or their caregivers were able to don the device components, check EEG signal recording quality and initiate the BCI therapy. Patients were instructed to use the device 5 days per week for 12 weeks. Research team members regularly checked EEG and task performance data on a secure server to ensure proper device function and patient compliance.

One session of BCI therapy took approximately 1 hour to complete and consisted of 1 calibration period and 5 BCI therapy runs. Pre-therapy calibration was implemented for data quality assurance and to adjust the power threshold for detecting motor imagery activity during the BCI task. During calibration, patients rested quietly for one minute then completed a series of rest and motor imagery task trials. During task blocks, patients were instructed to imagine moving their affected hand. The orthosis did not move during calibration. Following calibration, patients began BCI therapy runs. Each run contained 30 motor imagery trials and 30 rest trials. Trial order was randomized, and 3 seconds of "fidget" time were included between each 8-second trial. The BCI system paused after the completion of a run to allow patients to rest before continuing with their therapy.

4.2.4 BCI Performance and Usage

Trial success rates are reported as mean for each trial type. Success rates were calculated for each run of 30 movement imagery and 30 rest trials and averaged within patients to find individual success rates. Patient rates were then averaged to find group success rates. Usage data is reported as the mean number of unique sessions with at least 1 trial, as well as the mean number of total trials completed.

4.2.5 EEG Processing and Analysis

EEG data collected during quiet rest in pre-therapy calibration was prepared for analysis with common average referencing, 0.05-128 Hz bandpass filtering, and a 60 Hz notch filter to remove

environmental noise. A visual outline of the EEG analysis pipeline is shown in **Figure 4.1C**. Data from electrodes F3, F4, C3, C4, P3, and P4 (Frontal, Central-Motor, and Parietal) were acquired. We visually inspected recordings and excluded from further processing and analysis those with excessive noise, defined as greater than 10 seconds of artifact or one or more spikes larger than a five-fold increase in the magnitude of the baseline signal. Pre- and post-therapy EEG measures were estimated by averaging the first and last 5 calibration recordings (i.e., the first and last week of use) from each patient.

Magnitude-squared coherence was computed in 1-Hz bins from 1-40 Hz using the mscohere() function in MATLAB (Mathworks, Natick, MA). Coherence for each calibration recording was then split into canonical frequency bands by averaging over frequency. Coherence was thus the average of coherence within each frequency band (Delta: 1-4Hz, Alpha: 8-12 Hz, Beta: 16-25 Hz, Gamma: 30-40 Hz). Coherence was calculated between the contralesional motor electrode (C3 or C4 depending on the patient) and all other electrodes. Motor coherence was defined as C3-C4 coherence. Coherence topography was visualized using the EEGLab topoplot() function.[196] Paired t-tests were used to define differences in coherence pre- and post-therapy across all patients. Relationships between coherence change or baseline coherence and motor recovery were evaluated via Spearman correlation. Multiple comparisons corrections were applied with MATLAB's implementation of Storey's direct FDR method.[197] Reported p-values for these tests are FDR-corrected.

4.3 Results

4.3.1 Motor Outcomes

Chronic stroke patients using a contralesionally-driven brain-computer interface achieved a mean increase in UEFM score of 7.9 points (**Table 4.1**). This increase is statistically significant and

surpasses the minimal clinically significant difference (MCID) threshold of 5.25.[175] A total of 14

of the 17 patients reached the MCID. Secondary motor outcomes (MI, AMAT, Grip Strength,

and MAS) are tabulated in **Table 4.S1**. Statistically significant (p < 0.01) mean score increases

of 2.1 on the MI, 11.3 on the AMAT, and 4.9 lbs. of grip strength were recorded. No mean

changes in MAS were observed at the wrist or elbow. Secondary measure MCID thresholds were

not available for a chronic stroke population.

4.3.2 BCI Performance

Mean trial success rates and BCI usage are listed in **Table 4.2**. Rest trial success rates are

lower than movement imagery success rates due to the stricter criteria for a rest success.

Table 4.2. BCI Performance and Usage Data.

	Move Success Rate (%)	Rest Success Rate (%)	Total Sessions	Total Runs
Mean	85%	47%	68	302

4.3.3 Electrophysiology Changes

Alpha coherence between the C3 and C4 electrodes (i.e., motor electrodes) showed a statistically

significant increase between pre-therapy and post-therapy timepoints (**Figure 4.2**, p = 0.006).

Alpha power fluctuations in these electrodes become more similar over time. Alpha coherence

measured prior to every BCI session in an exemplar patient illustrates the non-linear progression

of coherence throughout the intervention. No other frequency bands (delta, beta, or gamma

bands) showed statistically significant changes over time (**Figure 4.S1**).
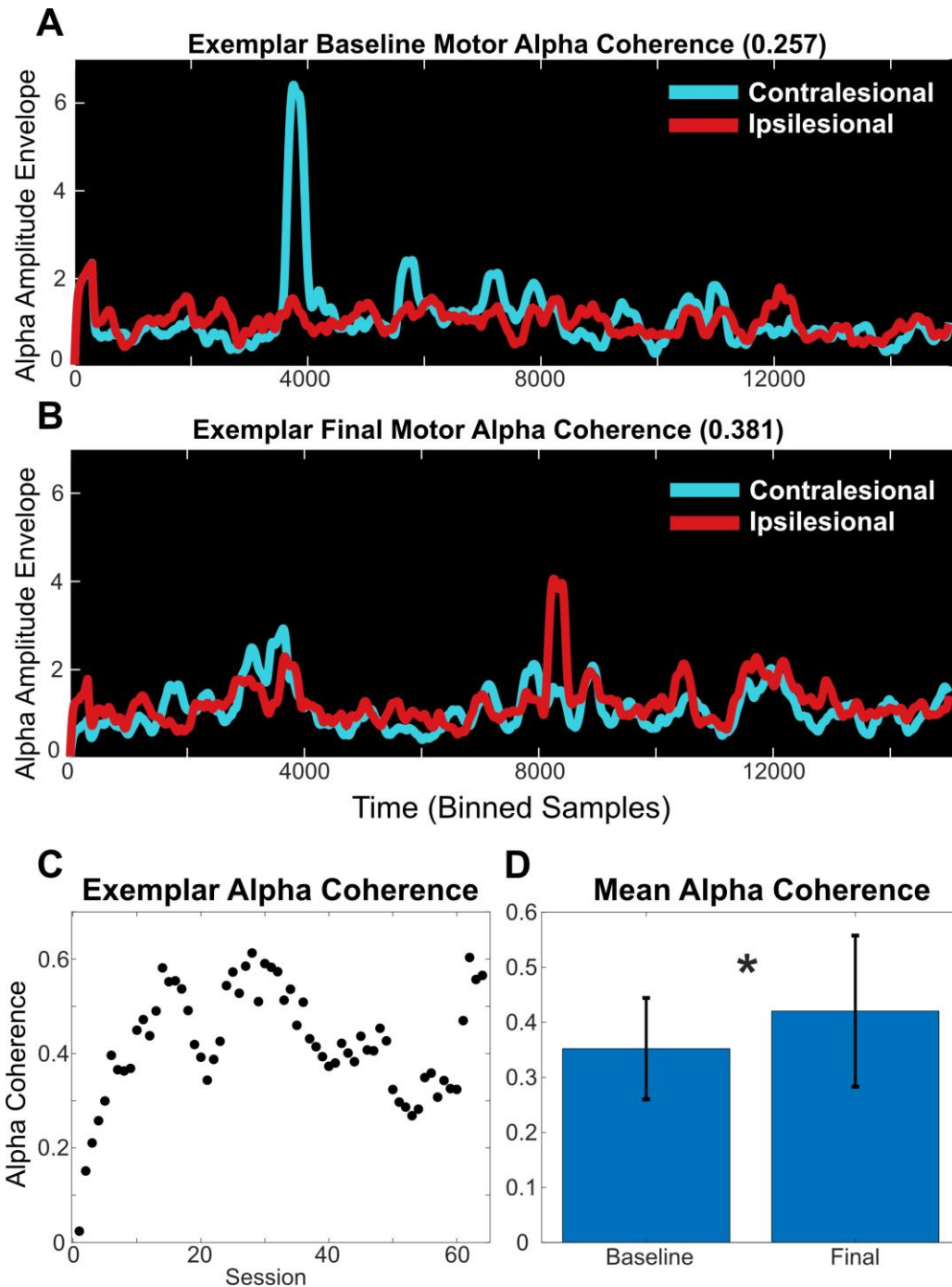
Figure 4.2. Motor Alpha Coherence Increases Following BCI Therapy. A,B) Alpha power envelope before (A) and after (B) 12 weeks of BCI therapy in an exemplar. Envelope timeseries are more similar post-therapy. **C)** Resting alpha motor coherence in each BCI calibration session over the entire therapy period. Change is nonlinear but positive over time. A smoothing filter with a width of five sessions was applied to the figure for visual clarity; analyses were performed on pre-filter data. **D)** Average and standard deviation of resting alpha motor coherence pre- and

post-therapy. A paired t-test revealed statistically significant differences between these timepoints.

The present study had too few therapy non-responders to perform subgroup analyses comparing the performance of responders to non-responders directly. However, Spearman correlations served to estimate relationships between EEG measures and motor recovery. These relationships were evaluated in two ways: predictive (the correlation of pre-therapy EEG measures to motor recovery) and concurrent (the correlation of EEG measure change to motor recovery). Pre-therapy alpha motor coherence did not correlate with motor recovery (**Figure 4.3A**). Alpha motor coherence change however, showed a strong correlation with motor recovery (**Figure 4.3B**, r = 0.64, p = 0.029). Specifically, larger increases in C3-C4 alpha coherence at rest were observed in patients who achieved greater recovery.

A

r = 0.36
p = 0.160

B

r = 0.64
p = 0.005
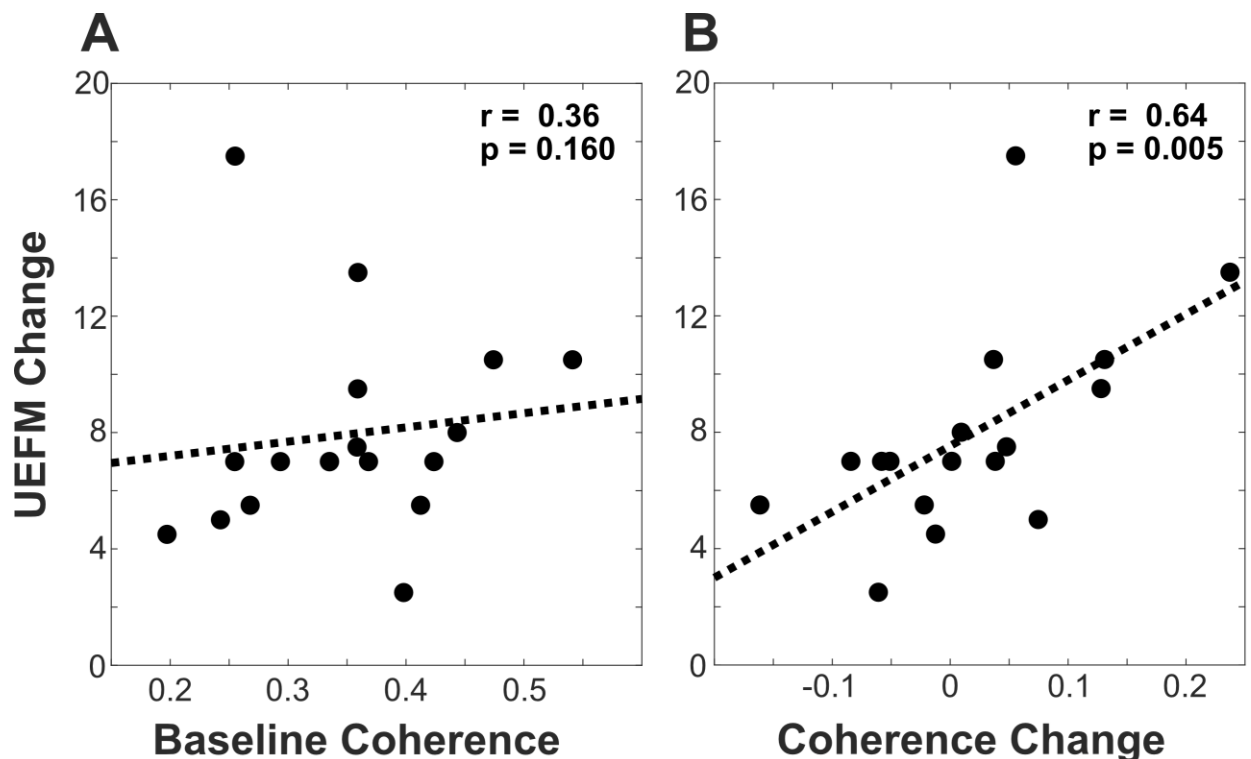
Figure 4.3. Alpha Coherence Change Correlates with Motor Recovery. A) Pre-therapy alpha coherence between C3 and C4 electrodes does not show a statistically significant correlation

with motor recovery. **B)** Alpha coherence change shows a statistically significant positive Spearman correlation with motor recovery.

Coherence in no other frequency bands in this electrode pair showed any predictive or concurrent correlations with recovery (**Figure 4.S2**). However, baseline delta coherence and beta coherence change showed trends toward significant correlations with motor recovery (**Figure 4.S2**).

Alpha coherence topography was examined using the contralesional motor electrode as a seed (**Figure 4.4**). The seed electrode was used for BCI control in all patients. The ipsilesional motor electrode showed the largest increase in alpha coherence (p = 0.006). Bilateral parietal electrodes also showed statistically significant coherence increases (contralesional p = 0.008, ipsilesional p = 0.008). Neither frontal electrode showed statistically significant changes, although the contralesional frontal electrode increased by a mean of 0.052 compared to the ipsilesional mean change of 0.010.

Change in Alpha Coherence to Contralesional Motor Electrode
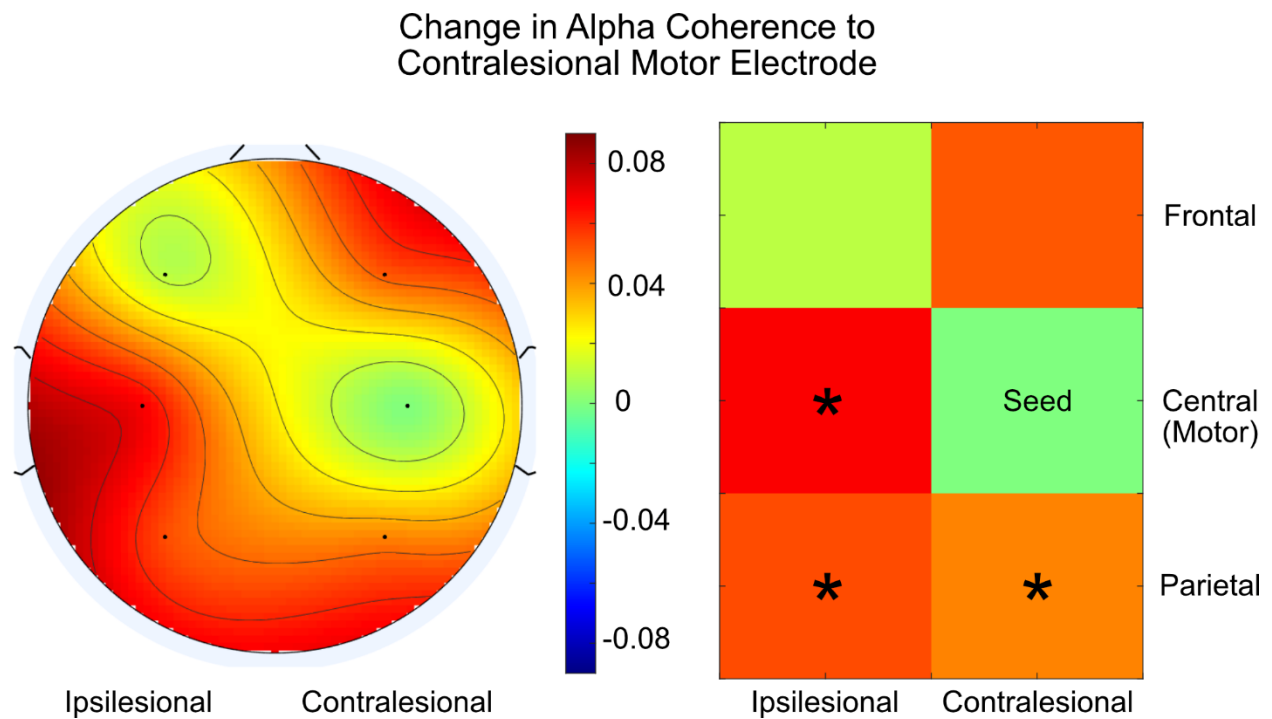
Figure 4.4 Alpha Coherence Topography of the Contralesional Motor Electrode. Alpha-band coherence change between contralesional motor electrode and all other electrodes. Asterisks indicate statistically significant differences found via paired t-test and FDR correction.

4.4 Discussion

In the present study we found that the use of a contralesional BCI for chronic stroke therapy induced motor function improvement that was significantly correlated with interhemispheric alpha coherence. Specifically, fourteen of seventeen study participants achieved clinically significant motor recovery, despite being an average of over 60 months post-stroke. Alpha band coherence between motor electrodes showed a statistically significant increase following therapy. Crucially, this increase in alpha coherence correlated strongly with motor recovery. Finally, alpha coherence also increased between the contralesional motor electrode and both parietal electrodes. Taken together, these findings support the notion of an increase in bihemispheric thalamo-cortical coordination for motor recovery in chronic stroke.

Increased resting-state functional similarity between brain hemispheres has been frequently associated with motor recovery in stroke patients.[110–112,148,149,154,178,198] Such similarity is often referred to as "functional connectivity" and is quantified with a variety of measures, including coherence.[199] Following an acute stroke, fMRI studies observed decreased interhemispheric functional connectivity corresponding with motor deficit severity.[110,112,148,149,154,178,198] In the early phase of recovery, interhemispheric connectivity recovery correlated with motor recovery.[149,150,178]. Since substantial motor improvement in chronic phase of stroke recovery is rare, there is less known about the cortical dynamics that occur with functional improvement during this time frame.[4–6,27,30] The advent of BCI therapy for chronic stroke patients has expanded the window of potential functional improvement.[31]

Generally, the results of this study follow a similar pattern of increased interhemispheric motor coherence correlating with motor ability or recovery seen in acute and subacute stroke. A longitudinal MEG study of alpha-band activity in stroke patients found that alpha coherence between a perilesional ROI and its homotopic, contralesional pair increased with motor recovery.[113] Additionally, alpha coherence three months post-stroke was decreased compared to healthy subjects in motor regions in patients with motor deficits.[129] Alpha coherence decreases may also correspond with other cognitive deficits in stroke patients.[129,130] Our results show a reversal of this decrease in alpha coherence in accordance with motor recovery. Another EEG study of stroke patients examining delta and beta coherence, but not alpha, found that decreases in M1-M1 delta coherence from inpatient rehabilitation admission to 90 days post-stroke were correlated with motor recovery.[126] Our findings were exclusive to the alpha frequency band, perhaps in part due to the unique contralesional BCI therapy.

The mechanistic implications of enhanced alpha coherence must be carefully considered. Alpha rhythms (also known as mu rhythms) are thought to represent inhibitory thalamocortical circuits [200,201]. Often considered an "idling rhythm," the brain signal has an elevated power at rest that reduces during the performance of a motor task.[117,121,202] Thus, we interpret increased alpha power coherence to represent enhanced coordination of the thalamic motor nuclei in their modulation of motor cortical regions. More specifically, this may represent enhanced coordination of thalamocortical inhibition, rather than an increase in cortico-cortical communication. Transcallosal M1-M1 white matter tract integrity is another potential anatomical substrate for this effect that has similarly been implicated in post-stroke motor recovery.[88–90,93,94,203] The use of contralesional BCI with proprioceptive sensory feedback may therefore be enhancing plasticity in these circuits to drive recovery.

Although BCI therapy in the home setting is a novel and effective approach, the EEG data quality is lower than if the recordings were performed in a laboratory setting. Additionally, usage was variable for some patients. We also assumed chronic stroke upper motor deficits in these patients were stable and thus did not have a separate control group or control arm in the study. Motor deficits vary little over time after the sub-acute stage of stroke.[27–30] Recovery in the chronic stage is typically the result of intentional behavioral adaptation as opposed to spontaneous improved motor control.[29] We therefore interpreted changes in motor function in this population as primarily due to the BCI intervention.

In conclusion, contralesional BCI therapy is effective for promoting motor recovery in chronic stroke patients. During rehabilitation, increased C3-C4 alpha coherence correlated with recovery. This suggests contralesional BCI therapy may drive plasticity in cortico-thalamic circuits to enhance recovery.

4.5 Supplemental Material
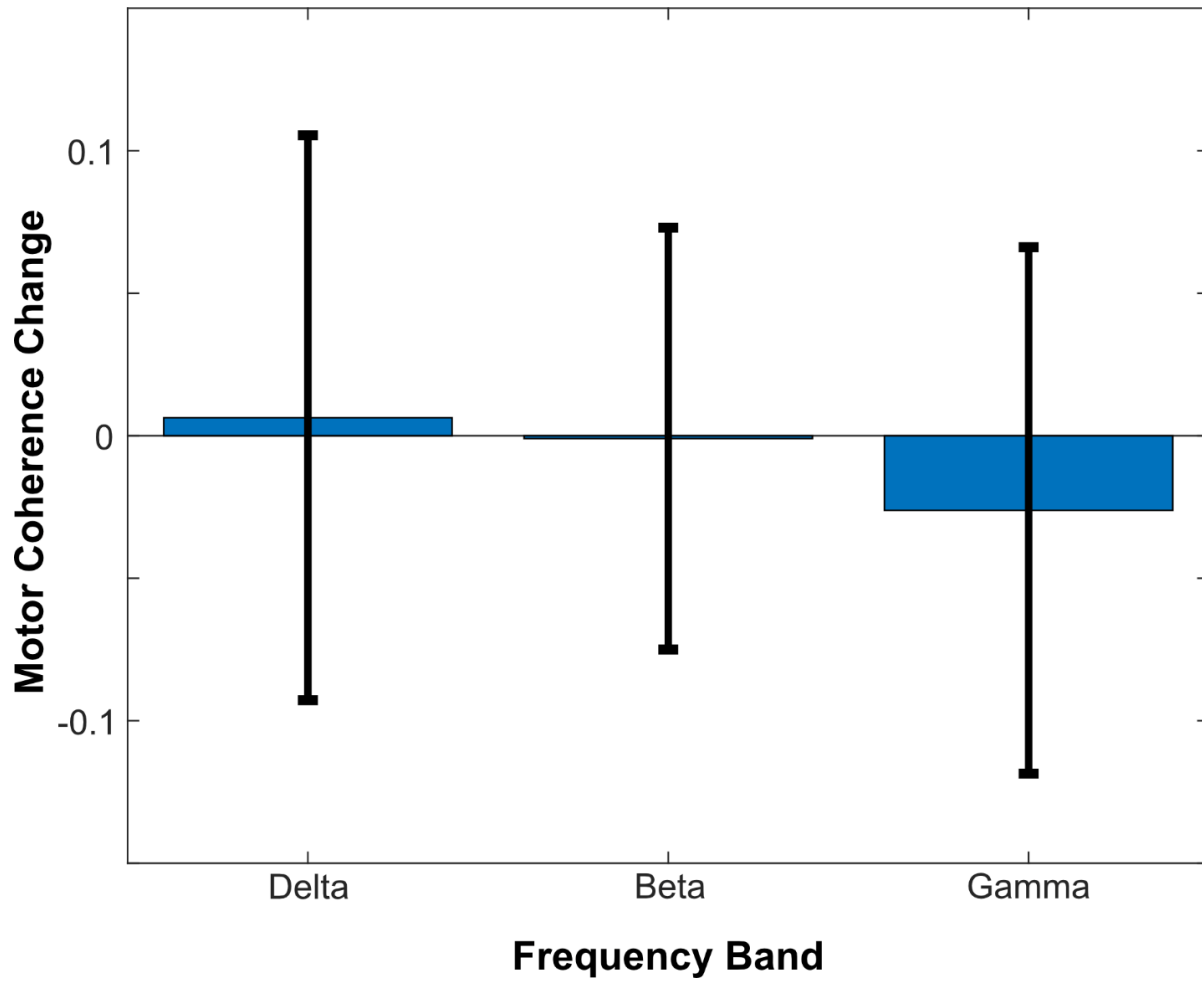
Figure 4.S1. No Motor Coherence Changes in Delta, Beta, or Gamma Bands. Bars indicate mean C3-C4 coherence change in each frequency band. Error bars show standard deviation. No changes were statistically significant as evaluated with a paired t-test.
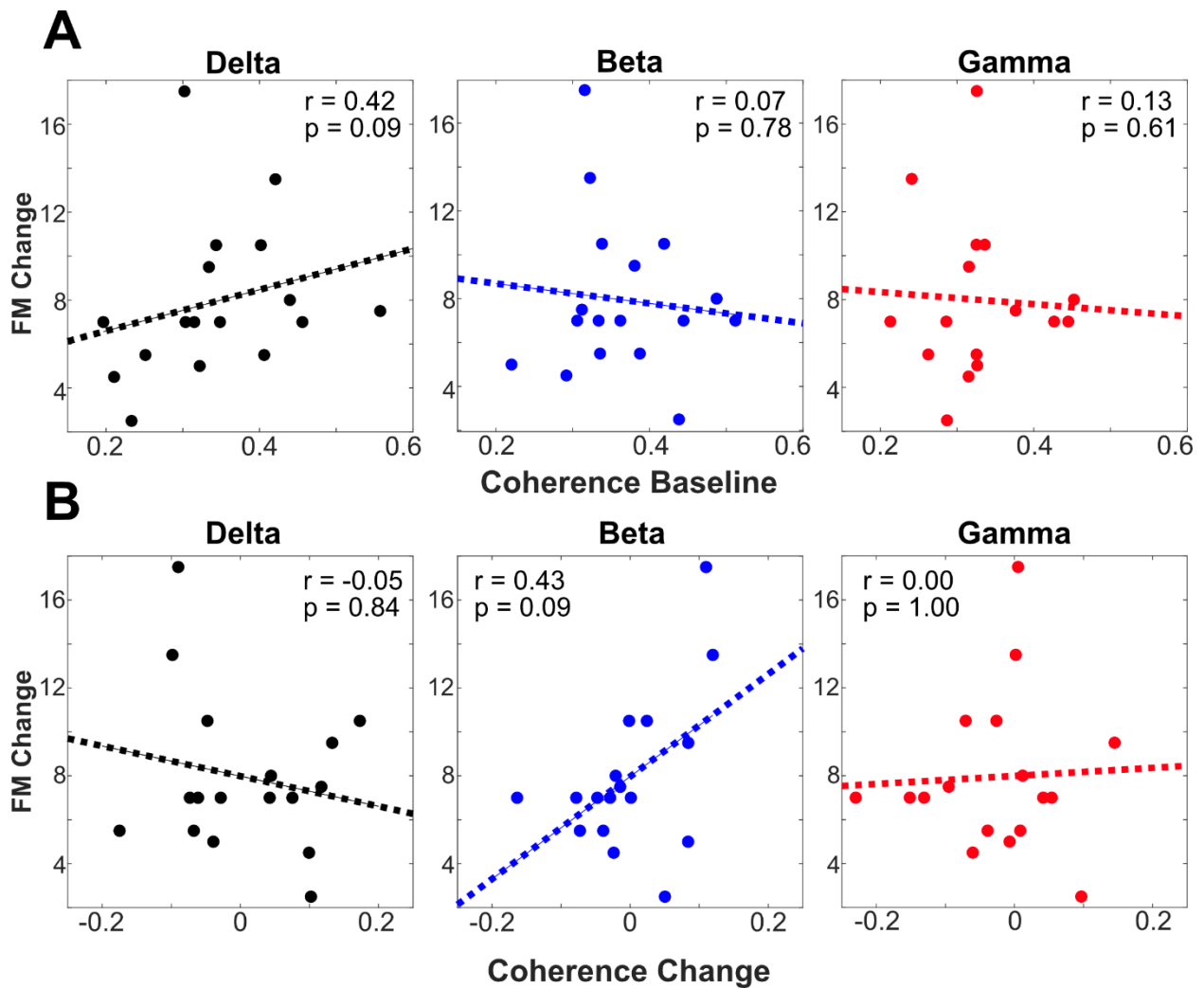
Figure 4.S2. No Correlation Between Motor Coherence and Motor Recovery in Delta, Beta, or Gamma Bands. A) Spearman correlations between baseline C3-C4 coherence and motor recovery (Fugl-Meyer score change). **B)** Spearman correlations between C3-C4 coherence change and motor recovery. Dotted lines indicate least-squares regression fits. No correlations were statistically significant.

Chapter 5: Conclusion

5.1 Summary of Findings

The goal of this dissertation is to show how a contralesional BCI promotes neural plasticity to drive motor rehabilitation in chronic stroke patients. Specifically, we hypothesized that the motor network would show resting-state functional reorganization that correlated with motor recovery. We succeeded in showing this effect in two modalities, leading to a suggestion of a mechanism for recovery with this therapy method. The ultimate goal of this research is to find the therapy design components and neural systems that can be targeted and modulated to achieve the greatest recovery possible for stroke patients. This dissertation is a major step towards that goal.

Chapter 3 illustrates a widespread decrease in resting-state functional connectivity in the motor network using BOLD signals acquired with functional MRI. These decreases were measured by combining all pairwise motor ROIs into pre- and post-therapy connectivity distributions. Crucially, the strength of the connectivity decrease correlated with motor recovery. This suggests that more independent activity in motor regions may be a key part of rehabilitation with contralesional BCI. To add context to this finding, we compared these results to an analysis of the same motor regions in a group of chronic stroke patients who attended intensive physical tehrapy sessions to achieve recovery. Although the overall therapy dosage and recovery levels were similar, the physical therapy patients showed none of the motor connectivity decreases or associations with recovery seen in the BCI patients. Therefore, contralesional BCI may drive recovery with a different mechanism than standard therapy approaches.

Chapter 4 similarly demonstrates systemic changes in motor function organization at rest. Alpha-band coherence between motor electrodes increased from pre- to post-therapy timepoints, and this increase correlated with motor recovery. Although activity in other frequency bands (delta and beta) are also disrupted by stroke or implicated in recovery, we only found effects in the alpha band of activity. Alpha activity in motor cortical regions is directly linked to motor function and is thought to reflect activity in thalamocortical circuits.[121,201] These circuits are inhibitory in nature; motor cortex is inhibited at rest, and is selectively disinhibited to perform movements.[116,117,121] This inhibition may be driving the decreased connectivity observed in fMRI data in Chapter 3. Direct M1-M1 white matter connections in the corpus callosum are also a potential substrate for functional reorganization during stroke recovery. These fibers are disrupted following stroke and show changes in structural integrity that correlate with motor recovery.[89,94,204] We also observed increased alpha coherence between the contralesional motor electrode and both parietal electrodes. Future research is necessary to fully characterize this finding, but it may indicate coordination between motor and attention networks necessary to perform the therapeutic BCI task. Together, these findings form a foundation for describing the mechanism for contralesional BCI rehabilitation and are an important step towards realizing individualized therapy approaches.

5.2 Future Directions

This research leads to several possible continuations that would be beneficial to chronic stroke patients and the field of neurorehabilitation. Further mechanistic studies of neural plasticity would better enable the application of individualized therapies. Refinement and augmentation of BCI systems used to promote rehabilitation is another major arm of future research.

5.2.1 Direct Comparisons to Multiple Therapy Strategies

Although Chapter 3 touches on this by comparing patients receiving BCI therapy to those receiving physical therapy, the data for those cohorts were collected in different studies, and with different scanning parameters. This constrains the strength of the findings. Comparisons of how various therapy methods change the brain during rehabilitation and which patients respond best to each approach are crucial for optimizing therapy. Intensive physical therapy and constraint-induced movement therapy are both used for chronic stroke rehabilitation and can be effective in some patients.[8,157] Additionally, other research groups have explored the use of ipsilesional BCI in chronic stroke.[75,205] Thorough collection of neural and motor function data before and after rehabilitation with each of these approaches would grant a much deeper understanding of how they influence system-level reorganization in the brain to achieve motor recovery. For example, it is currently unknown whether ipsilesional BCI works via the same mechanism as standard physical therapy or if it resembles contralesional BCI. Additionally, this data would allow for the analysis of baseline neural and behavioral data relative to performance with each type of therapy. Future patients could then be assigned to specific therapies based on the specific presentation of their stroke symptoms and neural system organization.

5.2.2 BCI Control Systems and Features

More complex BCI control schemes may be developed to further enhance activity in neural systems identified as important for BCI-driven motor recovery. BCI system control can be designed as a combination of features across different frequencies and electrodes. Alpha coherence between C3 and C4 electrodes calculated in a sliding window may be a useful feature for driving the neural signals shown in Chapter 4 to be a biomarker of recovery. Some studies have suggested coherence may be used as a robust feature for BCI control, and targeting alpha motor coherence specifically may further supplement rehabilitation.[206,207] Additionally,

comparisons among BCI systems are necessary to determine which patients respond best to contralesional and ipsilesional control, and in both subacute and chronic phases of stroke. Most current studies of BCI rehabilitation focus on subacute recovery (CITE). We do not yet understand whether contralesional BCI therapy in the chronic stage works by the same mechanism as it would in the subacute phase. Optimizing features both for individual patients and for time post-stroke is crucial for improving rehabilitation strategies.

5.2.3 BCI Efficacy Augmentation

BCI effects on motor recovery may be augmented through noninvasive stimulation. The most promising approaches to achieve this are transcranial magnetic stimulation (TMS), vagus nerve stimulation (VNS), and transcutaneous direct current stimulation (TDCS). Intermittent theta-burst TMS applied to the cerebellum of subacute stroke patients over 3 weeks resulted in improvements in gait and balance.[208] Additionally, a clinical trial is currently underway to assess the feasibility of targeting the dentate nucleus with deep brain stimulation to assist in the rehabilitation of stroke-induced hemiparesis.[209] Vagus nerve stimulation (VNS) is yet another method for enhancing plasticity with applications for stroke recovery. Several studies have shown that VNS is effective at improving recovery when paired with traditional physical and occupational therapy in subacute and chronic stroke rat models.[210–213] Clinical trials assessing invasive and non-invasive VNS for stroke therapy in human patients have similarly shown promising results with a variety of paired rehabilitation strategies.[214–217] Similarly, TDCS has been explored as a method to promote stroke recovery by enhancing plasticity. Thus far, TDCS has not shown strong or consistent effects in driving recovery.[218,219] Despite mixed reports of efficacy, TDCS may be useful in combination with BCI therapy. Each of the stimulation

approaches described here are of interest to potentially boost the effectiveness of contralesional BCI therapy.

5.2.4 Investigations Via Additional Modalities

Many studies have illustrated the impact of stroke and rehabilitation on the brain using resting state magnetoencephalography (MEG) and task activations. These approaches would be useful additions to the resting state fMRI and EEG studies described in this dissertation. A consistent finding in stroke is the acute shift in function to the non-lesioned hemisphere, followed by a remapping back to the lesioned hemisphere during recovery.[41,75] This result has been replicated across several studies, including with ipsilesional BCI, and was key in identifying one of the rehabilitation mechanisms driving stroke recovery.[75] Therefore, investigating motor task activations pre- and post-therapy with contralesional BCI and in a chronic stroke population is a critical next step in comparing its rehabilitation mechanism to existing therapy approaches. Due to the focus on activating the non-lesioned hemisphere, contralesional BCI therapy may not follow this established trend. Adding MEG as an imaging modality would allow for EEG-level temporal resolution of neural data with much more detailed spatial resolution. Chapter 4 illustrates cortical alpha effects, and Chapter 3 shows decreases in motor network BOLD connectivity. MEG data would be useful in understanding how these findings work together, since frequency-specific activity in both cortical and subcortical regions can be evaluated.

5.3 Final Thoughts

The rapid progress and recent FDA approval of BCIs for stroke rehabilitation make for an exciting and hopeful time in the field of neurorehabilitation. This dissertation represents the next important step in expanding access to chronic stroke rehabilitation. Now that the basic efficacy

of these systems has been established, it is vital to determine how BCIs change the brain to promote recovery. Some studies have been previously conducted on ipsilesional BCIs in the subacute phase of stroke; these generally showed the same post-stroke functional reorganization as standard physical therapy. The analysis of contralesional BCI therapy in a chronic stroke population presented here offers two key points of comparison in the differing BCI design and the different stage of stroke. The observed decrease in resting state BOLD connectivity in the motor network, and the increase in EEG alpha coherence differ from previously reported subacute findings. Additional comparisons to other therapies as well as continued analysis of the effects of contralesional BCI on neural reorganization are crucial for continuing to enhance rehabilitation. Although much work remains, the eventual goal of effective, individualized stroke rehabilitation grows closer each day.

References

1. Lawrence ES, Coshall C, Dundas R, et al. Estimates of the Prevalence of Acute Stroke Impairments and Disability in a Multiethnic Population. *Stroke*. 2001;32(6):1279-1284.

2. Sunderland A, Tinson D, Bradley L, Hewer RL. Arm function after stroke. An evaluation of grip strength as a measure of recovery and a prognostic indicator. *J Neurol Neurosurg Psychiatry*. 1989;52(11):1267-1272.

3. Wade DT, Langton-Hewer R, Wood VA, Skilbeck CE, Ismail HM. The hemiplegic arm after stroke: measurement and recovery. *J Neurol Neurosurg Psychiatry*. 1983;46(6):521-524.

4. Duncan PW, Goldstein LB, Matchar D, Divine GW, Feussner J. Measurement of motor recovery after stroke. *Stroke*. 1992;23(8):1084-1089.

5. Jorgensen HS, Nakayama H, Raaschou HO, Vive-Larsen J, Stoier M, Olsen TS. Outcome and time course of recovery in stroke. Part II: Time course of recovery. The copenhagen stroke study. *Arch Phys Med Rehab*. 1995;76(5):406-412.

6. Lloyd-Jones D, Adams R, Carnethon M, et al. Heart disease and stroke statistics - 2009 update. A report from the American heart association statistics committee and stroke statistics subcommittee. *Circulation*. 2009;119(3):480-486.

7. Taub E, Uswatte G, Pidikiti R. Constraint-Induced Movement Therapy: A New Family of Techniques with Broad Application to Physical Rehabilitation--A Clinical Review. *J Rehabil Res Dev*. 1999;36(3).

8. Grotta JC, Noser EA, Ro T, et al. Constraint-induced movement therapy. In: *Stroke*. Vol 35. Stroke; 2004:2699-2701. doi:10.1161/01.STR.0000143320.64953.c4

9. Stinear CM, Byblow WD, Ackerley SJ, Smith MC, Borges VM, Barber PA. Proportional Motor Recovery after Stroke: Implications for Trial Design. *Stroke*. 2017;48(3):795-798. doi:10.1161/STROKEAHA.116.016020

10. Kwakkel G, Veerbeek JM, van Wegen EEH, Wolf SL. Constraint-induced movement therapy after stroke. *Lancet Neurol*. 2015;14(2):224-234. doi:10.1016/S1474-4422(14)70160-7

11. Fritz SL, Light KE, Patterson TS, Behrman AL, Davis SB. Active finger extension predicts outcomes after constraint-induced movement therapy for individuals with hemiparesis after stroke. *Stroke*. 2005;36(6):1172-1177. doi:10.1161/01.STR.0000165922.96430.d0

12. Stinear C. Prediction of recovery of motor function after stroke. *Lancet Neurol*. 2010;9(12):1228-1232. doi:10.1016/S1474-4422(10)70247-7

13. Wolf SL, Newton H, Maddy D, et al. The Excite Trial: Relationship of intensity of constraint induced movement therapy to improvement in the wolf motor function test. *Restor Neurol Neurosci*. 2007;25(5-6):549-562. Accessed January 6, 2021. https://europepmc.org/article/med/18334772

14. Bundy DT, Wronkiewicz M, Sharma M, Moran DW, Corbetta M, Leuthardt EC. Using Ipsilateral Motor Signals in the Unaffected Cerebral Hemisphere as a Signal Platform for Brain Computer Interfaces in Hemiplegic Stroke Survivors. *J Neural Eng*. 2012;9(3):1-23.

15. Bundy DT, Souders L, Baranyai K, et al. Contralesional Brain–Computer Interface Control of a Powered Exoskeleton for Motor Recovery in Chronic Stroke Survivors. *Stroke*. 2017;48(7):1908-1915.

16. Virani SS, Alonso A, Benjamin EJ, et al. Heart disease and stroke statistics—2020 update: A report from the American Heart Association. *Circulation*. 2020;141:E139-E596. doi:10.1161/CIR.0000000000000757

17. Stinear CM. Prediction of motor recovery after stroke: advances in biomarkers. *Lancet Neurol*. 2017;16(10):826-836. doi:10.1016/S1474-4422(17)30283-1

18. Stinear CM, Byblow WD, Ackerley SJ, Smith MC, Borges VM, Barber PA. PREP2: A biomarker-based algorithm for predicting upper limb function after stroke. *Ann Clin Transl Neurol*. 2017;4(11):811-820. doi:10.1002/acn3.488

19. Barker AT, Jalinous R, Freeston IL. Non-invasive magnetic stimulation of human motor cortex. *Lancet*. 1985;325(8437):1106-1107. doi:10.1016/S0140-6736(85)92413-4

20. Prabhakaran S, Zarahn E, Riley C, et al. Inter-individual variability in the capacity for motor recovery after ischemic stroke. *Neurorehabil Neural Repair*. 2008;22(1):64-71. doi:10.1177/1545968307305302

21. Zarahn E, Alon L, Ryan SL, et al. Prediction of motor recovery using initial impairment and fMRI 48 h poststroke. *Cereb Cortex*. 2011;21(12):2712-2721. doi:10.1093/cercor/bhr047

22. Winters C, Van Wegen EEH, Daffertshofer A, Kwakkel G. Generalizability of the Proportional Recovery Model for the Upper Extremity After an Ischemic Stroke. *Neurorehabil Neural Repair*. 2015;29(7):614-622. doi:10.1177/1545968314562115

23. Byblow WD, Stinear CM, Barber PA, Petoe MA, Ackerley SJ. Proportional recovery after stroke depends on corticomotor integrity. *Ann Neurol*. 2015;78(6):848-859. doi:10.1002/ana.24472

24. Stinear CM, Barber PA, Smale PR, Coxon JP, Fleming MK, Byblow WD. Functional potential in chronic stroke patients depends on corticospinal tract integrity. *Brain*. 2007;130(1):170-180. doi:10.1093/brain/awl333

25. Hawe RL, Scott SH, Dukelow SP. Taking Proportional out of Stroke Recovery. *Stroke*. 2019;50(1):204-211. doi:10.1161/STROKEAHA.118.023006

26. Kundert R, Goldsmith J, Veerbeek JM, Krakauer JW, Luft AR. What the Proportional Recovery Rule Is (and Is Not): Methodological and Statistical Considerations. *Neurorehabil Neural Repair*. 2019;33(11):876-887. doi:10.1177/1545968319872996

27. Hatem SM, Saussez G, Della Faille M, et al. Rehabilitation of Motor Function after Stroke: A Multiple Systematic Review Focused on Techniques to Stimulate Upper Extremity Recovery. *Front Hum Neurosci*. 2016;10:442. doi:10.3389/fnhum.2016.00442

28. Krakauer JW. Motor learning: its relevance to stroke recovery and neurorehabilitation. *Curr Opin Neurol*. 2006;19(1):84-90. doi:10.1097/01.wco.0000200544.29915.cc

29. Kwakkel G, Kollen B, Lindeman E. Understanding the pattern of functional recovery after stroke: facts and theories. *Restor Neurol Neurosci*. 2004;22(3-5):281-299.

30. Langhorne P, Bernhardt J, Kwakkel G. Stroke rehabilitation. *Lancet (London, England)*. 2011;377(9778):1693-1702. doi:10.1016/S0140-6736(11)60325-5

31. Cervera MA, Soekadar SR, Ushiba J, et al. Brain-computer interfaces for post-stroke motor rehabilitation: a meta-analysis. *Ann Clin Transl Neurol*. 2018;5(5):651-663. doi:10.1002/acn3.544

32. Daly JJ, Wolpaw JR. Brain-computer interfaces in neurological rehabilitation. *Lancet Neurol*. 2008;7(11):1032-1043. doi:10.1016/S1474-4422(08)70223-0

33. Takeuchi N, Izumi SI. Rehabilitation with poststroke motor recovery: A review with a focus on neural plasticity. *Stroke Res Treat*. 2013;2013. doi:10.1155/2013/128641

34. Mrachacz-Kersting N, Jiang N, Stevenson AJT, et al. Efficient neuroplasticity induction in chronic stroke patients by an associative brain-computer interface. *J Neurophysiol*. Published online 2015:jn.00918.2015. doi:10.1152/jn.00918.2015

35. Barbero A, Grosse-Wentrup M. Biased feedback in brain-computer interfaces. *J Neuroeng Rehabil*. 2010;7:34. doi:10.1186/1743-0003-7-34

36. Fleury M, Lioi G, Barillot C, Lécuyer A. A Survey on the Use of Haptic Feedback for Brain-Computer Interfaces and Neurofeedback. *Front Neurosci*. Published online 2020. doi:10.3389/fnins.2020.00528

37. Neuper C, Scherer R, Wriessnegger S, Pfurtscheller G. Motor imagery and action observation: Modulation of sensorimotor brain rhythms during mental control of a brain-computer interface. *Clin Neurophysiol*. 2009;120(2):239-247. doi:10.1016/j.clinph.2008.11.015

38. McFarland DJ, McCane LM, Wolpaw JR. EEG-based communication and control: Short-term role of feedback. *IEEE Trans Rehabil Eng*. 1998;6(1):7-11. doi:10.1109/86.662615

39. Ramos-Murguialday A, Birbaumer N. Brain oscillatory signatures of motor tasks. *J Neurophysiol*. 2015;113(10):3663-3682. doi:10.1152/jn.00467.2013

40. Weiller C, Chollet F, Friston KJ, Wise RJ, Frackowiak RS. Functional reorganization of

the brain in recovery from striatocapsular infarction in man. *Ann Neurol*. 1992;31(5):463-472. http://www.ncbi.nlm.nih.gov/pubmed/1596081

41.   Cramer SC, Nelles G, Benson RR, et al. A Functional MRI Study of Subjects Recovered From Hemiparetic Stroke. *Stroke*. 1997;28(12):2518-2527.

42.   Tecchio F, Zappasodi F, Tombini M, et al. Brain plasticity in recovery from stroke: An MEG assessment. *Neuroimage*. 2006;32(3):1326-1334. doi:10.1016/j.neuroimage.2006.05.004

43.   Michel CM, Brunet D. EEG Source Imaging: A Practical Review of the Analysis Steps. *Front Neurol*. 2019;10:325. doi:10.3389/FNEUR.2019.00325

44.   Wisneski KJ, Anderson N, Schalk G, Smyth M, Moran D, Leuthardt EC. Unique cortical physiology associated with ipsilateral hand movements and neuroprosthetic implications. *Stroke*. 2008;39(12):3351-3359. doi:10.1161/STROKEAHA.108.518175

45.   Beloosesky Y, Streifler JY, Burstin A, Grinblat J. The importance of brain infarct size and location in predicting outcome after stroke. *Age Ageing*. 1995;24(6):515-518. doi:10.1093/ageing/24.6.515

46.   Chaudhuri G, Harvey RF, Sulton LD, Lambert RW. Computerized tomography head scans as predictors of functional outcome of stroke patients. *Arch Phys Med Rehabil*. 1988;69(7):496-498. Accessed March 26, 2021. https://europepmc.org/article/med/3389988

47.   Van Everdingen KJ, Van Der Grond J, Kappelle LJ, Ramos LMP, Mali WPTM. Diffusion-weighted magnetic resonance imaging in acute stroke. *Stroke*. 1998;29(9):1783-1790. doi:10.1161/01.STR.29.9.1783

48.   Saunders DE, Clifton AG, Brown MM. Measurement of infarct size using mri predicts prognosis in middle cerebral artery infarction. *Stroke*. 1995;26(12):2272-2276. doi:10.1161/01.STR.26.12.2272

49.   Pantano P, Formisano R, Ricci M, et al. Motor recovery after stroke Morphological and functional brain alterations. *Brain*. 1996;119(6):1849-1857. doi:10.1093/brain/119.6.1849

50.   Dromerick AW, Reding MJ. Functional outcome for patients with hemiparesis, hemihypesthesia, and hemianopsia: Does lesion location matter? *Stroke*. 1995;26(11):2023-2026. doi:10.1161/01.STR.26.11.2023

51.   Chen CL, Tang FT, Chen HC, Chung CY, Wong MK. Brain lesion size and location: Effects on motor recovery and functional outcome in stroke patients. *Arch Phys Med Rehabil*. 2000;81(4):447-452. doi:10.1053/mr.2000.3837

52.   Feng W, Wang J, Chhatbar PY, et al. Corticospinal tract lesion load: An imaging biomarker for stroke motor outcomes. *Ann Neurol*. 2015;78(6):860-870. doi:10.1002/ana.24510

53.   Thickbroom GW, Cortes M, Rykman A, et al. Stroke subtype and motor impairment

influence contralesional excitability. *Neurology*. 2015;85(6):517-520. doi:10.1212/WNL.0000000000001828

54.   Edwardson MA, Ding L, Park C, et al. Reduced upper limb recovery in subcortical stroke patients with small prior radiographic stroke. *Front Neurol*. 2019;10(MAY):454. doi:10.3389/fneur.2019.00454

55.   Karthikeyan S, Jeffers MS, Carter A, Corbett D. Characterizing Spontaneous Motor Recovery Following Cortical and Subcortical Stroke in the Rat. *Neurorehabil Neural Repair*. 2019;33(1):27-37. doi:10.1177/1545968318817823

56.   Honey CJ, Sporns O, Cammoun L, et al. Predicting human resting-state functional connectivity from structural connectivity. *Proc Natl Acad Sci U S A*. 2009;106(6):2035-2040. doi:10.1073/pnas.0811168106

57.   Alexander AL, Lee JE, Lazar M, Field AS. Diffusion tensor imaging of the brain. *Neurotherapeutics*. 2007;4(3):316-329. doi:10.1016/j.nurt.2007.05.011

58.   Pinter D, Gattringer T, Fandler-Höfler S, et al. Early Progressive Changes in White Matter Integrity Are Associated with Stroke Recovery. *Transl Stroke Res*. 2020;11(6):1264-1272. doi:10.1007/s12975-020-00797-x

59.   Wang Y, Liu G, Hong D, Chen F, Ji X, Cao G. White matter injury in ischemic stroke. *Prog Neurobiol*. 2016;141:45-60. doi:10.1016/j.pneurobio.2016.04.005

60.   Liu G, Dang C, Chen X, et al. Structural remodeling of white matter in the contralesional hemisphere is correlated with early motor recovery in patients with subcortical infarction. *Restor Neurol Neurosci*. 2015;33(3):309-319. doi:10.3233/RNN-140442

61.   Takenobu Y, Hayashi T, Moriwaki H, Nagatsuka K, Naritomi H, Fukuyama H. Motor recovery and microstructural change in rubro-spinal tract in subcortical stroke. *NeuroImage Clin*. 2014;4:201-208. doi:10.1016/j.nicl.2013.12.003

62.   Rüber T, Schlaug G, Lindenberg R. Compensatory role of the cortico-rubro-spinal tract in motor recovery after stroke. *Neurology*. 2012;79(6):515-522. doi:10.1212/WNL.0b013e31826356e8

63.   Choudhury S, Shobhana A, Singh R, et al. The Relationship Between Enhanced Reticulospinal Outflow and Upper Limb Function in Chronic Stroke Patients. *Neurorehabil Neural Repair*. 2019;33(5):375-383. doi:10.1177/1545968319836233

64.   Bradnam L V., Stinear CM, Byblow WD. Ipsilateral motor pathways after stroke: Implications for noninvasive brain stimulation. *Front Hum Neurosci*. 2013;7(APR 2013):184. doi:10.3389/fnhum.2013.00184

65.   K M, I H. Characteristics of the ipsilateral movement-related neuron in the motor cortex of the monkey. *Brain Res*. 1981;204(1):29-42. doi:10.1016/0006-8993(81)90649-1

66.   J B, HG K. Cerebral control of contralateral and ipsilateral arm, hand and finger movements in the split-brain rhesus monkey. *Brain*. 1973;96(4):653-674.

doi:10.1093/BRAIN/96.4.653

67. J T, K O, KC S. Neuronal activity in cortical motor areas related to ipsilateral, contralateral, and bilateral digit movements of the monkey. *J Neurophysiol*. 1988;60(1):325-343. doi:10.1152/JN.1988.60.1.325

68. P C, DJ C, JF K. Neural activity in primary motor and dorsal premotor cortex in reaching tasks with the contralateral versus ipsilateral arm. *J Neurophysiol*. 2003;89(2):922-942. doi:10.1152/JN.00607.2002

69. Ganguly K, Secundo L, Ranade G, et al. Cortical Representation of Ipsilateral Arm Movements in Monkey and Man. *J Neurosci*. 2009;29(41):12948-12956. doi:10.1523/JNEUROSCI.2471-09.2009

70. Scherer R, Zanos SP, Miller KJ, Rao RPN, Ojemann JG. Classification of contralateral and ipsilateral finger movements for electrocorticographic brain-computer interfaces. *Neurosurg Focus*. 2009;27(1). doi:10.3171/2009.4.FOCUS0981

71. Bundy DT, Szrama N, Pahwa M, Leuthardt EC. Unilateral, Three-dimensional Arm Movement Kinematics are Encoded in Ipsilateral Human Cortex. *J Neurosci*. Published online October 8, 2018:0015-0018. doi:10.1523/JNEUROSCI.0015-18.2018

72. Dodd KC, Nair VA, Prabhakaran V. Role of the contralesional vs. Ipsilesional hemisphere in stroke recovery. *Front Hum Neurosci*. 2017;11:469. doi:10.3389/fnhum.2017.00469

73. Buetefisch CM. Role of the contralesional hemisphere in post-stroke recovery of upper extremity motor function. *Front Neurol*. 2015;6(OCT):1-10. doi:10.3389/fneur.2015.00214

74. Carey JR, Kimberley TJ, Lewis SM, et al. Analysis of fMRI and finger tracking training in subjects with chronic stroke. *Brain*. 2002;125(Pt 4):773-788. doi:10.1093/brain/awf091

75. Ramos-Murguialday A, Broetz D, Rea M, et al. Brain-machine interface in chronic stroke rehabilitation: A controlled study. *Ann Neurol*. 2013;74(1):100-108.

76. Cramer SC, Riley JD. Neuroplasticity and brain repair after stroke. *Curr Opin Neurol*. 2008;21(1):76-82. doi:10.1097/WCO.0b013e3282f36cb6

77. Koralek AC, Jin X, Long 2nd JD, Costa RM, Carmena JM. Corticostriatal plasticity is necessary for learning intentional neuroprosthetic skills. *Nature*. 2012;483(7389):331-335. doi:10.1038/nature10845

78. Johansen-Berg H, Rushworth MFS, Bogdanovic MD, Kischka U, Wimalaratna S, Matthews PM. The role of ipsilateral premotor cortex in hand movement after stroke. *Proc Natl Acad Sci*. 2002;99(22):14518-14523. doi:10.1073/pnas.222536799

79. Marshall RS, Perera GM, Lazar RM, Krakauer JW, Constantine RC, DeLaPaz RL. Evolution of Cortical Activation During Recovery From Corticospinal Tract Infarction. *Stroke*. 2000;31(3):656-661.

80.   Schaechter JD, Kraft E, Hilliard TS, et al. Motor recovery and cortical reorganization after constraint-induced movement therapy in stroke patients: a preliminary study. *Neurorehabil Neural Repair*. 2002;16(4):326-338.

81.   Ward NS, Brown MM, Thompson AJ, Frackowiak RSJ. Neural correlates of outcome after stroke: A cross-sectional fMRI study. *Brain*. 2003;126(6):1430-1448. doi:10.1093/brain/awg145

82.   Ward NS, Brown MM, Thompson a. J, Frackowiak RSJ. Neural correlates of motor recovery after stroke: a longitudinal fMRI study. 2003;126(0 11):2476-2496. doi:10.1093/brain/awg245.Neural

83.   Young BM, Nigogosyan Z, Walton LM, et al. Changes in functional brain organization and behavioral correlations after rehabilitative therapy using a brain-computer interface. *Front Neuroeng*. 2014;7(July):26. doi:10.3389/fneng.2014.00026

84.   Kubis N. Non-Invasive Brain Stimulation to Enhance Post-Stroke Recovery. *Front Neural Circuits*. 2016;10:56.

85.   Takeuchi N, Chuma T, Matsuo Y, Watanabe I, Ikoma K. Repetitive transcranial magnetic stimulation of contralesional primary motor cortex improves hand function after stroke. *Stroke*. 2005;36(12):2681-2686.

86.   Volz LJ, Vollmer M, Michely J, Fink GR, Rothwell JC, Grefkes C. Time-dependent functional role of the contralesional motor cortex after stroke. *NeuroImage Clin*. 2017;16:165-174. doi:10.1016/j.nicl.2017.07.024

87.   Várkuti B, Guan C, Pan Y, et al. Resting state changes in functional connectivity correlate with movement recovery for BCI and robot-assisted upper-extremity training after stroke. *Neurorehabil Neural Repair*. 2013;27(1):53-62. doi:10.1177/1545968312445910

88.   Wang LE, Tittgemeyer M, Imperati D, et al. Degeneration of corpus callosum and recovery of motor function after stroke: A multimodal magnetic resonance imaging study. *Hum Brain Mapp*. 2012;33(12):2941-2956. doi:10.1002/hbm.21417

89.   Fan YT, Lin KC, Liu HL, Chen YL, Wu CY. Changes in structural integrity are correlated with motor and functional recovery after post-stroke rehabilitation. *Restor Neurol Neurosci*. 2015;33(6):835-844. doi:10.3233/RNN-150523

90.   Li Y, Wu P, Liang F, Huang W. The microstructural status of the corpus callosum is associated with the degree of motor function and neurological deficit in stroke patients. *PLoS One*. 2015;10(4):1-17. doi:10.1371/journal.pone.0122615

91.   Xu H, Qin W, Chen H, Jiang L, Li K, Yu C. Contribution of the resting-state functional connectivity of the contralesional primary sensorimotor cortex to motor recovery after subcortical stroke. *PLoS One*. 2014;9(1). doi:10.1371/journal.pone.0084729

92.   Di Pino G, Pellegrino G, Assenza G, et al. Modulation of brain plasticity in stroke: a novel model for neurorehabilitation. *Nat Rev Neurol*. 2014;10(10):597-608.

doi:10.1038/nrneurol.2014.162

93. Gupta RK, Saksena S, Hasan KM, et al. Focal Wallerian degeneration of the corpus callosum in large middle cerebral artery stroke: Serial diffusion tensor imaging. *J Magn Reson Imaging*. 2006;24(3):549-555. doi:10.1002/jmri.20677

94. Radlinska BA, Blunk Y, Leppert IR, Minuk J, Pike GB, Thiel A. Changes in Callosal Motor Fiber Integrity after Subcortical Stroke of the Pyramidal Tract. *J Cereb Blood Flow Metab*. 2012;32(8):1515-1524. doi:10.1038/jcbfm.2012.37

95. Bütefisch CM, Weβling M, Netz J, Seitz RJ, Hömberg V. Relationship Between Interhemispheric Inhibition and Motor Cortex Excitability in Subacute Stroke Patients. *Neurorehabil Neural Repair*. 2008;22(1):4-21. doi:10.1177/1545968307301769

96. Murase N, Duque J, Mazzocchio R, Cohen LG. Influence of interhemispheric interactions on motor function in chronic stroke. *Ann Neurol*. 2004;55(3):400-409. Accessed September 5, 2018. http://doi.wiley.com/10.1002/ana.10848

97. Levy CE, Nichols DS, Schmalbrock PM, Keller P, Chakeres DW. Functional MRI Evidence of Cortical Reorganization in Upper-Limb Stroke Hemiplegia Treated with Constraint-Induced Movement Therapy. *Am J Phys Med Rehabil*. 2001;80(1):4-12. doi:10.1097/00002060-200101000-00003

98. Sankarasubramanian V, Machado AG, Conforto AB, et al. Inhibition versus facilitation of contralesional motor cortices in stroke: Deriving a model to tailor brain stimulation. *Clin Neurophysiol*. 2017;128(6):892-902. doi:10.1016/J.CLINPH.2017.03.030

99. Plow EB, Sankarasubramanian V, Cunningham DA, et al. Models to tailor brain stimulation therapies in stroke. *Neural Plast*. 2016;2016. doi:10.1155/2016/4071620

100. Kleim JA, Barbay S, Cooper NR, et al. Motor Learning-Dependent Synaptogenesis Is Localized to Functionally Reorganized Motor Cortex. *Neurobiol Learn Mem*. 2002;77(1):63-77. doi:10.1006/nlme.2000.4004

101. Dancause N, Barbay S, Frost SB, et al. Extensive cortical rewiring after brain injury. *J Neurosci*. 2005;25(44):10167-10179. doi:10.1523/JNEUROSCI.3256-05.2005

102. Stroemer RP, Kent TA, Hulsebosch CE. Acute increase in expression of growth associated protein GAP-43 following cortical ischemia in rat. *Neurosci Lett*. 1993;162(1-2):51-54. doi:10.1016/0304-3940(93)90557-2

103. Nudo RJ. Mechanisms for recovery of motor function following cortical damage. *Curr Opin Neurobiol*. 2006;16(6):638-644. doi:10.1016/j.conb.2006.10.004

104. Nudo RJ. Postinfarct cortical plasticity and behavioral recovery. In: *Stroke*. Vol 38. Stroke; 2007:840-845. doi:10.1161/01.STR.0000247943.12887.d2

105. Alia C, Spalletti C, Lai S, et al. Neuroplastic changes following brain ischemia and their contribution to stroke recovery: Novel approaches in neurorehabilitation. *Front Cell Neurosci*. 2017;11. doi:10.3389/fncel.2017.00076

106. Gerloff C, Bushara K, Sailer A, et al. Multimodal imaging of brain reorganization in motor areas of the contralesional hemisphere of well recovered patients after capsular stroke. *Brain*. 2006;129(3):791-808. doi:10.1093/brain/awh713

107. Li S, Carmichael ST. Growth-associated gene and protein expression in the region of axonal sprouting in the aged brain after stroke. *Neurobiol Dis*. 2006;23(2):362-373. doi:10.1016/j.nbd.2006.03.011

108. Stowe AM, Plautz EJ, Eisner-Janowicz I, et al. VEGF protein associates to neurons in remote regions following cortical infarct. *J Cereb Blood Flow Metab*. 2007;27(1):76-85. doi:10.1038/sj.jcbfm.9600320

109. Alia C, Spalletti C, Lai S, Panarese A, Micera S, Caleo M. Reducing GABA A-mediated inhibition improves forelimb motor function after focal cortical stroke in mice. *Sci Rep*. 2016;6(1):1-15. doi:10.1038/srep37823

110. Siegel JS, Ramsey LE, Snyder AZ, et al. Disruptions of network connectivity predict impairment in multiple behavioral domains after stroke. *Proc Natl Acad Sci U S A*. 2016;113(30):E4367-76.

111. Chen JL, Schlaug G. Resting state interhemispheric motor connectivity and white matter integrity correlate with motor impairment in chronic stroke. *Front Neurol*. 2013;4 NOV(November):1-7. doi:10.3389/fneur.2013.00178

112. Carter AR, Astafiev S V, Lang CE, et al. Resting interhemispheric functional magnetic resonance imaging connectivity predicts performance after stroke. *Ann Neurol*. 2010;67(3):365-375.

113. Westlake KP, Hinkley LB, Bucci M, et al. Resting state α-band functional connectivity and recovery after stroke. *Exp Neurol*. 2012;237(1):160-169.

114. Burle B, Spieser L, Roger C, Casini L, Hasbroucq T, Vidal F. Spatial and temporal resolutions of EEG: Is it really black and white? A scalp current density view. *Int J Psychophysiol*. 2015;97(3):210-220. doi:10.1016/j.ijpsycho.2015.05.004

115. Kemna LJ, Posse S. Effect of Respiratory CO 2 Changes on the Temporal Dynamics of the Hemodynamic Response in Functional MR Imaging. Published online 2001. doi:10.1006/nimg.2001.0859

116. Pfurtscheller G, Lopes Da Silva FH. Event-related EEG/MEG synchronization and desynchronization: Basic principles. *Clin Neurophysiol*. 1999;110(11):1842-1857.

117. Pfurtscheller G, Aranibar A. Event related cortical desynchronization detected by power measurements of scalp EEG. *Electroencephalogr Clin Neurophysiol*. 1977;42(6):817-826.

118. Pfurtscheller G, Stancák A, Edlinger G. On the existence of different types of central beta rhythms below 30 Hz. *Electroencephalogr Clin Neurophysiol*. Published online 1997. doi:10.1016/S0013-4694(96)96612-2

119. Pfurtscheller G, Stancák A, Neuper C. Event-related synchronization (ERS) in the alpha

band - An electrophysiological correlate of cortical idling: A review. *Int J Psychophysiol*. Published online 1996.

120. Pfurtscheller G. Central beta rhythm during sensorimotor activities in man. *Electroencephalogr Clin Neurophysiol*. Published online 1981. doi:10.1016/0013-4694(81)90139-5

121. Pfurtscheller G, Neuper C. Event-related synchronisation of mu rhythms in the EEG over the hand area in man. *Neurosci Lett*. 1994;174(43):93-96.

122. Stępień M, Conradi J, Waterstraat G, Hohlefeld FU, Curio G, Nikulin V V. Event-related desynchronization of sensorimotor EEG rhythms in hemiparetic patients with acute stroke. *Neurosci Lett*. 2011;488(1):17-21. doi:10.1016/j.neulet.2010.10.072

123. Rossiter HE, Boudrias M-H, Ward NS. Do movement-related beta oscillations change after stroke? *J Neurophysiol*. 2014;112(9):2053-2058.

124. Platz T, Kim IH, Pintschovius H, et al. Multimodal EEG analysis in man suggests impairment-specific changes in movement-related electric brain activity after stroke. *Brain*. 2000;123(12):2475-2490.

125. Faught E. Current role of electroencephalography in cerebral ischemia. *Stroke*. 1993;24(4):609-613. doi:10.1161/01.STR.24.4.609

126. Cassidy JM, Wodeyar A, Wu J, et al. Low-Frequency Oscillations Are a Biomarker of Injury and Recovery after Stroke. *Stroke*. 2020;51(5):1442-1450. doi:10.1161/STROKEAHA.120.028932

127. Lu XCM, Williams AJ, Tortella FC. Quantitative electroencephalography spectral analysis and topographic mapping in a rat model of middle cerebral artery occlusion. *Neuropathol Appl Neurobiol*. 2001;27(6):481-495. doi:10.1046/j.1365-2990.2001.00357.x

128. Fanciullacci C, Bertolucci F, Lamola G, et al. Delta Power Is Higher and More Symmetrical in Ischemic Stroke Patients with Cortical Involvement. *Front Hum Neurosci*. 2017;11:385. doi:10.3389/fnhum.2017.00385

129. Dubovik S, Ptak R, Aboulafia T, et al. EEG alpha band synchrony predicts cognitive and motor performance in patients with ischemic stroke. *Behav Neurol*. 2013;26(3):187-189. doi:10.3233/BEN-2012-129007

130. Dubovik S, Pignat JM, Ptak R, et al. The behavioral significance of coherent resting-state oscillations after stroke. *Neuroimage*. 2012;61(1):249-257. doi:10.1016/j.neuroimage.2012.03.024

131. Foreman B, Claassen J. Quantitative EEG for the detection of brain ischemia. *Crit Care*. 2012;16(2):216. doi:10.1186/cc11230

132. Wu J, Srinivasan R, Quinlan EB, Solodkin A, Small SL, Cramer SC. Utility of EEG measures of brain function in patients with acute stroke. *J Neurophysiol*. 2016;115(5):2399-2405. doi:10.1152/jn.00978.2015

133. Finnigan S, Wong A, Read S. Defining abnormal slow EEG activity in acute ischaemic stroke: Delta/alpha ratio as an optimal QEEG index. *Clin Neurophysiol*. 2016;127(2):1452-1459. doi:10.1016/j.clinph.2015.07.014

134. Finnigan SP, Walsh M, Rose SE, Chalk JB. Quantitative EEG indices of sub-acute ischaemic stroke correlate with clinical outcomes. *Clin Neurophysiol*. 2007;118(11):2525-2532. doi:10.1016/j.clinph.2007.07.021

135. Leon-Carrion J, Martin-Rodriguez JF, Damas-Lopez J, Barroso y Martin JM, Dominguez-Morales MR. Delta-alpha ratio correlates with level of recovery after neurorehabilitation in patients with acquired brain injury. *Clin Neurophysiol*. 2009;120(6):1039-1045. doi:10.1016/j.clinph.2009.01.021

136. Schleiger E, Sheikh N, Rowland T, Wong A, Read S, Finnigan S. Frontal EEG delta/alpha ratio and screening for post-stroke cognitive deficits: The power of four electrodes. *Int J Psychophysiol*. 2014;94(1):19-24. doi:10.1016/j.ijpsycho.2014.06.012

137. Calautti C, Baron J-C. Functional neuroimaging studies of motor recovery after stroke in adults: a review. *Stroke*. 2003;34(6):1553-1566.

138. Grefkes C, Ward NS. Cortical Reorganization After Stroke: How Much and How Functional? *Neurosci*. 2014;20(1):56-70. doi:10.1177/1073858413491147

139. Buma FE, Raemaekers M, Kwakkel G, Ramsey NF. Brain Function and Upper Limb Outcome in Stroke: A Cross-Sectional fMRI Study. Cappello F, ed. *PLoS One*. 2015;10(10):e0139746. doi:10.1371/journal.pone.0139746

140. Biswal B, Yetkin FZ, Haughton VM, Hyde JS. Functional connectivity in the motor cortex of resting human brain using echo-planar MRI. *Magn Reson Med*. 1995;34(4):537-541. doi:10.1002/mrm.1910340409

141. Smitha KA, Akhil Raja K, Arun KM, et al. Resting state fMRI: A review on methods in resting state connectivity analysis and resting state networks. *Neuroradiol J*. 2017;30(4):305-317. doi:10.1177/1971400917697342

142. van den Heuvel MP, Hulshoff Pol HE. Exploring the brain network: a review on resting-state fMRI functional connectivity. *Eur Neuropsychopharmacol*. 2010;20(8):519-534. doi:10.1016/j.euroneuro.2010.03.008

143. Baldassarre A, Ramsey L, Hacker CL, et al. Large-scale changes in network interactions as a physiological signature of spatial neglect. *Brain*. 2014;137(12):3267-3283. doi:10.1093/brain/awu297

144. He BJ, Snyder AZ, Vincent JL, Epstein A, Shulman GL, Corbetta M. Breakdown of Functional Connectivity in Frontoparietal Networks Underlies Behavioral Deficits in Spatial Neglect. *Neuron*. 2007;53(6):905-918. doi:10.1016/j.neuron.2007.02.013

145. Ramsey LE, Siegel JS, Baldassarre A, et al. Normalization of network connectivity in hemispatial neglect recovery. *Ann Neurol*. 2016;80(1):127-141. doi:10.1002/ana.24690

146.   Gratton C, Nomura EM, Pérez F, D'Esposito M. Focal brain lesions to critical locations cause widespread disruption of the modular organization of the brain. *J Cogn Neurosci*. 2012;24(6):1275-1285. doi:10.1162/jocn_a_00222

147.   Siegel JS, Seitzman BA, Ramsey LE, et al. Re-emergence of modular brain networks in stroke recovery. *Cortex*. 2018;101:44-59.

148.   Lin LY, Ramsey L, Metcalf N V., et al. Stronger prediction of motor recovery and outcome post-stroke by cortico-spinal tract integrity than functional connectivity. Boltze J, ed. *PLoS One*. 2018;13(8):e0202504. doi:10.1371/journal.pone.0202504

149.   Fan Y, Wu C, Liu H, Lin K, Wai Y, Chen Y. Neuroplastic changes in resting-state functional connectivity after stroke rehabilitation. *Front Hum Neurosci*. 2015;9(OCT):546. doi:10.3389/fnhum.2015.00546

150.   Golestani AM, Tymchuk S, Demchuk A, Goodyear BG, Group V-S. Longitudinal evaluation of resting-state FMRI after acute stroke with hemiparesis. *Neurorehabil Neural Repair*. 2013;27(2):153-163. doi:10.1177/1545968312457827

151.   Park C, Chang WH, Ohn SH, et al. Longitudinal changes of resting-state functional connectivity during motor recovery after stroke. *Stroke*. 2011;42(5):1357-1362. doi:10.1161/STROKEAHA.110.596155

152.   Biasiucci A, Leeb R, Iturrate I, et al. Brain-actuated functional electrical stimulation elicits lasting arm motor recovery after stroke. *Nat Commun*. 2018;9(1):1-13. doi:10.1038/s41467-018-04673-z

153.   Pichiorri F, Morone G, Petti M, et al. Brain-computer interface boosts motor imagery practice during stroke recovery. *Ann Neurol*. 2015;77(5):851-865. doi:10.1002/ana.24390

154.   Baldassarre A, Ramsey LE, Siegel JS, Shulman GL, Corbetta M. Brain connectivity and neurological disorders after stroke. *Curr Opin Neurol*. 2016;29(6):706-713. doi:10.1097/WCO.0000000000000396

155.   Siegel JS, Mitra A, Laumann TO, et al. Data quality influences observed links between functional connectivity and behavior. *Cereb Cortex*. 2017;27(9):4492-4502. doi:10.1093/cercor/bhw253

156.   Lang CE, Strube MJ, Bland MD, et al. Dose response of task-specific upper limb training in people at least 6 months poststroke: A phase II, single-blind, randomized, controlled trial. *Ann Neurol*. 2016;80(3):342-354. doi:10.1002/ana.24734

157.   Waddell KJ, Strube MJ, Bailey RR, et al. Does Task-Specific Training Improve Upper Limb Performance in Daily Life Poststroke? *Neurorehabil Neural Repair*. 2017;31(3):290-300. doi:10.1177/1545968316680493

158.   Van der Lee JH, De Groot V, Beckerman H, Wagenaar RC, Lankhorst GJ, Bouter LM. The intra- and interrater reliability of the action research arm test: A practical test of upper extremity function in patients with stroke. *Arch Phys Med Rehab*. 2001;82(1):14-19.

doi:10.1053/apmr.2001.18668

159. Rabadi MH, Rabadi FM. Comparison of the Action Research Arm Test and the Fugl-Meyer Assessment as Measures of Upper-Extremity Motor Weakness After Stroke. *Arch Phys Med Rehabil*. Published online 2006. doi:10.1016/j.apmr.2006.02.036

160. Lang CE, Wagner JM, Dromerick AW, Edwards DF. Measurement of Upper-Extremity Function Early After Stroke: Properties of the Action Research Arm Test. *Arch Phys Med Rehabil*. Published online 2006. doi:10.1016/j.apmr.2006.09.003

161. Fugl-Meyer AR, Jääskö L, Leyman I, Olsson S, Steglind S. The post-stroke hemiplegic patient. 1. a method for evaluation of physical performance. *Scand J Rehabil Med*. 1975;7(1):13-31.

162. Duncan PW, Propst M, Nelson SG. Reliability of the Fugl-Meyer assessment of sensorimotor recovery following cerebrovascular accident. *Phys Ther*. 1983;63(10):1606-1610. doi:10.1093/ptj/63.10.1606

163. Lyle RC. A performance test for assessment of upper limb function in physical rehabilitation treatment and research. *Int J Rehabil Res*. 1981;4(4):483-492.

164. Barth J, Geed S, Mitchell A, Lum PS, Edwards DF, Dromerick AW. Characterizing upper extremity motor behavior in the first week after stroke. *PLoS One*. 2020;15(8):e0221668.

165. Sanford J, Moreland J, Swanson LR, Stratford PW, Gowland C. Reliability of the Fugl-Meyer assessment for testing motor performance in patients following stroke. *Phys Ther*. 1993;73(7):447-454. doi:10.1093/ptj/73.7.447

166. Sullivan KJ, Tilson JK, Cen SY, et al. Fugl-meyer assessment of sensorimotor function after stroke: Standardized training procedure for clinical practice and clinical trials. *Stroke*. 2011;42(2):427-432. doi:10.1161/STROKEAHA.110.592766

167. Gladstone DJ, Danells CJ, Black SE. The Fugl-Meyer Assessment of Motor Recovery after Stroke: A Critical Review of Its Measurement Properties. *Neurorehabil Neural Repair*. 2002;16(3):232-240. doi:10.1177/154596802401105171

168. Yozbatiran N, Der-Yeghiaian L, Cramer SC. A standardized approach to performing the action research arm test. *Neurorehabil Neural Repair*. 2008;22(1):78-90.

169. Power JD, Mitra A, Laumann TO, Snyder AZ, Schlaggar BL, Petersen SE. Methods to detect, characterize, and remove motion artifact in resting state fMRI. *Neuroimage*. 2014;84:320-341. doi:10.1016/j.neuroimage.2013.08.048

170. Fox MD, Zhang D, Snyder AZ, Raichle ME. The Global Signal and Observed Anticorrelated Resting State Brain Networks. *J Neurophysiol*. 2009;101(6):3270-3283. doi:10.1152/jn.90777.2008

171. Power JD, Plitt M, Laumann TO, Martin A. Sources and implications of whole-brain fMRI signals in humans. *Neuroimage*. 2017;146:609-625. doi:10.1016/j.neuroimage.2016.09.038

172.	Yarkoni T, Poldrack RA, Nichols TE, Van Essen DC, Wager TD. Large-scale automated synthesis of human functional neuroimaging data. *Nat Methods*. 2011;8(8):665-670. doi:10.1038/nmeth.1635

173.	Seitzman BA, Gratton C, Marek S, et al. A set of functionally-defined brain regions with improved representation of the subcortex and cerebellum. *Neuroimage*. 2020;206:116290. doi:10.1016/j.neuroimage.2019.116290

174.	Hagberg AA, Schult DA, Swart PJ. Exploring Network Structure, Dynamics, and Function using NetworkX. *Proc 7th Python Sci Conf (SciPy 2008)*. Published online August 2008:11-15.

175.	Page SJ, Fulk GD, Boyne P. Clinically important differences for the upper-extremity Fugl-Meyer scale in people with minimal to moderate impairment due to chronic stroke. *Phys Ther*. 2012;92(6):791-798. doi:10.2522/ptj.20110009

176.	Ono T, Shindo K, Kawashima K, et al. Brain-computer interface with somatosensory feedback improves functional recovery from severe hemiplegia due to chronic stroke. *Front Neuroeng*. 2014;7(July):19. doi:10.3389/fneng.2014.00019

177.	Mukaino M, Ono T, Shindo K, et al. Efficacy of brain-computer interface-driven neuromuscular electrical stimulation for chronic paresis after stroke. *J Rehabil Med*. 2014;46(4):378-382. doi:10.2340/16501977-1785

178.	van Meer MPA, van der Marel K, Wang K, et al. Recovery of sensorimotor function after experimental stroke correlates with restoration of resting-state interhemispheric functional connectivity. *J Neurosci*. 2010;30(11):3964-3972. doi:10.1523/JNEUROSCI.5709-09.2010

179.	Kraft AW, Bauer AQ, Culver JP, Lee JM. Sensory deprivation after focal ischemia in mice accelerates brain remapping and improves functional recovery through Arc-dependent synaptic plasticity. *Sci Transl Med*. 2018;10(426):31. doi:10.1126/scitranslmed.aag1328

180.	Kathleen Kelly M, Carvell GE, Kodger JM, Simons DJ. Sensory loss by selected whisker removal produces immediate disinhibition in the somatosensory cortex of behaving rats. *J Neurosci*. 1999;19(20):9117-9125. doi:10.1523/jneurosci.19-20-09117.1999

181.	Manger PR, Woods TM, Jones EG. Plasticity of the somatosensory cortical map in macaque monkeys after chronic partial amputation of a digit. *Proc R Soc B Biol Sci*. 1996;263(1372):933-939. doi:10.1098/rspb.1996.0138

182.	Jones EG. Cortical and subcortical contributions to activity-dependent plasticity in primate somatosensory cortex. *Annu Rev Neurosci*. 2000;23:1-37. doi:10.1146/annurev.neuro.23.1.1

183.	Hendry SHC, Jones EG. Reduction in number of immunostained GABAergic neurones in deprived-eye dominance columns of monkey area 17. *Nature*. 1986;320(6064):750-753. doi:10.1038/320750a0

184. Hendry SHC, Fuchs J, DeBlas AL, Jones EG. Distribution and plasticity of immunocytochemically localized GABAA receptors in adult monkey visual cortex. *J Neurosci*. 1990;10(7):2438-2450. doi:10.1523/jneurosci.10-07-02438.1990

185. DeFelipe J, Conley M, Jones EG. Long-range focal collateralization of axons arising from corticocortical cells in monkey sensory-motor cortex. *J Neurosci*. 1986;6(12):3749-3766. doi:10.1523/jneurosci.06-12-03749.1986

186. Rausell E, Bickford L, Manger PR, Woods TM, Jones EG. Extensive divergence and convergence in the thalamocortical projection to monkey somatosensory cortex. *J Neurosci*. 1998;18(11):4216-4232. doi:10.1523/jneurosci.18-11-04216.1998

187. Rausell E, Jones EG. Extent of intracortical arborization of thalamocortical axons as a determinant of representational plasticity in monkey somatic sensory cortex. *J Neurosci*. 1995;15(6):4270-4288. doi:10.1523/jneurosci.15-06-04270.1995

188. Hawasli AH, Kim DH, Ledbetter NM, Dahiya S, Barbour DL, Leuthardt EC. Influence of white and gray matter connections on endogenous human cortical oscillations. *Front Hum Neurosci*. 2016;10. doi:10.3389/fnhum.2016.00330

189. Soekadar SR, Birbaumer N, Slutzky MW, Cohen LG. Brain-machine interfaces in neurorehabilitation of stroke. *Neurobiol Dis*. 2015;83:172-179. doi:10.1016/j.nbd.2014.11.025

190. Young BM, Williams J, Prabhakaran V. BCI-FES: Could a new rehabilitation device hold fresh promise for stroke patients? *Expert Rev Med Devices*. 2014;11(6):537-539. doi:10.1586/17434440.2014.941811

191. Foong R, Tang N, Chew E, et al. Assessment of the Efficacy of EEG-Based MI-BCI with Visual Feedback and EEG Correlates of Mental Fatigue for Upper-Limb Stroke Rehabilitation. *IEEE Trans Biomed Eng*. 2020;67(3):786-795. doi:10.1109/TBME.2019.2921198

192. Ang KK, Chua KSG, Phua KS, et al. A Randomized Controlled Trial of EEG-Based Motor Imagery Brain-Computer Interface Robotic Rehabilitation for Stroke. *Clin EEG Neurosci*. 2015;46(4):310-320. doi:10.1177/1550059414522229

193. Giaquinto S, Cobianchi A, Macera F, Nolfe G. EEG recordings in the course of recovery from stroke. *Stroke*. 1994;25(11):2204-2209.

194. Shreve L, Kaur A, Vo C, et al. Electroencephalography Measures are Useful for Identifying Large Acute Ischemic Stroke in the Emergency Department. *J Stroke Cerebrovasc Dis*. 2019;28(8):2280-2286. doi:10.1016/j.jstrokecerebrovasdis.2019.05.019

195. Toro C, Deuschl G, Thatcher R, Sato S, Kufta C, Hallett M. Event-related desynchronization and movement-related cortical potentials on the ECoG and EEG. *Electroencephalogr Clin Neurophysiol Potentials Sect*. 1994;93(5):380-389.

196. Delorme A, Makeig S. EEGLAB: An open source toolbox for analysis of single-trial EEG

dynamics including independent component analysis. *J Neurosci Methods*. 2004;134(1):9-21. doi:10.1016/j.jneumeth.2003.10.009

197. Storey JD. A direct approach to false discovery rates. *J R Stat Soc Ser B Stat Methodol*. 2002;64(3):479-498. doi:10.1111/1467-9868.00346

198. Baldassarre A, Ramsey L, Rengachary J, et al. Dissociated functional connectivity profiles for motor and attention deficits in acute right-hemisphere stroke. *Brain*. 2016;139(7):2024-2038.

199. Wang HE, Bénar CG, Quilichini PP, Friston KJ, Jirsa VK, Bernard C. A systematic framework for functional connectivity measures. *Front Neurosci*. 2014;8(DEC):405. doi:10.3389/fnins.2014.00405

200. Yin S, Liu Y, Ding M. Amplitude of Sensorimotor Mu Rhythm Is Correlated with BOLD from Multiple Brain Regions: A Simultaneous EEG-fMRI Study. *Front Hum Neurosci*. 2016;10. doi:10.3389/fnhum.2016.00364

201. Hughes SW, Crunelli V. Thalamic mechanisms of EEG alpha rhythms and their pathological implications. *Neuroscientist*. 2005;11(4):357-372. doi:10.1177/1073858405277450

202. Pfurtscheller G, Neuper C. Motor imagery activates primary sensorimotor area in humans. *Neurosci Lett*. Published online 1997. doi:10.1016/S0304-3940(97)00889-6

203. Lindenberg R, Seitz RJ. *Impact of White Matter Damage After Stroke*. (Bright PP, ed.). InTech; 2012.

204. Lindenberg R, Zhu LL, Rüber T, Schlaug G. Predicting functional motor potential in chronic stroke patients using diffusion tensor imaging. *Hum Brain Mapp*. 2012;33(5):1040-1051. doi:10.1002/hbm.21266

205. Young BM, Nigogosyan Z, Nair V a, et al. Case report: post-stroke interventional BCI rehabilitation in an individual with preexisting sensorineural disability. *Front Neuroeng*. 2014;7(June):18. doi:10.3389/fneng.2014.00018

206. Krusienski DJ, McFarland DJ, Wolpaw JR. Value of amplitude, phase, and coherence features for a sensorimotor rhythm-based brain-computer interface. *Brain Res Bull*. 2012;87(1):130-134. doi:10.1016/j.brainresbull.2011.09.019

207. Salazar-Varas R, Gutiérrez D. An optimized feature selection and classification method for using electroencephalographic coherence in brain-computer interfaces. *Biomed Signal Process Control*. 2015;18:11-18. doi:10.1016/j.bspc.2014.11.001

208. Koch G, Bonnì S, Casula EP, et al. Effect of Cerebellar Stimulation on Gait and Balance Recovery in Patients with Hemiparetic Stroke: A Randomized Clinical Trial. *JAMA Neurol*. 2019;76(2):170-178. doi:10.1001/jamaneurol.2018.3639

209. Wathen CA, Frizon LA, Maiti TK, Baker KB, Machado AG. Deep brain stimulation of the cerebellum for poststroke motor rehabilitation: From laboratory to clinical trial.

Neurosurg Focus. 2018;45(2). doi:10.3171/2018.5.FOCUS18164

210. Khodaparast N, Hays SA, Sloan AM, et al. Vagus nerve stimulation during rehabilitative training improves forelimb strength following ischemic stroke. *Neurobiol Dis*. 2013;60. doi:10.1016/j.nbd.2013.08.002

211. Khodaparast N, Hays SA, Sloan AM, et al. Vagus nerve stimulation delivered during motor rehabilitation improves recovery in a rat model of stroke. *Neurorehabil Neural Repair*. 2014;28(7):698-706. doi:10.1177/1545968314521006

212. Khodaparast N, Kilgard MP, Casavant R, et al. Vagus Nerve Stimulation during Rehabilitative Training Improves Forelimb Recovery after Chronic Ischemic Stroke in Rats. *Neurorehabil Neural Repair*. 2016;30(7):676-684. doi:10.1177/1545968315616494

213. Hays SA, Khodaparast N, Hulsey DR, et al. Vagus nerve stimulation during rehabilitative training improves functional recovery after intracerebral hemorrhage. *Stroke*. 2014;45(10):3097-3100. doi:10.1161/STROKEAHA.114.006654

214. Kimberley TJ, Pierce D, Prudente CN, et al. Vagus nerve stimulation paired with upper limb rehabilitation after chronic stroke: A blinded randomized pilot study. *Stroke*. 2018;49(11):2789-2792. doi:10.1161/STROKEAHA.118.022279

215. Redgrave JN, Moore L, Oyekunle T, et al. Transcutaneous Auricular Vagus Nerve Stimulation with Concurrent Upper Limb Repetitive Task Practice for Poststroke Motor Recovery: A Pilot Study. *J Stroke Cerebrovasc Dis*. 2018;27(7):1998-2005. doi:10.1016/j.jstrokecerebrovasdis.2018.02.056

216. Dawson J, Pierce D, Dixit A, et al. Safety, feasibility, and efficacy of vagus nerve stimulation paired with upper-limb rehabilitation after ischemic stroke. *Stroke*. 2016;47(1):143-150. doi:10.1161/STROKEAHA.115.010477

217. Capone F, Miccinilli S, Pellegrino G, et al. Transcutaneous Vagus Nerve Stimulation Combined with Robotic Rehabilitation Improves Upper Limb Function after Stroke. *Neural Plast*. 2017;2017. doi:10.1155/2017/7876507

218. Feng W, Kautz SA, Schlaug G, Meinzer C, George MS, Chhatbar PY. Transcranial Direct Current Stimulation for Poststroke Motor Recovery: Challenges and Opportunities. *PM R*. 2018;10(9):S157-S164. doi:10.1016/j.pmrj.2018.04.012

219. Schlaug G, Renga V, Nair D. Transcranial direct current stimulation in stroke recovery. *Arch Neurol*. 2008;65(12):1571-1576. doi:10.1001/archneur.65.12.1571

Curriculum Vitae

EDUCATION

Washington University in St. Louis   **August 2014 – August 2021**
- Ph.D. candidate in Biomedical Engineering, Advisor: Eric Leuthardt, M.D.
- Cognitive, Computational, and Systems Neuroscience Fellowship
- Clinical and Translational Science (TL1) Fellowship

University of Alabama at Birmingham   **August 2010 - April 2014**
- B.S. in Biomedical Engineering
- Summa Cum Laude
- Departmental Honors

RESEARCH EXPERIENCE

Washington University in St. Louis   **September 2014 - August 2021**

PhD Project-Neural Mechanisms of Chronic Stroke Motor Recovery with a Brain-Computer Interface (BCI)

- Measured changes in EEG activity related to chronic stroke motor recovery
- Designed and implemented longitudinal neuroimaging experiment
- Analyzed volumetric time-series data from resting-state functional MRI scans to determine how the functional organization of the brain changes during BCI therapy

Rotation Project - Leuthardt Lab (January 2015 – May 2015)
- Designed and built an interactive task to evaluate hemispatial neglect severity using an eye-tracking system
- Designed ROC-based gaze distribution analysis technique

Rotation Project - Barbour Lab (August 2014-December 2014)
- Designed and implemented simulation of traditional audiology hearing threshold measurement
- Analyzed bias innate to traditional threshold measurement

Rotation Project - Bagnall Lab (May 2015 - August 2015)
- Bred zebrafish larvae and dyed spinal neurons for imaging
- Used confocal fluorescence microscopy to image vestibular neuron location and activity
- Analyzed activation of dyed neurons with ImageJ

University of Alabama at Birmingham   **August 2012 - August 2014**
Advisor: Vladimir Parpura, M.D., Ph.D.

- Measured effect of water-soluble carbon nanotubes on astrocyte morphology,

proliferation, and survival
- Compared efficacy of several fluorescent dyes in characterizing astrocyte morphology
- Combined fluorescent dyes to estimate area of astrocytes occupied by small processes

Teaching Experience

Graduate Teaching Assistant   **August 2015 – December 2015**
Biomedical Engineering Design
- Held weekly office hours and provided help sessions for design reports and presentations
- Gave class lecture on TRIZ design (Design strategy highlighting common combinations of abstract design problems and solutions)
- Evaluated design notebooks

Young Scientist Program, Continuing Mentoring   **September 2014 – May 2018**
- Mentored St. Louis public high school students throughout their high school careers to aid them in achieving future academic and professional success
- Gave lectures and demonstrations to high school students on several STEM topics, such as vision neuroscience, 3D printing, and introductory computer programming

Professional Experience

Biotechnology and Life Sciences Advising (BALSA) Group   **April 2018 - Present**

- Completed consulting project involving competitor analysis, SWOT analysis, and product and market viability analyses for early stage companies founded by researchers
- Collaborated with consulting team to compile and present findings to project manager
- Presented final recommendations to client with team of consultants

Sling Health Project Leader, Sevolytics   **August 2016 - April 2017**

- Identified business opportunity in surgical anesthesia monitoring
- Led diverse team of students from engineering, medicine, and business backgrounds
- Researched existing monitor devices and consulted with local anesthesiologists for design input
- Constructed monitor prototype using open-source electrophysiology equipment

Analytics Consultant, Neurolutions   **July 2015 – May 2020**

- Analyzed data quality and subject performance in clinical trial for a novel stroke therapy device
- Collaborated with CEO to develop action plan based on results
- Advised on device design and clinical trial implementation

Publications and Presentations

Papers:
Joseph B. Humphries, Daniela J. S. Mattos, Jerrel Rutlin, Andy G. S. Daniel, Kathleen Rybczynski, Theresa Notestine, Joshua S. Shimony, Harold Burton, Alexandre Carter, Eric Leuthardt. *Motor Network Reorganization Induced in Chronic Stroke Patients with the Use of a Contralesionally-Controlled Brain Computer Interface*. Manuscript in Submission. 2021.

Joseph B. Humphries, Kathleen Rybczynski, Theresa Notestine, Harold Burton, Alexandre Carter, Eric Leuthardt. *Alpha Coherence Increases with Motor Recovery During Chronic Stroke Rehabilitation with Contralesional EEG-BCI*. Manuscript in Submission. 2021.

Andy G. S. Daniel, Ki Yun Park, Jarod L. Roland, Donna Dierker, James Gross, **Joseph B. Humphries**, Carl D. Hacker, Abraham Z. Snyder, Joshua S. Shimony, Eric C. Leuthardt. *Functional connectivity within glioblastoma impacts overall survival*. Neuro-Oncology. 2021; 23 (3): 412-421.

Andy G. S. Daniel, Carl D. Hacker, John J. Lee, Donna Dierker, **Joseph B. Humphries**, Joshua S. Shimony, Eric C. Leuthardt. *Homotopic functional connectivity disruptions in glioma patients are associated with tumor malignancy and overall survival.* Manuscript in Submission. 2021.

Talks:
"Cortical Activity Changes in Chronic Stroke Motor Rehabilitation with a Contralesional Brain-Computer Interface," WUSTL Biomedical Engineering Department Retreat, September 2019

"Longitudinal Neural Correlates of Chronic Stroke Rehabilitation with a Contralesional Brain-Computer Interface," Cognitive, Computational, and Systems Neuroscience Mini-Retreat, January 2019

Posters:
Joseph B. Humphries, David T. Bundy, Thy N. Huskey, and Eric C. Leuthardt, "Longitudinal Changes in EEG Power are Proportional to Motor Recovery in Chronic Stroke Patients," Translational Science 2018, Washington, D.C., April 2018

Joseph B. Humphries, Isaac Mordukhovich, and Eric C. Leuthardt, "Smoothing and Test-Retest Reliability of Voxel-Based Morphometry in a Healthy Cohort," Organization for Human Brain Mapping 2018, Singapore, June 2018

Joseph B. Humphries, David T. Bundy, Ravi V Chacko, Byungchan Kim, Alexandre R. Carter, and Eric C. Leuthardt, "Longitudinal Shifts in Cross-Frequency Coupling Reflect Motor Recovery in Chronic Stroke Patients," WUSTL Clinical Research Training Center's Annual Research Training Symposium, St. Louis, MO, October 2018

Joseph B. Humphries, Byungchan Kim, David T. Bundy, Thy N. Huskey, and Eric C. Leuthardt, "Interhemispheric Neural Correlates of Chronic Stroke Recovery with a

Contralesional Brain Computer Interface," Translational Science 2019, Washington, D.C., March 2019

Joseph B. Humphries, Alexander Scott, Michael Olufawo, Ki Yun Park, Andy G.S. Daniel, Kathleen Rybczynski, Theresa Notestine, Alexandre R. Carter, Eric C. Leuthardt, "Resting-State Functional Connectivity Alterations Associated with Chronic Stroke Recovery via a Brain-Computer Interface," Society for Neuroscience 2019, Chicago, IL, October 2019.

Sarah N. Chiang, Siddharth Rana, **Joseph B Humphries**, Eric C Leuthardt, "Motor Recovery After Chronic Stroke Correlates With Diffusion Tensor Measures of Ipsilesional Cerebral and Cerebellar White Matter Integrity," International Stroke Conference (virtual), March 2021